

**DEVELOPMENT OF LONG-TERM STABLE MIXED
SODIUM CASEINATE AND PEA PROTEIN ISOLATE-STABILIZED
NANOEMULSIONS FOR THE DELIVERY OF CURCUMIN**



College of Agriculture
and Bioresources

A Thesis Submitted to the
College of Graduate Studies and Research
in Partial Fulfillment of the Requirements for the
Degree of Master of Science in the
Department of Food and Bioproduct Sciences
University of Saskatchewan
Saskatoon, SK

By

Manispuritha Yerramilli

PERMISSION TO USE

In presenting this thesis in partial fulfillment of the requirements for a Postgraduate degree from the University of Saskatchewan, I agree that the Libraries of this University may make it freely available for inspection. I further agree that permission for copying of this thesis/dissertation in any manner, in whole or in part, for scholarly purposes may be granted by the professor or professors who supervised my thesis work or, in their absence, by the Head of the Department or the Dean of the College in which my thesis work was done. It is understood that any copying or publication or use of this thesis or parts thereof for financial gain shall not be allowed without my written permission. It is also understood that due recognition shall be given to me and to the University of Saskatchewan in any scholarly use which may be made of any material in my thesis.

Requests for permission to copy or to make other uses of materials in this thesis in whole or part should be addressed to:

Head of the Department,
Food and Bioproduct Sciences,
University of Saskatchewan Saskatoon,
Saskatchewan S7N 5A8 Canada

ABSTRACT

Nanoemulsions (NEs) with extremely small droplet size (radius <100 nm) were found to possess characteristics that have many advantages over conventional emulsion systems. These nano-sized droplets were found to contribute to higher stability of the NEs and also found to improve the bioavailability of poorly water-soluble bioactive components. The overall aim of this thesis is to develop oil-in-water (O/W) NEs stabilized by a mixture of sodium caseinate (a dairy protein) and pea protein isolates (a pulse protein). The mixed protein stabilized NEs were utilized to encapsulate a bioactive compound, curcumin, where the goal is to investigate its stability, delivery and bioavailability through *in vitro* digestion studies.

Various concentrations (2.5 – 10 wt%) of sodium caseinate (SC) were used as the sole emulsifier in the development of 5 wt% O/W NEs and their long-term storage stability for 6 months was investigated. The sodium caseinate stabilized NEs (SCEs) developed in this work displayed an average droplet diameter less than 200 nm, which remained unchanged for an experimental time frame of 6 months. However, all of them displayed rapid creaming, which increased with an increase in protein concentration, in accordance with previous studies. It was postulated that excess unabsorbed protein caused depletion flocculation leading to creaming of oil droplets, which was confirmed using confocal laser scanning microscopy. Calculation of depletion interaction energy showed an increase in attraction with protein concentration and decrease with a reduction in droplet size, making NEs more resistant to flocculation than conventional emulsions.

Next, pea protein isolate (PPI), was utilized to partially replace SC and thereby PPIs efficacy in the formation and long-term stabilization of mixed protein NEs (MPEs) was investigated. Total aqueous phase-protein concentration of 5, 7.5 and 10 wt%, with SC and PPI in a 1:1 ratio, was used. As a control individual PPI-stabilized NEs (PPIE) were also prepared. PPI failed to produce stable flowable NEs displaying excessive droplet and protein aggregation. At higher concentrations of PPI (7.5 and 10 wt%), the emulsion transformed into viscoelastic gels. Interestingly, the mixed SC and PPI-stabilized NE did not display any creaming or aggregation and remained stable throughout the experimental timeframe of 6 months with average droplet diameter <200 nm. Results from interfacial protein composition (surface load) and SDS-PAGE indicated the presence of PPI at the interface along with SC confirming PPI's ability to take part in droplet formation and stabilization. It was hypothesized that the mutual presence of SC and PPI during high-pressure homogenization led to interactions between the proteins, which was

confirmed by FTIR spectroscopy, intrinsic fluorescence and surface hydrophobicity measurements. Interactions between the proteins not only prevented depletion flocculation effect of SC, but also interfered with PPI aggregation thereby preventing both the destabilizing mechanisms seen in individual protein-stabilized NEs. The mixed-protein stabilization could be a novel way to utilize plant proteins in the development of NEs.

In the final part, the efficacy of the MPE for stability, delivery and bioavailability of an encapsulated bioactive compound, curcumin was investigated and compared to the SCE . It was seen that over 54% of encapsulated curcumin was degraded in the MPE, while only ~42% was degraded in the SCE over a period of 8 weeks. *In vitro* digestion studies indicated that the amount of bioavailable curcumin from SCE was slightly higher (although not statistically significant) compared to that from MPE, which was attributed to a thicker droplet interface in the mixed protein NE (due to presence of globular protein PPI), thereby making the droplet less susceptible towards protein hydrolysis by pepsin in the stomach.

Overall, it was concluded that it is possible to develop mixed protein NEs utilizing PPI and SC, which displayed better stability when compared to the individual protein-stabilized NEs. The presented approach not only utilized pulse protein, PPI, in the development of NEs, but also showed good applicability in terms of encapsulating bioactive ingredients for prospective applications in food and pharmaceutical industries.

ACKNOWLEDGEMENTS

I would like to express my deep and sincere gratitude to my supervisor Dr. Supratim Ghosh, whose patience and expertise inspired and kept me going throughout my masters. Thank you Supratim! This work is a definite outcome of your trust in me and the continuous encouragement you showered.

I would like to acknowledge the Department of Food and Bioproduct Sciences for its continuous support throughout my masters. I would like to thank my graduate chairs, Drs. Robert T. Tyler, Takuji Tanaka, Qui Xiao and my advisory committee member Dr. Michael Nickerson for their support and suggestions. I thank my external examiner, Dr. Venkatesh Meda for his precious time in this endeavour.

I would like to thank all my colleagues from Food Nanotechnology lab for their help and co-operation (Vivek, Anzhelika, Maja, Chang, Wai Fun, Aakash, Pol, Rana, Nin, Srinivas, Akaysha and Sylavana). Special thanks to all my other colleagues and friends from U of S. I would also like to thank Ann Harley, Patricia Olesiuk and Donna Selby for their administrative assistance. Special thanks to Andrea Stone, Yuanlong Cao and Dr. Adrienne Wotowich for their help and training. I am also grateful to Tara McIntosh and Suneru Mohottalalage of the Protein Research Lab at Agriculture and Agri-food Canada, for their help in protein content determination and SDS-PAGE. Also, I would like to thank Jason Maley from Saskatchewan Structural Science Center for his help in ITC and FT-IR experiments. Helpful discussions with Dr. Michael Nickerson, Dr. Janitha Wanasundara and Dr. Ramaswami Sammynaiken are also deeply acknowledged.

Financial support for this work provided by the Agriculture Development Fund (ADF) from the Saskatchewan Ministry of Agriculture, CFI-John R. Evans Leaders Fund, Innovation and Science Fund (ISF) from the Saskatchewan Ministry of Advanced Education and University of Saskatchewan New Faculty Start-up Equipment Support grant is deeply acknowledged.

I would like to thank my parents (Dr. Ramaprabha & Mr. Srivatsa) and my brother (Sinjith) for their love and unconditional support. Your encouragement is all that bought me this far. Thanks to my in-laws (Mr. Venkateshwarlu & Mrs. Subhashini Kuppala) and Bhargav for their encouragement in this endeavor. Last but not the least, special thanks to my husband, Karthik without whose love and continuous support, this wouldn't have been possible! Thank you Karthik!

Finally, I thank, almighty god for everything!

DEDICATION

To,

My late grandfather

Mr. Kasturi Vijaya Ram Mohan

TABLE OF CONTENTS

PERMISSION TO USE	i
ABSTRACT	ii
ACKNOWLEDGEMENTS	iv
DEDICATION.....	v
TABLE OF CONTENTS.....	vi
LIST OF TABLES	ix
LIST OF FIGURES	x
LIST OF SYMBOLS AND ABBREVIATIONS	xv
1 INTRODUCTION	1
1.1 Summary	1
1.2 Objectives.....	3
1.3 Hypothesis	3
2 LITERATURE REVIEW	4
2.1 Emulsions and nanoemulsions	4
2.2 Protein stabilized nanoemulsions	16
2.3 Encapsulation and release of bio-active ingredients from emulsions	21
2.4 Bioavailability and <i>in vitro</i> digestion of nanoemulsions.....	24
2.5 Choice of materials.....	31

3	LONG-TERM STABILITY OF SODIUM CASEINATE-STABILIZED NANOEMULSIONS	34
3.1	Abstract	34
3.2	Introduction	35
3.3	Materials and methods.....	36
3.4	Results and discussion.....	39
3.5	Conclusion.....	51
3.6	Connection to next study.....	52
4	IMPROVED STABILIZATION OF NANOEMULSIONS BY PARTIAL REPLACEMENT OF SODIUM CASEINATE WITH PEA PROTEIN ISOLATE	53
4.1	Abstract	53
4.2	Introduction.....	54
4.3	Materials and methods	57
4.4	Results and discussion	62
4.5	Conclusion	80
4.6	Connection to next study.....	81
5	EFFECTS OF PARTIAL REPLACEMENT OF SODIUM CASEINATE WITH PEA PROTEIN ISOLATE IN NANOEMULSION ON THE STABILITY, DELIVERY AND BIOAVAILABILITY OF CURCUMIN.....	82
5.1	Abstract	82
5.2	Introduction.....	83
5.3	Materials and methods	85
5.4	Results and discussion	89

5.5	Conclusion	102
6	GENERAL DISCUSSION	104
7	OVERALL CONCLUSION	108
8	FUTURE STUDIES.....	111
9	REFERENCES.....	114

LIST OF TABLES

Table 5.3.1 Constituents and their concentration for simulated gastric, duodenal and bile juices used in the <i>in vitro</i> digestion model.....	88
--	----

LIST OF FIGURES

- Figure 2.1.1** Schematic representation of emulsions: (a) O/W emulsion (b) W/O emulsion 4
- Figure 2.1.2** Schematic representation of double emulsions. (a) Oil-in-water-in-oil emulsion. Here, o_1 internal oil phase, o_2 stands for external oil phase and w for water phase. (b) Water-in-oil-in water emulsion. Here, w_1 internal water phase, w_2 stands for external water phase and o for oil phase..... 5
- Figure 2.1.3** DLVO interdroplet pair potential between two droplets (adapted from Ghosh & Rousseau, 2010). The interdroplet interaction energy (JK^{-1}) is shown on Y axis and the distance of separation between two droplets is shown on X axis. 12
- Figure 2.1.4** Destabilization mechanisms in NEs (adapted from Rao & McClements, 2011).. 13
- Figure 2.4.1** The process of digestion in different sections of human gastrointestinal tract (picture adapted from www.catalog.niddk.nih.gov). 25
- Figure 2.4.2** Schematic representation of multiple step *in vitro* digestion model 28
- Figure 3.4.1** Droplet size distribution of 5 wt% canola oil-in water nanoemulsions stabilized by various concentrations of sodium caseinate for (a) freshly prepared and (b) 24 weeks old samples. Nanoemulsions prepared with protein concentrations of 2.5 wt% (●), 5 wt% (▲), 7.5 wt% (■), 10 wt% (◆) are compared. 40
- Figure 3.4.2** Surface average mean droplet diameter (d_{32}) of oil-in-water nanoemulsions stabilized with various concentrations of sodium caseinate (SC) as a function of time. 2.5 wt% (●), 5 wt% (▼), 7.5 wt% (■), 10 wt% (◆). Error bars represents \pm standard deviation of the average data (n =3). 41
- Figure 3.4.3** Visual observation of oil-in water nanoemulsions stabilized by various concentrations of sodium caseinate after (a) 8 weeks and (b) 24 weeks of storage at 4°C..... 42
- Figure 3.4.4** Change in creaming index for sodium caseinate (SC)-stabilized oil-in-water nanoemulsions as a function of time and protein concentrations: 2.5 wt% (●), 5 wt% (▼), 7.5 wt% (■), 10 wt% (◆). Error bars represents \pm standard deviation of the average data (n =3)..... 43
- Figure 3.4.5** Confocal micrographs of 5 wt% canola oil-in-water nanoemulsions stabilized by various concentrations of sodium caseinate (a) 2.5 wt%, (b) 5 wt%, (c) 7.5 wt% and

(d) 10 wt% (scale bar 20 μ m). The nanodroplet flocs are clearly visible in (e) which was captured by 5 times digital zooming on a 2.5 wt% sodium caseinate-stabilized nanoemulsion sample (scale bar 5 μ m). For a clear view of droplet flocculation an enlarged view of image (e) is shown..... 45

Figure 3.4.6 Optical micrographs of the cream layer from 5 wt% canola oil-in-water nanoemulsions stabilized by sodium caseinate at various concentrations on the day of preparation and after 8 and 24 weeks of storage. A working magnification of 400 \times was used. Scale bar represents 5 μ m..... 47

Figure 3.4.7 Instability index calculated from centrifugal separation analysis transmission profiles of the nanoemulsions prepared with various concentrations of sodium caseinate for freshly prepared, 4 weeks and 24 weeks old samples..... 48

Figure 3.4.8 Calculated values of depletion interaction energy ΔG_{dep} (units of $K_B T$) as a function of unadsorbed protein concentration in the aqueous phase of the nanoemulsions for (a) different caseinate submicelle radii: 5nm (\bullet), 10nm (\blacksquare), 20nm (\blacktriangle) for 78 nm average droplet diameter of nanoemulsion, and (b) different average droplet radii: 500 nm (\bullet), 250 nm (\blacksquare), 78 nm (\blacktriangle) for 10 nm caseinate submicelle..... 51

Figure 4.4.1 Droplet size distributions of 5 wt% canola oil-in-water nanoemulsions stabilized with sodium caseinate (SC) (---), pea protein isolates (PPI) (.....) and 1:1 mixture of SC and PPI (mixed protein, MP) (—). Freshly prepared emulsions (a, c, e) and at the end of 24 weeks (b, d, f) are compared with total protein concentration of 5 wt% (a) and (b); 7.5 wt % (c) and (d); 10 wt% (e) and (f). The additional curve (—) represents 5 wt% PPI emulsion diluted with SDS. 63

Figure 4.4.2 Change in surface mean droplet diameter (d_{32}) as a function of time for 5 wt% canola oil-in-water nanoemulsions stabilized at a total protein concentration of 5 wt% (a); 7.5 wt % (b) and 10 wt% (c) with sodium caseinate (SC) (\bullet) and 1:1 mixture of SC and pea protein isolate (PPI) , (MP) (\circ). d_{32} values considered for this figure are taken from the first peak of droplet size distribution alone. 65

Figure 4.4.3 Visual observation of oil-in-water nanoemulsions after 24 weeks of storage. Samples of emulsions stabilized by 1:1 mixture of sodium caseinate (SC) and pea protein isolates (PPI) (mixed protein, MP), and individual proteins at (a) 5 wt%, (b)

7.5 wt% and (c) 10 wt% total protein concentrations. Horizontal vial images at the bottom indicates the flowability of PPI emulsions at various concentrations..... 67

Figure 4.4.4 Viscosity of freshly prepared nanoemulsions stabilized with various concentration of sodium caseinate (SC) (■), pea protein isolates (PPI) (▲) and 1:1 mixture of SC and PPI (MP) (◆). 68

Figure 4.4.5 Change in Creaming index of nanoemulsions stabilized with a total protein concentration of (a) 5 wt%; (b) 7.5 wt % and (c) 10 wt% sodium caseinate (SC) (●) and 1:1 mixture of sodium caseinate and pea protein isolate (MP) (○). 69

Figure 4.4.6 Confocal laser scanning micrographs of freshly prepared (a) 5 wt% sodium caseinate (SC) nanoemulsion, (b) pea protein isolate (PPI) nanoemulsion, (c) 5 wt% mixed protein (1:1 of SC:PPI) nanoemulsion and (d) emulsion made up by mixing 1:1 ratio of 5 wt% SC and 5 wt% PPI nanoemulsions. All images captured at a working magnification of 600× with a 5 times digital zoom. Nanoemulsions' oil phase was stained with 0.01 wt% Nile red, and the proteins were stained with 0.01 wt% fast green. Scale bars represent 5µm. 71

Figure 4.4.7 Surface load of freshly prepared nanoemulsions stabilized with various concentration of sodium caseinate (SC) (■), pea protein isolates (PPI) (▲) and 1:1 mixture of SC and PPI (MP) (◆)..... 72

Figure 4.4.8 SDS-PAGE of separated serum phase and cream phase from the nanoemulsions. MWM on Lane 1 represents molecular weight marker, with pre-stained standards ranging from 10 kDa to 130 kDa. Lanes from left to right (2-5) represent serum phase from 5 wt % PPI nanoemulsion (PPIE), serum phase from 5 wt % mixed protein nanoemulsion (MPE), protein extracted from cream phase of 5 wt % mixed protein nanoemulsion (MPE), serum phase from 5 wt % sodium caseinate nanoemulsion (SCE). 73

Figure 4.4.9 Confocal laser scanning micrographs of solutions (homogenized and un-homogenized) of pea protein isolate (PPI), 1:1 mixture of SC and PPI (MP). Fast green (0.01 wt%) was used to stain these protein solutions. Working magnification of 600×. Scale bar represents 20 µm. 75

Figure 4.4.10	Deconvoluted amide I region of FT-IR spectra of freeze dried protein solution containing mixed protein (1:1 mixture of SC and PPI) mixed protein un-homogenized (----). And homogenized (—).	77
Figure 4.4.11	(a) Surface hydrophobicity expressed in arbitrary units at an excitation and emission wavelengths of 390 nm and 470 nm, respectively and (b) Zeta potential expressed in mV of mixed protein (MP), sodium caseinate (SC) and pea protein isolate; un-homogenized (UH) □ and homogenized (H) ■	78
Figure 4.4.12	Fluorescence spectra of protein solutions carried out at constant excitation wavelength of 295 nm. Fluorescence is given as arbitrary units (AU) as a function of wavelength (nm). Spectra of un-homogenized s (----) and homogenized (—) protein solutions.	8080
Figure 5.2.1	Chemical structure of curcumin (adapted from Anand et al., 2007).....	84
Figure 5.4.1	Droplet size distribution of 5 wt% canola oil-in water nanoemulsions with curcumin encapsulated in the oil phase and stabilized by (a) 5 wt% sodium caseinate (b) 5 wt% mixed protein (1:1 ratio of sodium caseinate and pea protein isolate). Data for freshly prepared (----) and 8 weeks old (....) samples are shown.	90
Figure 5.4.2	Change in surface mean droplet diameter (d_{32}) as a function of time for 5 wt% canola oil-in-water nanoemulsions containing curcumin and stabilized by 5 wt% mixed protein (1:1 ratio of sodium caseinate and pea protein isolate) (5 MPE) (●) and 5 wt% sodium caseinate (5 SCE) (○).	90
Figure 5.4.3	Visual observation of fresh and 8 weeks old oil-in-water nanoemulsions containing curcumin and stabilized by (a) 5 wt% mixed protein (1:1 ratio of sodium caseinate and pea protein isolate) and (b) 5 wt% sodium caseinate	91
Figure 5.4.4	Stability of curcumin encapsulated in 5 wt% oil-in-water nanoemulsions stabilized by 5 wt% mixed protein (1:1 ratio of sodium caseinate and pea protein isolate) (5 MPE) (●) and 5 wt% sodium caseinate (5 SCE) (○) and as a function of time. Theoretically the NEs should have a curcumin concentration of 0.005 wt%.	92
Figure 5.4.5	Change in droplet size distribution of curcumin encapsulated oil-in-water nanoemulsions stabilized by 5 wt% mixed protein (1:1 ratio of sodium caseinate and pea protein isolate) (MPE) (a, c) and 5 wt% sodium caseinate (5 SCE) (b, d) as a function of digestion time with respect to various digestion steps of stomach (with	

and without digestive enzymes). Distribution represented as: stomach blank and small intestine blank (----), Fresh NE (—), at the beginning of digestion 0 hour (- - - - -), and after 2 hours of digestion (.). 93

Figure 5.4.6 Change in droplet size distribution of curcumin encapsulated oil-in-water nanoemulsions stabilized by 5 wt% mixed protein (1:1 ratio of sodium caseinate and pea protein isolate) (MPE) (a, c) and 5 wt% sodium caseinate (5 SCE) (b, d) as a function of digestion time with respect to various digestion steps of small intestine (with and without digestive enzymes). Distribution represented as: small intestine blank (----), Fresh NE (—), at the beginning of digestion 0 hour (- - - - -), and after 2 hours of digestion (.). 94

Figure 5.4.7 Confocal laser scanning micrographs from simulated gastric digestion of 5 wt% mixed protein and sodium caseinate stabilized nanoemulsions as a function of digestion time; 0 hour (a, b), after two hours of digestion (c, d), after two hours of digestion without enzymes (e, f). Micrographs captured at a magnification of 600X, with a 5 times digital zoom. Scale bar represents 5 μm 96

Figure 5.4.8 Confocal laser scanning micrographs from simulated intestinal digestion as a function of digestion time; 0 hour (a, b), after two hours of digestion (c, d) with enzymes. Micrographs captured at a magnification of 600X. Scale bar represents 10 μm 98

Figure 5.4.9 Confocal laser scanning micrographs from simulated intestinal digestion as a function of digestion time; 0 hour (a, b), after two hours of digestion (c, d) without enzymes. Micrographs captured at a magnification of 600X. Scale bar represents 10 μm 100

Figure 5.4.10 Bioaccessibility of curcumin from the micelle phase of 5 wt% canola oil-in water nanoemulsions after *in vitro* digestion, stabilized by 5 wt% sodium caseinate and 5 wt% mixed protein (1:1 ratio of sodium caseinate and pea protein isolate) 101

LIST OF ABBREVIATIONS AND SYMBOLS

BHA	Butylated hydroxyanisole
BHT	Butylated hydroxytoluene
C_{aq}	Aqueous phase excess protein concentration (g/ 100 g)
CITREM	Citric acid ester of monoglyceride
CLSM	Confocal laser scanning microscope
d_{32}	Volume surface mean droplet diameter (micrometer/ nanometer)
DAG	Diacylglycerols
DATEM	Diacetyl tartaric acid ester of monoglyceride
DLVO	Derjaguin, Landau, Verwey and Overweek
DTAB	Dodecyl trimethyl ammonium bromide
ΔP	Laplace pressure
$\Delta\rho$	Density difference of the two phases in the emulsion
EFSA	European Food Safety Authority
F	Bioavailability of an encapsulated lipophilic component
$f(\kappa\alpha)$	Function related to the ratio of particle radius (α) and the Debye length (κ)
F_A	Fraction of lipophilic component released from delivery system bioaccessible
F_B	Fraction of released component absorbed across the intestinal epithelial cells
FDA	Food and Drug Administration
FFA	Free fatty acids
F_M	Fraction of the absorbed component without being metabolized
FT-IR	Fourier transform infrared spectroscopy

<i>g</i>	Acceleration due to gravity (9.81 m/ s ²)
GI	Gastrointestinal
GRAS	Generally recognized as safe
HPLC	High performance liquid chromatography
K_B	Boltzmann's constant (1.3807 x 10 ⁻²³ J/ K)
$K_B T$	Thermal energy of the system (J)
<i>M</i>	Effective molecular weight (kg/ mol)
MAG	Monoacylglycerols
MPE	Mixed protein nanoemulsion
<i>n</i>	Number density of the SC submicelles
N_A	Avogadro number (6.022 ×10 ²³ / mol)
NE	Nanoemulsion
O/W	Oil-in-water
O/W/O	Oil-in-water-in-oil
Pa	Pascal
P_{osm}	Osmotic pressure (Pa)
PPI	Pea protein isolate
PPIE	Pea protein isolate nanoemulsion
<i>r</i>	Radius of the droplet
r_d	Radius of nanoemulsion droplets (meter)
r_m	Radius of casein submicelle (meter)
SC	Sodium caseinate
SCE	Sodium caseinate nanoemulsion

SCJ	Simulated colonic juice
SDS-PAGE	Sodium dodecyl sulfate polyacrylamide gel electrophoresis
SEM	Scanning electron microscope
SGJ	Simulated gastric juice
SIJ	Simulated intestinal juice
T	Temperature (K)
TAG	Triacylglycerol
TEM	Transmission electron microscopy
U_E	Electrophoretic mobility
V_d	Velocity of the droplet
V	Volume of the emulsifier depleted layer
W/O	Water-in-oil
W/O/W	Water-in-oil-in-water
γ	Interfacial tension between oil and water
ΔG_{dep}	Depletion interaction energy (J)
ϵ	Permittivity
η	Viscosity (Pa.s)
ρ	Density of the sub-micelle particles (1050 kg/m ³)
η_d	Viscosity of dispersed phase
η_c	Viscosity of continuous phase

1 INTRODUCTION

1.1 Summary

Nanoemulsions (NEs) as a research discipline have drastically improved over the last decade. They were found to possess properties that have advantages over conventional emulsion systems in terms of practical applications in the food industry. The nano-sized droplets poorly scatter light and hence visual appearance of food containing NEs may remain unaffected. The improved stability of NEs to various destabilization phenomena as compared to their conventional counterparts is attributed to their nanoscale droplets (Mason et al., 2006). NEs are also known to significantly increase bioavailability of encapsulated bioactive components which is one of the most important attributes that may lead to improved health benefits (Rao & McClements, 2012).

To develop oil-in-water (O/W) NEs with extremely small droplet size, a suitable water-soluble emulsifier is required. If an emulsifier is used it would lower the interfacial tension by adsorbing onto the freshly created nanodroplets' surface during homogenization. Small molecule emulsifier, sodium dodecyl sulfate (SDS) and Tween 20, aid in this process, but larger quantities of these are required thereby raising toxicological issues for food-based applications (He et al., 2011a; Lawrence & Rees, 2000). Therefore, food proteins can be considered as an ideal alternative as they do not raise toxicological concerns and additionally improve consumer acceptance (Can Karaca et al., 2011b). The O/W NEs in this study utilized sodium caseinate (SC), a dairy protein and the proteins extracted from pea, pea protein isolate (PPI), a pulse proteins. Pulse-based plant proteins remain relatively underutilized for their functionality and applicability in various foods when compared to animal-based proteins (Adebisi & Aluko, 2011). In this regard, there is limited work done in the development of NEs stabilized by pulse-based proteins (Donsi et al., 2010; Kuhn et al., 2014). Therefore, in this work PPI was one of the emulsifiers utilized to develop long-term stable NEs. Since, not much literature support was available, it was important to start with a protein that was well established and consequently utilize pea to partially or wholly replace it. Proteins derived from bovine milk (whey, casein) are one of the most widely used emulsifying agents in a variety of food products (McClements, 2005). The sodium salt of casein, most popularly referred to as sodium caseinate, is a soluble mixture of all four fractions of caseins and has been extensively

utilized not only to develop emulsions but also NEs (Hunt & Dalgleish, 1994; Lee & Norton, 2013; Qian & McClements, 2011; Radford & Dickinson, 2004; Zeeb et al., 2014; Zhao et al., 2015). Therefore, SC was the other emulsifier chosen such that individual SC stabilized NEs (SCE), PPI stabilized NEs (PPIE) and mixed SC and PPI (in 1:1 ratio) stabilized NEs (MPE) were developed.

In the next part of the research curcumin, a polyphenolic compound, was used to encapsulate in the oil phase of the MPE and SCE to study its stability and bioavailability through *in vitro* digestion studies. Kinetically stable O/W NEs have been widely used in encapsulating bioactive ingredients to deliver and enhance their bioavailability (McClements et al., 2007; Sari et al., 2015). Curcumin is an oil soluble phytochemical extracted from powdered rhizomes of turmeric spice, has a number of beneficial biological effects on the human body, e.g., anti-tumour, anti-oxidant, anti-microbial and anti-inflammatory properties (Anand et al, 2007). However, due to low water solubility it is difficult to incorporate curcumin into food where it can have higher chance of getting absorbed into the body through small intestine (Ahmed et al., 2012). Studies have shown that NEs were successful in encapsulating and delivering this compound (Ahmed et al., 2012).

In vitro digestion studies are conducted using components isolated from their usual biological surroundings in order to permit a more detailed or convenient analysis (Stipanuk & Caudill, 2013). These studies mimic human gastrointestinal conditions. *In vivo* experiments are conducted with living organisms in their normal intact state (Stipanuk & Caudill, 2013). Bioavailability is the fraction of ingested components that enters into or gets absorbed in the bloodstream (Holst & Williamson, 2008) while bioaccessibility is the fraction released from food matrix into the GI tract and thus becomes available for intestinal absorption (Fernández-García et al., 2009). Hence, what is bioaccessible, enters the bloodstream, gets absorbed, and become bioavailable. *In vitro* studies reveal the bioaccessibility of a compound rather than bioavailability, which is accurately understood through *in vivo* studies. Li and co-workers have shown that results from *in vitro* studies were qualitatively similar when compared to *in vivo* studies (Li et al., 2012). Therefore, an improved bioaccessibility is an indication of improved bioavailability of bioactives. Hence, it was hypothesized that through the *in vitro* studies carried out in the research, bioaccessibility of curcumin would be an indication of its bioavailability.

The overall goal of this research is to develop oil-in-water (O/W) NEs stabilized by a mixture of sodium caseinate (a dairy protein) and pea protein isolate (a pulse protein), encapsulate

a bioactive compound, curcumin and investigate its stability, delivery and bioavailability through *in vitro* digestion studies.

1.2 Objectives

To reach the overall research goal the following objectives were developed:

- 1) Develop SC-stabilized NEs and investigate their long term stability.
- 2) To partially replace SC with PPI and investigate the long-term stability of mixed SC and PPI-stabilized NEs.
- 3) To encapsulate curcumin, a bioactive ingredient, in the NEs and investigate their stability and release behavior with time.
- 4) To perform *in vitro* digestion studies for determination of bioaccessibility of curcumin encapsulated in mixed SC and PPI-stabilized NEs.

1.3 Hypotheses

The following hypotheses were tested to support the above objectives.

- 1) Mixture of SC and PPI will be able to stabilize NEs such that the pulse protein would be incorporated at the oil droplet interface by partially replacing SC and aid in the stabilization of NEs.
- 2) Under high-pressure homogenization condition denaturation of PPI would lead to hydrophobic interactions between SC and PPI which could significantly influence NE formation and stability.
- 3) Incorporation of bioactive ingredient in the oil droplets will not influence the physical stability of the NEs.
- 4) The mixed protein-stabilized NE will protect the bioactive ingredient from environmental degradation during storage.
- 5) Bioavailability of curcumin encapsulated in mixed protein-stabilized NEs will not be affected compared to dairy protein-stabilized NEs.

2 LITERATURE REVIEW

2.1 Emulsions and nanoemulsions

Emulsions are dispersions of two or more immiscible phases, one being dispersed as droplets in the other (McClements, 2005). The phase which makes droplets is referred to as the dispersed, discontinuous or internal phase and the phase surrounding these droplets is called continuous or external phase (McClements, 2005). Emulsions find applications in various fields, e.g., food, agro-chemical, chemical, pharmaceutical, cosmetic, paint, printing and oil industries. In foods, these are found in a number of products where either a major constituent (e.g., sauces, soups) or the whole food (e.g., milk, mayonnaise) is made of emulsion (McClements, 2005; Muschiolik, 2007).

2.1.1 Types of emulsions

Emulsions are classified as oil-in-water (O/W) (Figure 2.1.1a) and water-in-oil (W/O) (Figure 2.1.1b), based on the dispersed and continuous phase composition. In O/W emulsions, oil droplets are dispersed in the continuous water phase, e.g., mayonnaise and salad dressings. In W/O emulsions water droplets are dispersed in the continuous oil phase, e.g., butter and margarine.

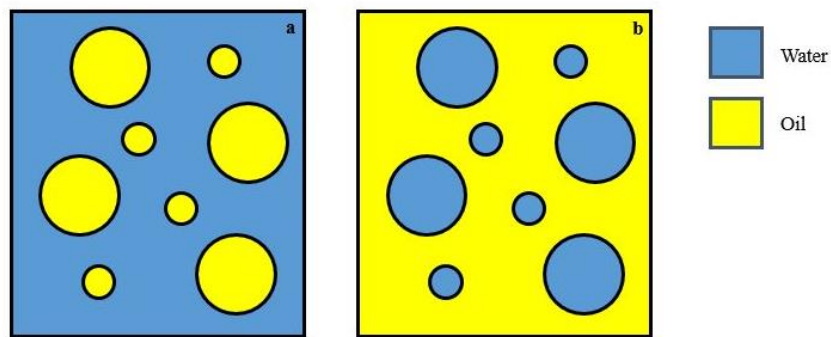


Figure 2.1.1 Schematic representation of emulsions: (a) O/W emulsion (b) W/O emulsion.

Based on the number of dispersed phases that exist in an emulsion, there could be single or multiple emulsions. Single emulsions have only one dispersed phase, while multiple emulsions have two or more dispersed phases, one dispersed as droplets in the other, which in turn dispersed

in another continuous phase (Muschiolik, 2007). These include oil-in-water-in-oil (O/W/O) emulsions (Figure 2.1.2 a) and water-in-oil-in-water (W/O/W) emulsions (Figure 2.1.2 b).

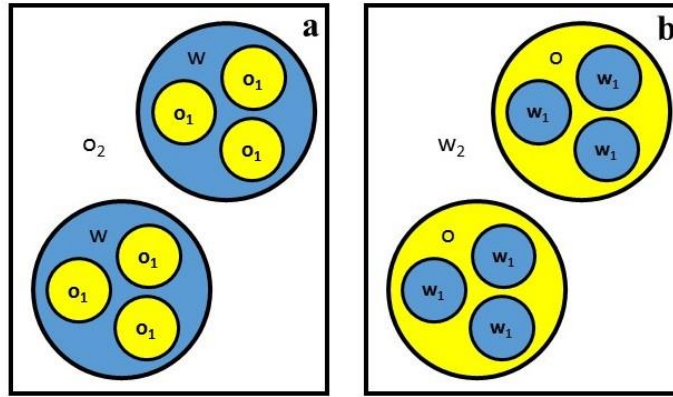


Figure 2.1.2 Schematic representation of double emulsions. (a) Oil-in-water-in-oil emulsion. Here, o_1 internal oil phase, o_2 stands for external oil phase and w for water phase. (b) Water-in-oil-in water emulsion. Here, w_1 internal water phase, w_2 stands for external water phase and o for oil phase.

Depending on the stability of the dispersed phase, emulsions are classified as conventional emulsions and microemulsions (McClements, 2012). Conventional emulsions are those that are thermodynamically unstable. They separate into oil and water phases respectively with time. However, the stability of the two phases could be controlled kinetically such that conventional emulsions can be stabilized for a long period of time from few days to several months (Mason et al., 2006). Microemulsions are a class of emulsions which are thermodynamically stable under a given set of conditions. In these emulsions, the surfactant molecules are arranged in such a way that their non-polar tails associate with each other forming a hydrophobic core which reduces thermodynamically unfavorable contact area between non-polar groups and water thus making the emulsion stable (McClements, 2012). The droplet radii of these emulsions are typically in the range of 2-50 nanometers, whereas a conventional emulsion has a broader range of droplet radii from few hundred nanometers to several micrometers (100nm-100 μ m) (McClements, 2012).

A new class of emulsion, called nanoemulsion (NE) had taken form in the recent years which are claimed to possess much improved stability as compared to conventional emulsions (Rao & McClements, 2012). By definition NEs are emulsions with droplet radii less than 100 nm (McClements, 2012). However, this range of droplet size is arbitrary and some authors consider

the upper range to be 200 nm (Gutiérrez et al., 2008). These small sized droplets (radius less than 100 nm) display number of potential advantages over the conventional emulsions, e.g., higher stability to droplet aggregation and gravitational separation, high optical clarity, ability to modulate product texture, and increase bioavailability (Rao & McClements, 2012). These advantages bring in potential applications of NEs not only in food and beverages, but also in chemical and pharmaceutical industries.

2.1.2 Nanoemulsion formulation

Apart from the oil and water phase constituents, emulsions and NE also consist of emulsifiers, thickening agents, preservatives, antioxidants, sweeteners, flavors etc. The concentration and distribution of these ingredients influence the physicochemical properties and stability of the emulsions. The chief ingredients in food emulsions and NE can be categorized into the following groups:

Oil phase: The composition of the oil phase of food emulsions has a significant influence on the nutritional, physicochemical and organoleptic properties (McClements, 2005). The lipid phase also contains other oil soluble ingredients like vitamins, anti-oxidants, preservatives, waxes, weighting agents, essential oils, lipophilic nutraceuticals such as carotenoids, curcumin (McClements, 2005). The perceived flavor of an emulsion is largely dependent on the type and concentration of the lipid and lipophilic ingredients present (McClements, 2005) which is important in terms of consumer acceptability of any food product. Formation and stability of NE also depends on the bulk physicochemical characteristics like viscosity, interfacial tension, water solubility, density, polarity of the oil phase. For instance lower interfacial tension promotes both droplet formation as well as disruption (Rao & McClements, 2012).

In food industry, NEs can be prepared from lipids like triacylglycerols (TAGs) and essential oils (McClements, 2005). Soybean oil, sunflower oil, flaxseed oil are TAGs that are commonly used because of their availability, low cost and better nutritional and functional attributes. Most of these oils are dominated by long chain fatty acids and they tend to be hydrophobic in nature exhibiting higher levels of viscosity and interfacial tension compared to other oils with medium chain and short chain fatty acids. Hence, these tend to form more stable NEs. Conversely, some NEs prepared from low viscous edible oils like flavor and essential oils facilitate in formation of

very small droplets due to the lower interfacial tension and viscosity (McClements, 2005), but breakdown rapidly due to Ostwald ripening that is one of the major destabilization phenomena for NEs (discussed in detail in later sections). The oil phase may also contain other ingredients like weighting agents (which match the density of oil and aqueous phase, thereby further improving NE stability to gravitational separation) and ripening inhibitors (components which are soluble in oil and insoluble in aqueous phase and reduce the solubility of oil phase in water thus inhibiting Ostwald ripening) (Gutiérrez et al., 2008).

Aqueous phase: The aqueous phase of NEs contains primarily water, emulsifiers and other water-soluble ingredients which influence stability organoleptic properties and flowability (McClements, 2005). These other water-soluble components include co-solvents (such as simple alcohols and polyols), colorants, preservatives, carbohydrates, proteins, minerals, acids and bases.

The viscosity ratio of dispersed to continuous phase (η_d/η_c) influences droplet breakup and NE stability (Walstra, 1993). It has been proposed that for η_d/η_c greater than 4, the flow behavior inside a homogenizer turns less turbulent, making it difficult to achieve droplet breakdown and thus formation of smaller droplet size of NE (Walstra, 1993). It was also shown that if η_d/η_c is greater than 10, droplets cannot be broken down (Walstra, 1993), indicating, increase in the oil phase viscosity will make it difficult to prepare NEs. Hence, the formation of nanosized droplets for a NE is often facilitated by the addition of water-soluble co-solvents to the aqueous phase to control the η_d/η_c .

Emulsifier: If an oil phase and aqueous phase are homogenized together, the system will eventually break down into two separate phases. For this reason, an emulsifier is added which will stabilize the system. The term emulsifier is used to describe any surface-active substance that is capable of adsorbing to an oil-water interface and protecting emulsion droplets from destabilization through aggregation, flocculation and coalescence (these emulsion destabilization mechanisms are discussed in later sections). Selection of proper emulsifier is one of the most important factors in designing NE. The most commonly used emulsifiers in food industries are small molecule surfactants and amphiphilic biopolymers (McClements, 2005).

Small molecule surfactants: The term “surfactant” is used to refer to those relatively small surface active molecules that consist of a hydrophilic head which has affinity for aqueous phase and a hydrophobic tail with affinity for oil phase. The nature and characteristics of the surfactant

depends on the type of head and tail groups present (McClements, 2005). Depending on the charge of the head group small molecule surfactants can be classified into anionic, cationic, zwitterionic and non-ionic. Examples of anionic small molecule surfactant include citric acid ester of monoglyceride (CITREM) or, diacetyl tartaric acid ester of monoglyceride (DATEM). Examples of cationic surfactant include lauric arginate, dodecyl trimethyl ammonium bromide (DTAB). Lecithin is an example of zwitterionic emulsifier where both positive and negative charge is present on the molecule. Non-ionic emulsifiers include polyol esters of fatty acids like polyoxyethylene sorbitan esters (which carry the trade name of Tween) and sorbitan esters of fatty acids (trade name Span). The tail group of small molecule surfactants usually consists of one or two linear or branched hydrocarbon chains.

Amphiphilic biopolymers: Proteins and certain polysaccharides are naturally occurring polymers that are used as emulsifiers. Proteins are amino acid polymers and polysaccharides are monosaccharide polymers. These have covalent linkages between their monomer units (known as peptide bonds in proteins and glycolytic bonds in polysaccharides), around which the polymer chain rotates at well-defined angles. When added to an emulsion as emulsifiers, biopolymers adopt fairly well defined conformation such that all the lipophilic groups are towards the oil phase and the hydrophilic groups towards the aqueous phase. The conformation and state of the biopolymer plays an important role in determining their functional attributes, which ultimately decides the stability of the emulsions (McClements, 2005). Some commonly used protein emulsifiers include whey, casein, gelatin, pea and soy. Polysaccharides used as emulsifiers include gum Arabic, pectin, modified starches and chitosan. However, formation of a stable emulsion by utilization of a polysaccharide alone is rare. They are often accompanied by considering another polysaccharide or another protein in combination (Akhtar & Dickinson, 2007; Dickinson, 2009; Schmitt et al., 2005).

Co-emulsifier: Certain methods of formation of emulsions employ the addition of co-emulsifier. Co-emulsifiers are amphiphilic, surface-active molecules which generally possess a hydrocarbon chain and small sized polar head group (Garti et al., 2001). Some of the commonly used co-emulsifiers include short-chain and medium-chain alcohols. Due to the small size of the polar head group, these molecules are not as efficient as the surfactant itself, but aid in emulsion formation by reduction of interfacial tension and modifying emulsifier packing at the oil/water

interface (Gradzielski, 1998). Some commonly used co-emulsifiers include ethyl alcohol and lecithin (McClements, 2005).

2.1.3 Nanoemulsion formation

The formation of a NE may involve single step or multiple steps depending on the type and nature of the ingredients present in oil and aqueous phases (McClements, 2005). As the two phases in emulsions are immiscible, external energy is required to disperse one phase as droplets into other. This energy supplied should be sufficient for droplet deformation and disruption, which is opposed by the internal pressure of the droplets (also known as Laplace pressure, ΔP) and is given by the equation:

$$\Delta P = \frac{2\gamma}{r} \quad (\text{eq. 2.1})$$

where, ' γ ' is interfacial tension between oil and water and ' r ' is the radius of the droplet (Walstra, 1993). From equation 2.1 it can be inferred that the Laplace pressure is directly proportional to the interfacial tension and inversely proportional to the droplet size. Therefore, as the droplet radius becomes smaller during homogenization, it becomes increasingly difficult to further break them up, hence high energy is required to form NEs compared to conventional emulsions (Tadros et al., 2004).

A number of different approaches can be employed to form an emulsion, but these can be broadly categorized as high-energy and low-energy approaches (McClements, 2005).

High-energy approaches: These utilize mechanical devices that are capable of generating intensive disruptive forces produce oil droplets of smaller size. Examples of these devices include the high pressure valve homogenizers, microfluidizers, sonicators etc. This is the most commonly and widely used method to prepare NEs, because they are capable of producing desired small droplets required for NE. If employed, these methods are also capable of production in large scale for industries (Tadros et al., 2004).

Low-energy approaches: In low-energy approaches small oil droplets are spontaneously formed when the solution conditions (e.g., oil and dispersed phase concentration, emulsifier type and concentration) or environmental conditions (e.g., temperature) are altered accordingly (Solans & Solé, 2012). A number of methods for preparing NEs are based on low-energy approaches like spontaneous emulsification and phase inversion methods. In spontaneous emulsification process,

a NE is spontaneously formed when two liquids are mixed together along with a suitable surfactant. Use of proteins or polysaccharides as emulsifiers in this approach is highly unlikely, because these do not aid in the spontaneous formation of the small sized droplets for NEs. Interfaces covered with these emulsifiers tend to be more elastic in nature and have higher interfacial tension than those compared with small molecule surfactants. Hence, unlike the high-energy approaches, only a few kinds of emulsifiers can be used during low-energy approaches (Solans & Solé, 2012). In phase inversion method, a W/O emulsions changes to O/W emulsion or vice versa. This phase inversion could be induced by altering the temperature (Phase inversion temperature method), or composition of the dispersed phase (phase inversion composition method). Low-energy approaches often produce smaller droplet sizes as compared to high-energy approaches, but have limited acceptability in food industry because of usage of synthetic emulsifier and that too in high concentrations (Rao & McClements, 2012).

Stability enhancement techniques: After NEs are formed using either high-energy or low-energy approaches it is possible to further reduce the droplet size or change the characteristics of interfacial layer, using various methods that ultimately aid in enhancing the stability of the prepared NE (Rao & McClements, 2012). Some of them include:

Change in nature of the interfacial layer surrounding the oil droplets: The interfacial layer is altered by the addition of emulsifiers that alter the adsorption, or create an electric charge around the layer or cross link the already adsorbed layer (Rao & McClements, 2012).

Solvent displacement/ evaporation: In this method the O/W emulsion is initially prepared by homogenizing the oil phase containing organic solvent and the aqueous phase followed by solvent displacement or evaporation resulting in the shrinkage or further decrease in the oil droplets size of a NE (Lee & McClements, 2010). This method was proven successful in producing a NE stabilized by whey protein isolate, using ethyl acetate as the solvent. It was proven that size of the droplets proportionally reduces with increase in the solvent quantity (Lee & McClements, 2010). However, the problem with this approach is that, large amount of solvent is required. This is because; volume is directly proportional to the cube of diameter. So, to reduce the size of a droplet to say half its original diameter, volume of the droplet must be reduces to $1/8^{\text{th}}$ its original volume and this demands large amount of solvent.

2.1.4 Inter-droplet interactions in nanoemulsions

Droplet interactions have a significant impact in deciding whether they will remain separate or form aggregates (Friberg et al., 2004). Droplet interactions are expressed in terms of the interdroplet pair potential. It is the energy required to bring two droplets from an infinite distance to a close separation (Figure 2.1.3) (Ghosh & Rousseau, 2010). The interdroplet pair potential in Figure 2.1.3, is the sum of van der Waal and electrostatic interactions. Electrostatic potential component is repulsive which increases exponentially with a decrease in distance between the droplets. Whereas, van der Waal forces are attractive and increases as the droplets approach each other. The total interaction potential is the sum of these two forces. It decreases as the particles come near and the droplets form loose aggregates when the interaction potential drops to a secondary minimum. Upon further droplet approach, the electrostatic repulsion dominate over the van der Waal interaction and if the thermal energy of the droplets is not enough to overcome the repulsive energy barrier they return back to initial non-aggregated state (also known as reversible flocculation, discussed in later sections). On the other hand, if thermal energy of the droplet pair is more than the repulsive energy barrier, the interaction potential passes through the energy barrier and the droplets form strong irreversible aggregates (also known as coagulation, discussed in later sections) at the primary energy minima. This theory of interdroplet potential was first proposed by Derjaguin, Landau, Verwey and Overweek and is known as DLVO theory (Ghosh & Rousseau, 2010). The original DLVO theory did not take into account steric repulsions, depletion forces, hydrophobic and hydration interactions, so it is only an approximate estimate of droplet interactions. However, for specific cases, these factors can be included in a modified DLVO theory that could be used to predict inter-droplet interactions and hence emulsion stability (McClements, 2005). Understanding the forces acting on an emulsion will help in prediction of the stability of the NE. Hence, the DLVO theory is an important factor in terms of evaluation of formation of a NE.

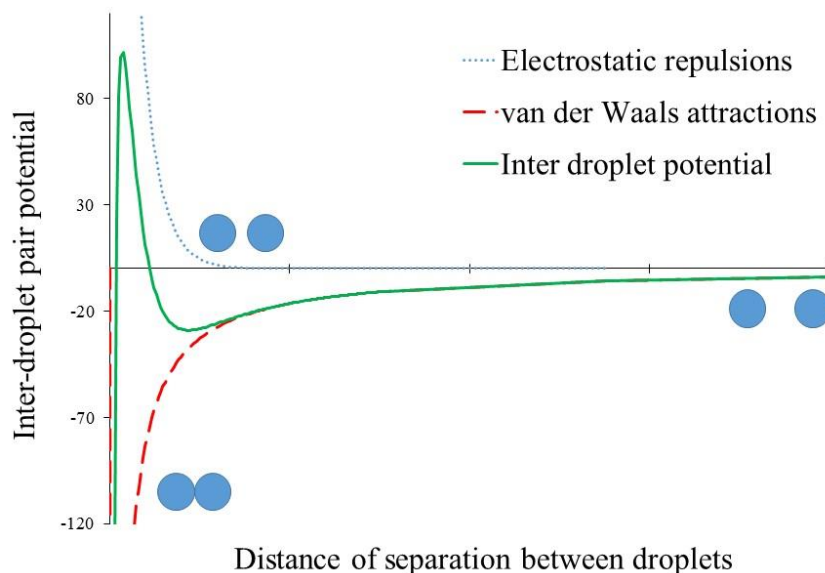


Figure 2.1.3 DLVO interdroplet pair potential between two droplets (adapted from Ghosh & Rousseau, 2010). The interdroplet interaction energy (JK^{-1}) is shown on Y axis and the distance of separation between two droplets is shown on X axis.

2.1.5 Stability of nanoemulsions

Stability of an emulsion is its ability to resist changes in its properties with time (McClements, 2005). Instability of an emulsion may be due to number of physical and chemical changes that it undergoes. These are often interrelated and occur simultaneously (McClements, 2007). Creaming, flocculation, coalescence, phase inversion, Ostwald ripening are examples of physical instability. Biopolymer hydrolysis, lipid oxidation, color or flavor degradation are examples of chemical instability (Walstra, 1996). As such emulsions are thermodynamically unstable systems and they tend to separate out as oil and aqueous phases over time which is energetically more favored. They could be made stable kinetically by incorporating emulsifiers and other ingredients. In the following section, each of these instability mechanisms will be discussed in terms of NEs.

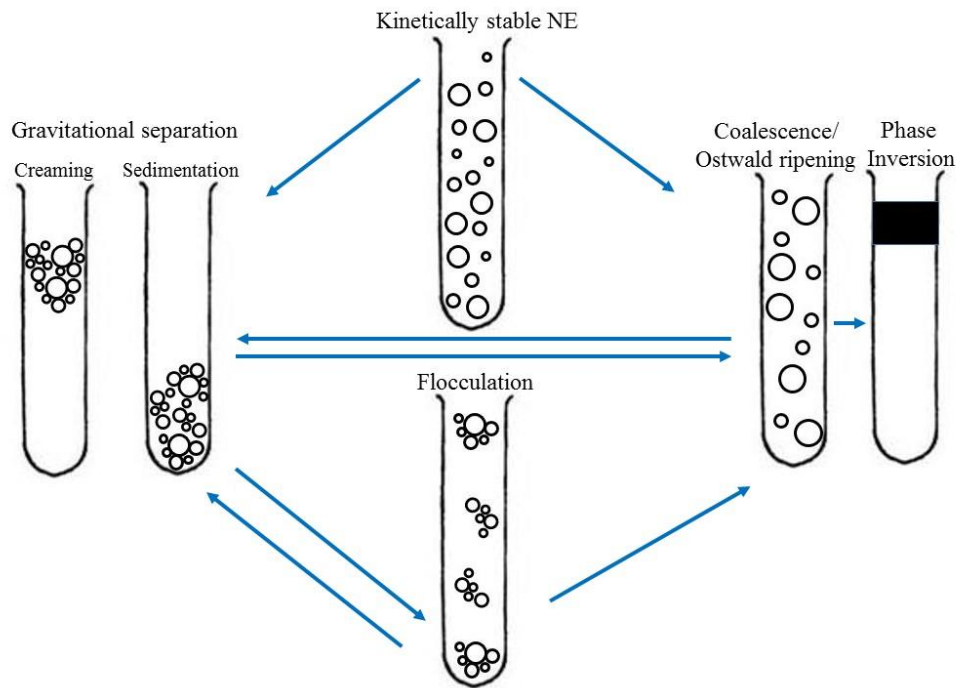


Figure 2.1.4 Destabilization mechanisms in NEs (adapted from Rao & McClements, 2011).

Gravitational separation: Gravitational separation is the process in which the two immiscible phases with different densities tend to separate under the influence of gravity (McClements, 2007). In the case of O/W emulsion, where the droplet density is less than that of the continuous phase, creaming takes place. Whereas, in W/O emulsions droplet density is more than that of the continuous phase and sedimentation takes place. The rate of creaming/sedimentation is measured by Stokes' law, which states that a particle moving at a constant velocity through surrounding liquid will have an opposing hydrodynamic frictional force equal to the gravitational force acting on it. The velocity of creaming of an isolated spherical particle in an emulsion can be determined by Stokes' formula (eq. 2.2):

$$V_d = \frac{2g\Delta\rho r^2}{9\eta} \quad (\text{eq. 2.2})$$

where ' V_d ' is the velocity of the droplet, ' $\Delta\rho$ ' is the density difference of the two phases in the emulsion, ' r ' is the radius of the droplet, ' η ' is the viscosity of the surrounding continuous phase and ' g ' is the acceleration due to gravity. From equation 2.2, we can deduce that the rate of creaming in an O/W emulsion can be reduced by decreasing the droplet size and increasing the continuous phase viscosity.

Studies have showed that, if the particle radius falls below the range of 70 nm for a NE, creaming is not observed (McClements, 2005). These small particles are not influenced by gravitational forces and display movement due to Brownian motion which are associated with the thermal energy of the system. Consequently, particle movement is dominated by gravity for the relatively large particles in emulsions, but dominated by Brownian motion for relatively small particles like those in some NEs. Therefore, in the case of NEs gravitational separation is mostly not considered as a major destabilization mechanism.

Flocculation: It is the process where two or more droplets associate with each other, without losing their individual identity (McClements, 2005). It tends to occur when the attractive forces between two or more droplets dominate the repulsive forces (electrostatic). Hence, the rate of flocculation depends on the nature and degree of colloidal interactions (McClements, 2007). It can be prevented by inducing electrostatic or steric repulsion among the droplets. As a result of flocculation, the overall size of the droplet aggregates increase which in turn increases the creaming (McClements, 2005).

Coalescence: It is the process in which two or more droplets merge together to form a larger droplet (McClements, 2005). The rate of creaming or sedimentation of an emulsion increases rapidly with coalescence. In coalescence, inter-droplet film is ruptured when the droplets encounter each other. Hence, the rate of coalescence also depends on the degree and nature of inter-droplet interactions (McClements, 2007). NEs have much better stability to both flocculation and coalescence than conventional emulsions because of the influence of their small particle size on colloidal interactions. Also, due to the high Laplace pressure (equation 2.1) of these nanodroplets, it is difficult to break them apart (Tadros et al., 2004).

Ostwald ripening: In Ostwald ripening (OR) mass transport of the molecules of dispersed phase droplets occurs from smaller droplets to larger droplets, increasing the size of larger droplets at the expense of smaller ones (McClements, 2007). As a result of this phenomenon, larger droplets tend to grow in size at the expense of smaller droplets. As the size of the droplet decreases, the solubility of the material increases with increasing Laplace pressure. In a NE, the small sized droplets possess very high Laplace pressure (equation 2.1) which leads to an increased level of solubility. Hence, these small droplets tend to give material to the largest one through mass transfer across the continuous phase. Therefore, OR depends on the solubility and diffusion of the dispersed

phase molecules in the aqueous phase (Weiss & McClements, 2000). Hence, the main factor determining the stability of a NE to OR is the water-solubility of the oil phase.

The effect of OR could be negligible if the oil (TAGs with long-chain fatty acids) and the aqueous phases are insoluble in the NE. However, if the NEs are prepared by flavor oils, essential oils or TAGs with short-chain and medium-chain fatty acids, they are more susceptible to OR because of higher levels of solubility in aqueous phase. In such cases, OR can be inhibited by proper selection of oil that is insoluble in the aqueous phase (e.g., TAGs with long-chain fatty acids, like vegetable oils) (Tadros et al., 2004). Ripening inhibitors (e.g., polyvinyl alcohol) are also used which reduces the solubility of dispersed phase molecules in the continuous phase (Chang et al., 2012).

Phase inversion: Phase inversion is the process whereby an O/W emulsions changes in W/O emulsion or vice versa. This could happen due to alteration in the conditions of an emulsion like, change in dispersed phase volume fraction, change emulsifier type or concentration, change in temperature or mechanical agitation (McClements, 2005). This is desirable and important in the manufacture of certain food products like butter and margarine. Or otherwise, it is an undesirable phenomenon and causes undesirable changes in the texture, appearance, stability and taste of the product.

2.1.6 Applications of nanoemulsions

NEs have current applications in the field of food and beverage industry. These are highly stable when compared to conventional emulsions which make them easier to incorporate into a wide variety of food applications (Silva et al., 2012). These are significantly less turbid or translucent compared to conventional emulsions with similar dispersed phase concentrations. This property of NEs makes them suitable for incorporation into products like fortified soft drinks and water, soups, sauces and dips (Mason et al., 2006; Velikov & Pelan, 2008; Wooster et al., 2008).

NEs hold great promise for use in food application due to their stability and flow behavior ranging from liquid to viscoelastic gels at a lower oil phase volume fraction compared to conventional emulsions (Mason et al., 2006; Tadros et al., 2004). This property of NE may be desirable for producing reduced fat products that need to be highly viscous or gel like including products like cheese, mayonnaise and yogurt. The ability of NEs to encapsulate lipophilic

functional components, such as vitamins, flavors, colors, antioxidants, preservatives, and nutraceuticals have been finding an important application in food and beverage industry (Graves & Mason, 2008). Smaller droplets in NEs have large surface-to-volume ratio that promote higher release of bioactive compounds in the gut. Studies have shown that the bioavailability of bioactive components encapsulated in NEs was higher making them more preferable over the conventional emulsions (Acosta, 2009). This property of NEs is explored in nutraceutical and pharmacological applications.

2.2 Protein stabilized nanoemulsions

2.2.1 Proteins as emulsifiers

Proteins have been widely used as emulsifiers to facilitate the formation of emulsions. They are said to provide desirable physicochemical properties which are important for improving the stability of emulsions. Proteins are amphiphilic in nature. The interfacial activity of proteins is because of the hydrophilic and hydrophobic groups distributed in their structure. The major driving force for adsorption of these amphiphilic groups at the oil-water interface is the non-polar hydrophobic interactions (Damodaran, 2007). Hydrophobic interactions act between two non-polar surfaces dispersed in water which force them to aggregate in order to minimize the unfavorable interactions between their surfaces in water. When a protein molecule is dispersed in an aqueous phase, the non-polar groups present in the protein orient towards water, which is thermodynamically unfavorable because of these hydrophobic interactions. Hence, at the interface the protein molecule tries to adapt a conformation by undergoing structural rearrangements, where the non-polar groups are in the oil phase and the polar groups are in aqueous phase (thermodynamically favorable situation). It is also well known that proteins facilitate droplet disruption by lowering the interfacial tension (Walstra, 2002). The contact area between the oil and water molecules at the interface is reduced because of adsorption of proteins, and this eventually reduces the interfacial tension. Therefore, hydrophobic interactions and reduced interfacial tensions favor the adsorption of protein at the oil-water interface.

Proteins generate repulsive interactions (steric and electrostatic) between the oil droplets and form a thick interfacial membrane that is resistant to rupture. This membrane acts as a protective coating and retards droplet coalescence and flocculation, thus stabilizing emulsions

(Walstra, 2002). Random-coil (e.g., napin), flexible proteins (e.g., casein) adopt an arrangement where the nonpolar segments protrude into the oil phase and polar segments into the aqueous phase and the neutral regions lie flat at the interface. The membranes formed by this type of molecules tend to be relatively open and thick. Globular proteins (e.g. soy protein, whey protein) adsorb at the interface such that the nonpolar amino acids face the oil phase and the polar amino acids face the aqueous phase, and the protein molecule tends to have an orientation at the interface. It was found that flexible proteins that have a disordered structure are most surface-active compared to the globular proteins that required to be unfolded before adsorption to the interface (Dickinson & McClements, 1995). In both the cases, these proteins form a viscoelastic film at the interface. These membranes are usually electrically charged, and major mechanism that prevents destabilization of protein stabilized emulsions is electrostatic repulsion. Consequently, protein stabilized emulsions are sensitive to pH and ionic strength. They flocculate at pH values closer to the isoelectric point (point where the net charge carried by the protein is zero) of the adsorbed protein (Dickinson & McClements, 1995). Proteins also increase the viscosity of the continuous phase, which contributes to emulsion stability by decreasing the rate of droplets movement (Sikorski, 2001).

In general, the stability of protein-stabilized NE depends on the following factors: protein characteristics (source, concentration, type of extraction, solubility, groups present etc.), environmental conditions (temperature, pH, ionic strength etc.), and oil-phase to aqueous phase concentration, emulsions droplet properties, emulsion viscosity, type and time of homogenization (McClements, 2005). For a protein to be an effective emulsifier, it should be able to readily adsorb to the oil-water interface, unfold at the interface and be able to form a cohesive film around the oil droplet and thus stabilize the emulsion (Damodaran, 2007).

It was observed that proteins take longer time to move to the interface and stabilize the emulsion when compared to the small-molecule surfactants because of their large molecular size (Rao & McClements, 2012). Therefore, the formation of smaller droplets for a protein stabilized NE will be limited. Larger quantities of protein are required by a NE because the droplet surface needs to be fully covered by the protein to prevent aggregation. Here, the free and unabsorbed protein might interact with each other to form flocs of proteins. This phenomenon is known as depletion flocculation (Dickinson & McClements, 1995). On long term basis, proteins can form a cross-linked and close packed network at the oil-water interface and hence create a stable NE (Rao & McClements, 2012).

2.2.2 Protein sources

Animal proteins: A wide range of animal based proteins are incorporated into food emulsions as stabilizers. Proteins isolated from bovine milk are widely used as emulsifying agents in a variety of food products including beverages, frozen desserts, ice creams, sports supplements, infant formula, salad dressings etc. (McClements, 2005). Milk proteins are divided into two major categories: caseins (~80 wt %) and whey proteins (~20 wt %). There are four main protein fractions in casein: α_{s1} (~44 %), α_{s2} (~11 %), β (~32 %), and κ (~11 %). Whey protein contains β -lactoglobulin (~55 %), α -lactalbumin (~24%), serum albumin (~5%), and immunoglobulins (15%) (Aleandri et al., 1968).

Plant proteins: The application of plant proteins as emulsifiers in food and bioproduct systems is less well understood compared to more widely used animal proteins due to their ease in production, availability and acceptability. However, there has been a growing interest towards utilization of these proteins as substitutes for animal-based proteins in new product formulations (Can Karaca et al., 2011a). Functional properties of these proteins provide suitable emulsifying properties for the preparation of food emulsions and also offer the advantage of using natural products together with the health-beneficial properties of the proteins themselves. These are an important sources of proteins, with essential amino acids (Duranti, 2006). Plant proteins could be classified as cereal proteins (wheat, rye, barley, oats, corn, sorghum etc.), legume proteins (peas, faba beans, lentils, chick pea etc.) and oilseed proteins (canola, sunflower etc.). However, some of the examples stated could fall into more than one of the categories stated above. Like soybean and peanut could be both oilseed and legume protein.

The foaming and emulsifying properties of gluten protein from wheat has been studied (Linares et al., 2000). Legume proteins have been finding more importance recently due to their nutritional value, easy availability, low cost and beneficial health effects (Duranti, 2006). In addition to that nowadays these are used as animal protein substitutes which could lead to new types of novel foods with improved nutritional value, texture, and shelf life (Tsoukala et al., 2006). For instance, instead of egg yolk in mayonnaise, alternative, vegetable emulsifiers are said to contribute to decreasing cholesterol and fat contents as well as increasing microbiological stability (Donsi et al., 2010). Proteins from several legumes such as beans, chickpea, faba bean, lentil, pea, cow pea and lupine have been investigated for emulsifying properties.

Out of all the plant proteins used to stabilize emulsions, soy is most widely applied and accepted (McClements, 2005). Pulse proteins include pea, chickpea, beans and lentils. These are dominated by salt-soluble globulin protein (legumin and vicilin) and water-soluble albumin protein. The globulin proteins contain two major protein components the legumin (11S) and the vicilin (7S). Legumin (Iso-electric point, pI: 4.8 and molecular weight, MW: 300-400 kDa) is a hexamer and consists of acidic and basic amino acid groups, linked by disulfide bridges. Vicilin is a trimer with its iso-electric point, pI at 5.5, and MW 150-180 kDa (Damodaran, 2007). The ratios of globulins to albumins and legumin to vicilin affect the emulsifying property of pulse proteins. For example purified vicilin pea protein had higher emulsifying index when compared to pure legumin component (Dagorn Scaviner et al., 1987).

2.2.3 Emulsions stabilized with multiple components

Proteins, polysaccharides or a combination of these two are often used in the food industry not only for the development of emulsions but also for a wide range of other products (microencapsulants, coacervates etc.) (Ye, 2008). Apart from these, small molecule surfactants are also used as emulsifier along with these components. When there is more than one component present at the oil droplet interface, often it leads to either competitive or co-operative adsorption that usually depends on surface hydrophobicity, interfacial tension, size and mobility of these components during emulsification (Chen & Dickinson, 1995; Liu et al., 2007; Ye, 2008). Competitive adsorption is when the components competes to get to the interface thereby replacing the one already present at the interface. This could happen due to the lowering of interfacial tension and bringing in more thermodynamic stability by the process of replacement (Dickinson et al., 1989). For example, it has been well documented that addition of small molecule emulsifiers (e.g., Tweens) would completely replace proteins from oil droplet surface (Morris & Gunning, 2008). Co-operative adsorption, on the other hand, is the simultaneous presence of both components at the interface thereby enhancing the stability of the emulsions. This is more the case when there are polysaccharides present in combination with proteins as emulsifiers (Dickinson, 1992a, 1994). In such case, although, proteins are primarily adsorbed onto the oil-water interface, polysaccharides form a secondary layer, thereby stabilizing the droplet through steric interactions (Dickinson et al., 1988, 1989).

When there is more than one protein present to stabilize emulsion it could be any combination of dairy and plant-based proteins. Using a combination of two dairy protein is far more prevalent and well-studied (Dickinson et al., 1988, 1989). A combination of the casein and whey protein and their components has been well documented (Dickinson, 1986; Dickinson et al., 1988, 1989). However, combination of dairy protein with plant-based protein has not been studied in detailed. Kuhn et al. (2014) are the only group that assessed the potential of flax seed protein (a plant based protein) in combination with whey protein isolate (a dairy protein) in the development of emulsions. If both the proteins were present in equal ratios or flax seed in higher quantities, the emulsions consequently destabilized due to depletion and led to creaming. The authors found that a stable emulsion system was developed when lower ratio of flax seed protein (0.14% w/v) was used in combination with whey protein isolate (3% w/v) (Kuhn et al., 2014). However, the reason for stability or the mechanism through which the mixed system was stabilized was not discussed.

2.2.4 Proteins as nanoemulsion stabilizer

In preparing NEs, the choice of emulsifier plays a very important role because both, a high interface adsorption rate and a high interfacial area are required to stabilize the nanosized droplets. These properties are readily available for food-grade artificial emulsifiers, whereas for most proteins, significant pre-treatment is necessary in order to utilize them in emulsions (Damodaran, 1996). Hence, it is relatively difficult to prepare and stabilize NEs with proteins as stabilizers. Nevertheless, protein modifications before utilizing them as emulsifiers may enhance the stability of the resulting emulsions. For example, lentil protein dispersed at a pH of 3.0 had much higher emulsifying activity index ($\sim 130.2 \text{ m}^2/\text{g}$) than that dispersed at pH 5.0 ($\sim 6.1 \text{ m}^2/\text{g}$) (Joshi et al., 2012). Enzymatic modifying pea protein with papain was also observed to improve the emulsifying index (Barac et al., 2010).

He et al (2011) studied the effects of pH, ionic strength, thermal treatment, freeze-thaw stability on whey protein stabilized O/W NE and compared that with conventional emulsions. It was observed that NE was more stable to droplet aggregation and creaming over the conventional emulsion. In addition, the NE (at pH 7) was stable to salt addition, thermal treatment, and freezing/thawing (He et al., 2011a). Over the last few years, proteins have been studied for incorporation into NEs as emulsifiers for certain additional benefits as compared to the small

molecule surfactants in delivery of hydrophobic drugs (McClements, 2012). NEs stabilized by traditional emulsifiers raise toxicological concerns for long-term treatment, while food proteins are generally considered as safer alternatives as NE (He et al., 2011a).

2.3 Encapsulation and release of bio-active ingredients from emulsions

2.3.1 Encapsulation

Encapsulation is the technique by which one material or a mixture of materials is coated with or entrapped within another material or system. The coated material is called active or core material, and the coating material is called shell, wall material, carrier or encapsulant (Madene et al., 2006). Encapsulation technology is one of the most widely accepted technologies within the pharmaceutical, chemical, cosmetic, food and printing industries. In food industries, a variety of products including fats, oils, aroma compounds, oleoresins, vitamins, minerals, colorants, enzymes and probiotics are being encapsulated (Madene et al., 2006). Encapsulation of these ingredients has various advantages; it retains the aroma of the ingredient in foods during storage, protects the ingredient from undesirable interactions with food, minimizes ingredient-interactions, guards against light-induced reactions and/or oxidation, allow a controlled release of these ingredients, masks unpleasant feelings during eating, such as bitter taste and astringency (Baldwin et al., 2011).

Wall materials used for encapsulation: A variety of materials are used to coat or encapsulate substances. However, there are regulations that are set by certain governmental agencies (e.g., European Food Safety Authority (EFSA) or Food and Drug Administration (FDA) in the USA) on the type and kind of materials that could be used for this purpose. These should be certified for food applications as “generally recognized as safe” (GRAS) (Madene et al., 2006). It should be capable of forming a barrier between the internal phase and the surrounding environment thereby preventing the core materials from any possible light or oxidation reactions (Nedovic et al., 2011). The most widely used and accepted wall material for encapsulation in food industry are polysaccharides. Commonly used materials include starches, maltodextrins, polydextrose, gum Arabic, pectins, carrageenans and alginate (Nedovic et al., 2011). Proteins are also used as encapsulation materials, especially when they act as emulsion stabilizers where lipophilic active compounds are trapped inside the oil droplets of O/W emulsions (Gibbs et al., 1999).

Bioactive ingredients for encapsulation: Bioactive compounds are compounds that occur in nature, as a part of the food chain, and are shown to have beneficial effect on human health (Biesalski et al., 2009). Some of the examples include antioxidants (e.g., Butylated hydroxyanisole or BHA, Butylated hydroxytoluene or BHT), minerals, vitamins, phytosterols, fatty acids, plant polyphenols (e.g., curcumin, resveratrol, epigallocatechin gallate) and carotenoids (e.g., lycopene, β -carotene, lutein, zeaxanthin) (Biesalski et al., 2009).

The general increase in dietary-intake-related illnesses such as cardiovascular diseases, hypertension, diabetes and cancer in recent years led to the development of health-and-wellness promoting foods commonly called functional foods (Biesalski et al., 2009). However incorporation of most of these components into food matrices is complicated, due to their low solubility in water. This may also lead to lower absorption in the GI track and therefore limited bioavailability. The term bioavailability refers to the fraction of an ingested component that enters into or absorbed in the bloodstream (Holst & Williamson, 2008). Another problem associated with these compounds is that they undergo degradation when exposed to the environment once extracted from plant tissues (Velikov & Pelan, 2008). Hence, consistent efforts have been invested by the food industry to develop edible and efficient delivery systems to encapsulate these bioactive ingredients with improved solubility, stability and bioavailability.

Curcumin is a bioactive compound that has been drawing considerable interest by researchers, due to its numerous health benefits (for example, anti-tumor, anti-carcinogenic, anti-inflammatory properties) (Wang et al., 2007). Derived from the dietary spice, turmeric (*Curcuma longa*), it has long been used in curing many health ailments in Asian countries (Anand et al., 2007; Biesalski et al., 2009). However, its poor water solubility makes it challenging to incorporate into foods (Anand et al., 2007). Among the numerous systems, emulsions and nanoemulsions have been investigated and proven in being efficient in delivering curcumin (Ahmed et al., 2012; Wang et al., 2008). Due its better solubility in oil, when compared to water, oil-in-water emulsions have been utilized to encapsulate and consequently deliver curcumin for improved bioavailability (Ahmed et al., 2012).

2.3.2 Emulsification for encapsulation of bioactive ingredients

A number of techniques are employed for encapsulation of food compounds, including spray-drying, fluid bed coating, spray-cooling/ spray-chilling, melt injection and melt extrusion, coacervation, co-extrusion, freeze-drying/ vacuum drying and emulsification (Madene et al., 2006). Emulsification is one of the widely used techniques for the encapsulation where the encapsulation matrix are stabilized through different physicochemical phenomenon of emulsion itself. (McClements, 2007). Presence of both hydrophilic and lipophilic phases in emulsion makes it easy to incorporate a wide variety of bioactive components within the same delivery system that could be either lipophilic, hydrophilic or amphiphilic (Coupland & McClements, 1996). There is always this flexibility that exists in using emulsions either in wet form or in dry powdered form (spray dried) that makes them convenient in an industrial scale point of view. Another advantage of using emulsion as delivery systems is that they could be created from entirely food-grade ingredients (water, oil, and protein/polysaccharide emulsifier) using simple processing operations (like blending or homogenization). The human body has enzymes (lipases and pepsins) to digest the lipid phase and interfacial proteins in a protein-stabilized emulsion which enhances the bioavailability of the bioactive ingredients from emulsion-based delivery systems (McClements, 2007). High surface area of oil droplets makes it even better for enzyme attack and release of bioactive components in the small intestine of human gastrointestinal (GI) tract.

Encapsulation of bioactives in nanoemulsions: Encapsulation of bioactive ingredients in NE is an effective approach for their delivery in food (McClements, 2007). NEs based delivery systems have been proved to be efficient enough to carry the bioactive ingredients into the human GI tract and also said to increase their bioavailability when compared to the conventional emulsions. The delivery of any bioactive component through NEs was observed to be more efficient compared to conventional emulsions, due to a larger surface area for interaction with the biological substrates i.e., the epithelial cells (Acosta, 2009). Especially in carrying poorly water-soluble bioactives such as curcumin, resveratrol, O/W NEs have been proven quite efficient (Huang et al., 2010; Lin et al., 2011). It was found that the extremely small droplet size aided in the transportation of dibenzoylmethane (DBM, a phytochemical with anti-cancer activities, found in licorice root) through the cell membranes much more efficiently than the conventional counterparts (Huang et al., 2010). As a result, it can be concluded that there is an increased

concentration of the bioactive in the plasma leading to enhanced bioavailability of bioactives when delivered through NEs.

2.4 Bioavailability and in-vitro digestion of nanoemulsions

2.4.1 Bioavailability and Bioaccessibility:

Bioavailability: It refers to that fraction of ingested components that enters into or absorbed in the bloodstream (Holst & Williamson, 2008). On the other hand, uptake refers to the fraction of ingested component that is absorbed through the intestinal walls. Although these two phenomena can be related, a bioactive compound that is absorbed through the intestine may not be bioavailable, due to the complexity of the biological mechanisms involved in the digestion of nutrients (Acosta, 2009). The overall bioavailability of an encapsulated lipophilic component (F) depends on a number of physicochemical and physiological factors:

$$F = F_A \times F_B \times F_M \quad (\text{eq. 2.3})$$

Where, F_A is the fraction of lipophilic component released from the delivery system into the GI tract to become bioaccessible, F_B is the fraction of the released component that is absorbed across the intestinal epithelial cells and F_M is the fraction of the absorbed component without being metabolized (Ahmed et al., 2012). The overall bioavailability of bioactives is dependent on the characteristics of the NEs including droplet size, charge, type of oil, and interfacial composition (Acosta, 2009; Ahmed et al., 2012)

Bioaccessibility: It is a term that is more often associated with bioavailability. Bioaccessibility is defined as that fraction of a compound released from its encapsulation matrix into the GI tract and thus becomes available for intestinal absorption to enter into the blood stream (Fernández-García et al., 2009). Consequently, bioavailability is a fraction of bioaccessibility that has entered into the blood stream after absorption.

2.4.2 Digestion within the human GI tract

To understand the bioavailability and uptake of a component encapsulated in an emulsion, it is important to understand the basic physicochemical and physiological processes behind human digestion and in particular the process of digestion of emulsified lipids within the human GI tract. The ingested food undergoes a set of complex physical and chemical changes as it passes through

the mouth, stomach, small and large intestines which affect its ability to digest or absorb through the intestinal wall (Acosta, 2009) (Figure 2.4.1)

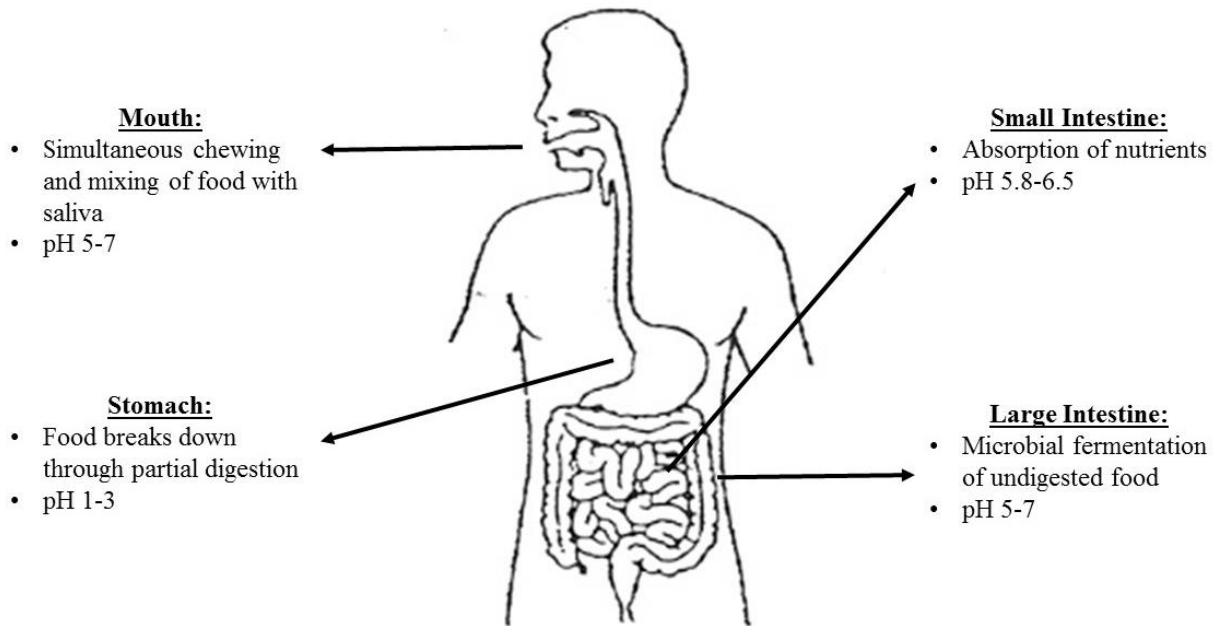


Figure 2.4.1 The process of digestion in different sections of human gastrointestinal tract (picture adapted from www.catalog.niddk.nih.gov).

Mouth: The process of digestion begins in the mouth. Here food is mixed with saliva and broken down into smaller pieces by mastication. Human saliva is usually around pH 5.5 - 6.1 during fasting and around pH 7 to 8 after food ingestion. It contains about 99% water, less than 1% minerals and 0.1 - 0.2% enzymes (amylase, lingual lipase) (Guerra et al., 2012). The masticated material that gets into the stomach through esophagus is known as “bolus” (Stipanuk & Caudill, 2013).

Stomach: Once the bolus reaches the stomach it is subjected to acidic digestive juices (pH 1 - 3) containing proteases, phospholipids, gastric lipases and proteases. It is also exposed to shear stress and mixing action due to contractions of the stomach (Stipanuk & Caudill, 2013). Although gastric lipase is present in the stomach to break down the triglycerols into diglycerols, monoglycerols and free fatty acids, most of the lipid digestion occurs in small intestine. Proteases present in stomach initiate protein digestion. The partially digested food from the stomach called “chyme” enters the small intestine (McClements & Li, 2010b).

Small Intestine: It is the region where most of the digestion and absorption takes place. It mainly comprises of three regions: duodenum, jejunum, and ileum. The chyme is mixed with sodium bicarbonate, bile salts, phospholipids and enzymes secreted by the liver pancreas and gall bladder. Bile salts are bile acids compounded with a cation, usually sodium. In human taurocholic acid, glycocholic acid and taurochenodeoxycholic acid and glycochenodeoxycholic acid represent approximately 80% of all bile acids (Hu et al., 2009). The pH of small intestine ranges between 5.8 - 6.5. This increase in pH compared to stomach is due to the presence of sodium bicarbonate in intestine. The products of digestion are transported through the mucous layer to the enterocyte cell (enterocytes, or intestinal absorptive cells, are epithelial cells found in the small intestine) where they are absorbed (Ahmed et al., 2012). Absorption through the intestinal walls occurs via paracellular mechanism where extremely small nanoparticles pass through the narrow gaps separating the epithelial cells; and transcellular mechanism where nanoparticles are absorbed directly through the epithelial cell membranes (McClements & Li, 2010b; Sahay et al., 2010). Once these nanoparticles are absorbed, they may be transported directly into the blood/lymph system or they may accumulate within specific location in the cell itself (Hu et al., 2009).

Large intestine: The material that remains unabsorbed within the small intestine moves to the large intestine, also known as colon. The pH of large intestine usually ranges between 5-7. Normally lipids are fully digested in the small intestine (Stipanuk & Caudill, 2013) and here water, electrolytes and bile salts (if present) are absorbed. Further, fermentation of undigested polysaccharides and proteins takes place by colonic microbiota. There by, formation, storage and elimination of feces out of the body through rectum and anus (Guerra et al., 2012; Stipanuk & Caudill, 2013).

2.4.3 *In vitro* digestion

In vitro (meaning glass in Latin) are studies in experimental biology that are conducted using components of an organism that have been isolated from their usual biological surroundings in order to permit a more detailed or convenient analysis. *In vivo* experiments are conducted with living organisms in their normal intact state, and *ex vivo* are studies conducted on functional organs that have been removed from an intact organism (refers to functional organs from experimental species that is intact to mimic the human systems) (Stipanuk & Caudill, 2013).

In vitro studies however aid in understanding the bioaccessibility rather than bioavailability which is accurately understood through *in vivo* studies. In a study carried out by Li and co-workers (Li et al., 2012), it has been shown that results from *in vitro* studies were qualitatively similar when compared to *in vivo* studies. Thus it can be hypothesized that an improved bioaccessibility is an indication of improved bioavailability of bioactives.

2.4.3.1 *In vitro* digestion models for emulsions

In vitro digestion models for emulsified lipids can be classified as: 1) single-step models where one particular region of the GI tract is simulated, e.g., the mouth, stomach, small intestine or colon, and 2) multiple step models, where two or more regions of the GI tract are simulated (Figure 2.4.2). All the samples and solutions for *in vitro* digestion studies are maintained at 37°C to mimic human body temperature. The samples to be tested are usually mixed with simulated digestive fluids employing controlled agitation (McClements & Li, 2010b). To accurately mimic the human GI conditions, it is important to understand the fluids that are secreted in each component and their physicochemical interactions with the sample.

Mouth: The emulsion sample to be tested is mixed with a simulated saliva fluid (SSF) under conditions mimicking the mouth (under controlled temperature, pH and shear). The composition of the SSF used in various research studies ranges from simple buffer solution at pH 7 to mimicking oral conditions using biopolymers, enzymes, and other materials (Hur et al., 2009).

Stomach: The key factors for stomach are the high acidic conditions, specific activity of enzymes and mechanical flow. The simulated gastric juice (SGJ) used for this experiments may contain, pH buffer, pepsin, lipase or other minerals depending on the complexity of the model incorporated (Hur et al., 2009).

Small Intestine: Here, the sample moves from highly acidic conditions in the stomach to a near neutral condition. Many physicochemical phenomena that attribute to lipid digestion and absorption of bioactives take place in this step. The simulated small intestine juice (SIJ) is a mixture of pancreatic lipases, bile salts, phospholipids, various enzymes, salts and co-enzymes (McClements & Li, 2010b; Stipanuk & Caudill, 2013).

Colon: This is considered as one of the most difficult regions to mimic because of the difficulty involved in understanding the type and variety of bacteria present in the colon. Incubating

them to produce simulated colonic juice (SCJ) is one of the most difficult tasks of in-vitro digestion studies (McClements & Li, 2010b).

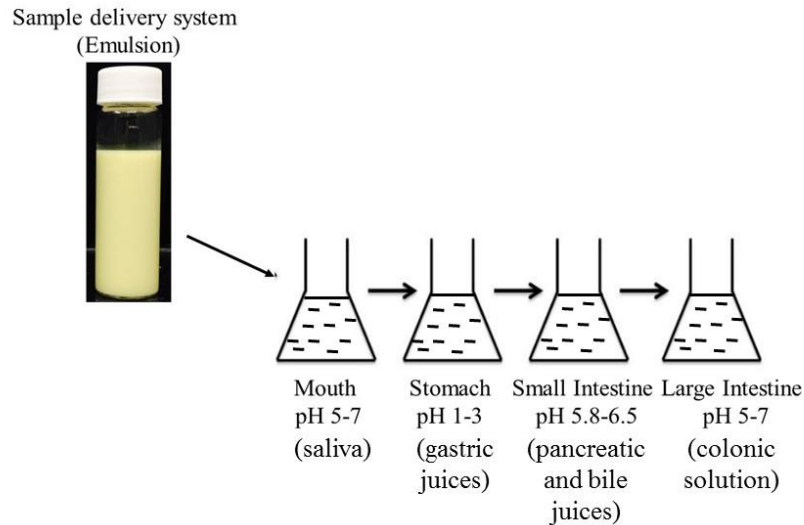


Figure 2.4.2 Schematic representation of multiple step *in vitro* digestion model.

2.4.3.2 Physicochemical parameters measured in digestion studies

Enzyme activity: Lipases, phospholipases, proteases, amylases and glycosidases are few of the prominent enzymes that are active in different locations of the human GI tract (Hur et al., 2009).

Lipases: The rate of lipid digestion due to lipase activity is measured by estimating the conversion of triacylglycerols (TAG) and diacylglycerols (DAG) to monoacylglycerols (MAG) and free fatty acids (FFA). Simple acid/base titration is carried out with standard alkali solution and the quantity of MAG and FFA are determined to understand the extent of digestion.

Proteases: If the emulsion is stabilized by proteins, their rate of digestion should also be monitored. Digestion of interfacial proteins involves exposing the oil droplets and the lipophilic bioactive components present inside them. Protease conversion of proteins into amino acids and peptides is generally monitored by employing chromatography (HPLC) or electrophoresis (SDS-PAGE) techniques (Hur et al., 2009; McClements, 2007).

Particle size distribution and microstructure: The rate of lipid digestion depends on the size of the oil droplets present in an emulsion. This also governs the amount of bioactive ingredient that encapsulated in the oil phase, which underwent digestion. The oil droplets size may change as emulsion passes through different regions of the GI tract. In general, particle size distribution

(PSD) of oil droplets from *in vitro* digestion studies can be determined using static or dynamic light scattering technique (McClements, 2007). It should be noted that, no particle size measurement technique is accurate for digestion systems. This is because, the light scattering responsible for producing the distribution of the emulsions comes not only from the droplets, but also from enzymes and salts present in the simulated digestive mixture, which take part in digestion process. To understand the accurate change in droplet size, all the other particles (other than droplets) should be filtered out. However, this requires further understanding and research about the size and nature of these enzymes.

Optical microscopy techniques could also be incorporated to study the size of the droplets up to a certain level. At nano level, electron microscopy like the transmission electron microscope (TEM) or the scanning electron microscope (SEM) could be used. Specific fluorescent dyes can also be used to highlight particular components (e.g., oil soluble dye or protein stain) to determine their presence and location using confocal microscopy (McClements & Li, 2010a).

Release of lipophilic components: Determination of release of bioactive components encapsulated within an emulsion is one of the most important aspects of in-vitro digestion studies. The digested sample is centrifuged separating into different layers. The pellet at the bottom of the centrifuge tube contains dense insoluble matter, an aqueous phase in the middle contains lipid digestion products (FFA, MAG) and lipophilic bioactive components bound in micelles, and the top cream layer contains undigested lipid phase. These layers could be separated and analyzed using various techniques, namely, chromatography and spectroscopy to determine the amount of bioactive compounds that has been released (Porter & Charman, 2001). It has been proposed that *in vitro* release of these components could not provide a real estimation of bioavailability, rather the fraction of a component released after digestion should be taken as a measure of its bioaccessibility (McClements, 2007).

2.4.3.3 Determination of bioavailability of bioactive components

The absorption and bioavailability of encapsulated lipophilic bioactive components within an emulsion can be assessed using different ways (McClements & Li, 2010a)

Physical method: This method assumes that the amount of digested product released from the sample is the amount that absorbed by the epithelium cells of the small intestine wall (Porter & Charman, 2001). However, as mentioned before this is actually the measure of bioaccessibility.

Ex-vivo permeation method: In this method a section of GI tract is cut from an animal (e.g., rats, pigs, guinea pig etc.) after it has been sacrificed. After cleaning part of the intestine is clamped between two chambers; one chamber contains the sample to be analyzed and the other contains buffer solution. The transport of sample across the chamber is measured analytically using chromatography or spectroscopy (Dahan & Hoffman, 2007).

Cell culture methods: Caco-2 are cell cultures that mimic the human intestinal epithelium (Donsì et al., 2010). Alternatively, the amount of digestion products absorbed by the cell can be determined employing chromatography or spectroscopic studies (Dhuique Mayer et al., 2007).

2.4.4 Scope of nanoemulsions as delivery vehicle

The main driving force in creating emulsions based encapsulation matrices is to increase the bioavailability of the encapsulated bioactive components. Hence, a thorough understanding of the digestion and release behavior of these systems in the human GI tract is a pre-requisite (Ahmed et al., 2012). Moreover, improvisation of emulsions to nano-scale was shown to have enhanced absorbance of encapsulated components in the human GI tract. The application of NEs in delivering bioactives made considerable advances through the past decade, owing to the increased demand of functional foods containing bioactive compounds to prevent ailments like heart diseases, diabetes, cancer, hypertension etc. (Acosta, 2009). Studies carried out by Patel and Sawant indicated enhanced bioavailability and uptake of lipophilic drug (acyclovir, an anti-viral agent utilized in the treatment of Herpes Simplex Virus infections), in NE than in conventional emulsion (Patel & Sawant, 2007). In contrast, Ahmed & co-workers found that the bioavailability of curcumin was fairly similar in both NEs (droplet diameter < 100 nm) and conventional emulsions (droplet diameter > 10 µm) systems (Ahmed et al., 2012). Nevertheless, as lipid digestion in case of O/W emulsion systems occurs at the oil droplet interface, rate of lipid digestion increases with a decrease in droplet size owing to the increase in surface area of the lipid exposed to digestive enzymes (Acosta, 2009; McClements & Li, 2010a). Therefore in NEs, digestion should happen rapidly and to a greater extent compared to conventional emulsions leading to a higher

bioavailability of the bioactives. However, this may not be true in case of protein stabilized NEs. Protein stabilized NEs have a relatively thicker interfacial layer compared to the other emulsifier stabilized NEs, which may hinder the digestive enzymes from reaching the inner lipid core. This results in lower rate of digestion and consequently lesser bioavailability than the conventional systems (Acosta, 2009; McClements & Li, 2010a). Nevertheless potential toxicity of food grade NEs is also an aspect to be considered while inspecting their prospective applications in the food. At present, there is no standard testing protocol for measuring NEs extent of toxicity in food products (Bouwmeester et al., 2009; Maynard et al., 2006). When remained undigested, the nanoparticles can even cross the epithelium cell layer present in the human GI tract and might get circulated throughout the body for absorption and deposition. If the emulsion is made up of synthetic or non-food grade ingredients this could also cause substantial harm to the body. Hence, it is very important to develop NEs with completely food grade ingredients (McClements & Li, 2010a).

There is a growing interest within the food industry to develop foods with improved functionality. In this regards, application of emulsion-based delivery systems especially, NE to encapsulate and deliver bioactive components has been of prime interest. In the present research the goal is to develop a NE-based delivery system encapsulating a bioactive component, curcumin. The NE for this research were developed using a mixture of dairy and pulse proteins as emulsifiers. Usage of pulse protein not only is a value addition to the pulse crops, but also removes the potential threats caused by non-food grade emulsifiers in typically used in NE systems. The efficacy of the dual protein-stabilized NE as a delivery vehicle for curcumin will also be assessed via *in vitro* digestion studies where bioaccessibility of curcumin encapsulated in the NEs will be determined.

2.5 Choice of materials

2.5.1 Emulsifier

Food markets are now shifting away from the widely used animal based proteins toward alternative sources of plant-based proteins, (Adebiyi & Aluko, 2011). This could be attributed to various reasons; perceived fears about consuming animal-derived products, dietary choices based on religious or moral preferences, allergenicity, and genetic modification (Can Karaca et al., 2011a; 2011b). Additionally, pulse-based plant proteins remain relatively underutilized as food ingredients, where information on their structural and functional properties is limited (Adebiyi &

Aluko, 2011). Canada being one of the most important player in world pulse production, utilization of these pulse based proteins would not only enhance their applicability and functionality, it would also be a value addition to the agricultural commodity of the nation. Hence pea protein isolate (PPI), a generous gift from Nutri Pea Limited (Manitoba, Canada) has been utilized as one of the emulsifiers for the development of NEs. The two major components in pea protein are the 11S legumin and 7S vicilin (Donsi et al., 2010). The legumin fraction, possess a hexameric structure has a beta-sheet rich structure with an average molecular weight of about 380 kDa, while the vicilin fraction, possess a trimeric structure with an average molecular weight of about 150 kDa (Gharsallaoui et al., 2009). At pH 7, both of these components exist in hexameric or trimeric forms. Being globular in nature, a number of approaches are followed in order to break down its larger aggregates to make it applicable for emulsification. High pressure homogenization is one such technique where large aggregates of protein is broken down into smaller fractions, thus exposing the hydrophobic groups and enhancing the emulsifying properties (Donsi et al., 2010). Pea protein is one of those pulse based ingredients that is less exploited when compared to the other dairy based proteins that have been previously utilized in the development of stable NEs (Lee et al., 2009). Hence, it was important to start with a system that was well established and then utilize pea (partially or wholly). In this regard, protein derived from bovine milk (casein and whey) are most commonly and widely utilized in the food industry for a number of nutritional and functional applications (Aleandri et al., 1968). They are widely used as emulsifying agents in a variety of food products including beverages, ice creams, sports supplements, infant formula and coffee creamer (McClements, 2005). The protein casein consists of four fractions: α_{s1} (~44 wt%), α_{s2} (~11 wt%), β (~32wt%), and κ (~11 wt%). It has well-defined hydrophobic and hydrophilic regions that help in rapid adsorption at the oil-water interface (Aleandri et al., 1968). The sodium salt of casein, most popularly referred to as sodium caseinate (SC), is a soluble mixture of all four fractions of caseins (Radford & Dickinson, 2004). Due its high solubility and well defined hydrophobic and hydrophilic regions, SC has been widely utilized not only in the development of emulsions but also NEs (Dickinson et al., 1997; Hunt & Dalgleish, 1994; Lee & Norton, 2013; Qian & McClements, 2011; Zeeb et al., 2014; Zhao et al., 2015). Therefore, SC was the other emulsifier chosen in this work to develop long-term stable NEs.

2.5.2 Oil phase

Vegetable oils are most widely used in the development of NEs. Canola oil, primarily used for cooking and biodiesel production, has been previously utilized in development of NEs (Erramreddy & Ghosh 2014; Wu & Muir 2008). Saskatchewan being the largest producers of canola in Canada, canola oil was utilized as the oil phase of the NEs for this research project.

2.5.3. Bioactive ingredient

In this work, curcumin, a lipophilic bioactive ingredient, was encapsulated in the NEs. Curcumin is a natural polyphenolic phytochemical extracted from the powdered rhizomes of turmeric (*Curcuma longa*) spice. It was found to have a number of potential benefits on human health, e.g., anti-tumour, anti-oxidant, anti-microbial and anti-inflammatory properties etc., (Ahmed et al., 2012). Due its extremely low water solubility (11 ng/ml), it is difficult to incorporate into many food products and consequently lower bioavailability when ingested (Tonnesen et al., 2002). Studies indicate that emulsion based systems have proven efficient not only to encapsulate but also deliver curcumin to the human gut when compared to that dispersed in water (Ahmed et al., 2012; Wang et al., 2008).

3 LONG-TERM STABILITY OF SODIUM-CASEINATE STABILIZED NANOEMULSIONS ¹

3.1 Abstract

Nanoemulsions (NEs) have recently been widely investigated for higher stability against gravitational separation and improved bioavailability of poorly water-soluble bioactive components. However, their application in food has been compromised due to lack of suitable food-grade emulsifiers that can create nanodroplets and provide long-term stability without the issues of toxicity due to excess concentration. The goal of the present work is to use different concentration (2.5 – 10 wt%) of sodium caseinate (SC) as a sole emulsifier in the preparation of 5 wt% oil-in-water NEs and investigate their long-term storage stability for 6 months. Previous studies in literature associated with SC looked only into NE formation; hence the challenges with long-term stability were not addressed. All NEs displayed an average droplet size less than 200 nm, which remained unchanged over 6 months. However, all of them displayed rapid creaming, whose extent increased with protein concentration. The cream layer formed was weak and re-dispersible upon gentle mixing. Microstructural analysis of the cream layer showed that at higher protein concentration compaction of the cream layer was due to re-organization of the flocculated nanodroplet network leaving the aqueous phase out. It was postulated that excess unabsorbed protein caused depletion flocculation leading to creaming of oil droplets. Calculation of depletion interaction energy showed an increase in attraction with protein concentration and decrease with a reduction in droplet size, making NE more resistant to flocculation than conventional emulsions. This work aids in understanding the dependence of protein concentration on long-term stability of SC stabilized NEs.

¹ Submitted to Journal of Food Science and Technology on 15th April, 2016

3.2 Introduction

Nanoemulsions (NEs) are emulsions where the majority of the dispersed droplets fall within the nanoscale range. It has been proposed that average droplet radii of NEs should be less than 100 nm (McClements, 2012), however, others considered the upper range to be 200 nm or at times even higher (Fernandez et al., 2004; Gutiérrez et al., 2008). Due to their small droplet sizes, NEs have several advantages compared to conventional emulsions. They were found to have higher stability to droplet aggregation and gravitational separation, high optical clarity and display potential to modulate product texture (Erramreddy & Ghosh, 2014). Oil-in-water (O/W) NEs are being utilized in food applications to encapsulate and deliver poorly water-soluble active ingredients (e.g., vitamins, antioxidants, nutraceuticals, preservatives and flavors) (Rao & McClements, 2012). Studies have shown that the bioavailability of these encapsulated components was significantly higher in NEs than conventional emulsions due to the high surface-to-volume ratio of nanodroplets (Acosta, 2009; Ahmed et al., 2012). These advantages of NEs not only improve their applications in food and beverages, but also in chemical, agriculture and pharmaceutical industries where higher release of chemicals, pesticides or drug molecules may lead to better utilization and cost-effectiveness (Ahmed et al., 2012; Rao & McClements, 2012).

To create extremely small droplets of O/W NEs, a lot of water-soluble emulsifiers are required. An essential criterion for the selection of emulsifiers is their ability to lower interfacial tension so that nano-size droplets can be created, and fast movement to freshly created bare nanodroplet surfaces during homogenization. Many small molecule emulsifiers, including sodium dodecyl sulfate (SDS), Tweens, etc., can meet both of these criteria, but large quantities of these emulsifiers in food and drug is not preferred due to toxicological concerns (He et al., 2011a; Lawrence & Rees, 2000). In this respect, food proteins are ideal candidate to stabilize NEs as they do not raise toxicological concerns and improve consumer acceptance (Can Karaca et al., 2011b), although their ability to lower interfacial tension and movement towards bare interfaces during homogenization are significantly lower than small molecule emulsifiers. Nevertheless, if a NE can be formed with proteins, they tend to provide better long-term stability due to the formation of a thick viscoelastic membrane on droplet surface that acts as a protective coating (Walstra, 2002).

Among the various food proteins, those isolated from bovine milk (casein and whey proteins) are widely used as emulsifying agents in a variety of food products including beverages, ice creams, sports supplements, infant formula and coffee creamer (McClements, 2005). The

protein casein consists of four fractions: α_{s1} (~44 wt%), α_{s2} (~11 wt%), β (~32wt%), and κ (~11 wt%) and it has well-defined hydrophobic and hydrophilic regions that help in rapid adsorption at the oil-water interface (Aleandri et al., 1968). The sodium salt of casein, popularly referred to as sodium caseinate (SC), is essentially a soluble mixture of all four fractions of caseins (Radford & Dickinson, 2004). High solubility of SC has been exploited widely for its use as an emulsifier for conventional emulsions and also NEs (Hunt & Dalgleish, 1994; Lee & Norton, 2013; Qian & McClements, 2011; Zeeb et al., 2014; Zhao et al., 2015).

It has also been observed that the stability of SC-stabilized emulsions and NEs was largely influenced by the presence of un-adsorbed free proteins in the continuous phase (as sub micelles in the order of 15-20 nm) (Dickinson & Golding, 1997) leading to depletion flocculation (Aronson, 1989). Extensive attempts have been made on SC-stabilized conventional emulsions in order to prevent depletion flocculation by keeping protein concentration level below a critical limit or by including other components in the system that curbed the depletion effects associated with SC (Liang et al., 2014; Zhao et al., 2015). In this regard, whey protein isolate (Hunt & Dalgleish, 1994), polysaccharides (maltodextrin or xanthan gum) (Liang et al., 2014), various alcohols (ethanol, 1-propanol, 1-butanol) (Zeeb et al., 2014) and flaxseed protein (Zhao et al., 2015) have been used. However, preparation of NEs stabilized with SC alone as an emulsifier has not been explored in details. Most of the studies associated with SC looked into NE formation by measuring droplet size and did not include any long-term stability study. Hence, the issues of depletion flocculation were not addressed (Lee & Norton, 2013; Qian & McClements, 2011). The objective of the current research is to investigate long-term stability of SC-stabilized O/W NEs (SCEs) against depletion flocculation. All NEs were prepared with 5 wt% canola oil with different concentrations of SC, and their storage stability was studied for 6 months using droplet size, microstructure, gravitational and accelerated stability analysis.

3.3 Materials and methods

3.3.1 Materials

Canola oil was purchased from local grocery store. Milli-Q™ water (Millipore Corporation, MA, USA) was used for the preparation of continuous aqueous phase. Casein sodium salt from bovine milk (SC) was purchased from Sigma Aldrich (Oakville, ON, Canada). SDS was

purchased from Fisher Scientific (Nepean, ON, Canada). All the other chemicals were purchased from Sigma Aldrich (Oakville, ON, Canada).

3.3.2 Preparation of aqueous phase

A 10 wt% protein stock solution was prepared by dispersing SC in Milli-Q™ water and left overnight stirring on a bench top magnetic stirrer (VWR International, AB, Canada) at room temperature. To this, 0.01 wt% sodium azide was added to avoid microbial contamination. This stock solution was serially diluted to obtain solutions containing 2.5, 5 and 7.5 wt% SC. pH of these solutions (measured when freshly prepared) always ranged between 6.8 and 7.2.

3.3.3 Preparation of nanoemulsions

The oil phase (5 wt% canola oil) and aqueous phase (95 wt%) containing the different amount of SC were coarsely mixed on a benchtop magnetic stirrer. An oil-in-water coarse emulsions was prepared from this pre-mix using a rotor/stator mixer (Polytron, Brinkmann instruments, ON, Canada) for 2 minutes at 20,000 rpm which was then passed through a high-pressure homogenizer (Emulsiflex-C3, Avestin Inc., Ottawa, ON, Canada) at a pressure of 20,000 psi (137.9 MPa) for 6 cycles in order to develop NE. Emulsification was done at room temperature although the final temperature of NEs rose to ~40° C. The pH and conductivity of all NEs ranged between 6.8-7.1 and 10-20 µS/cm, respectively.

3.3.4 Emulsion storage stability

All freshly prepared NEs were stored in 40 mL clear glass vials (VWR international, AB, Canada) for long-term stability analysis (6 months) through visual observation and creaming index measurement. For all the other experiments NEs were stored in two separate 50 mL clear polypropylene centrifuge tubes (VWR international, AB, Canada), one exclusively for microscopy (to understand the microstructure of the cream layer and the serum layer without disturbing the sample) and the other for the rest of the experiments (droplet size, bulk microscopy and accelerated stability analysis). All sample vials were stored in a refrigerator at 4°C.

3.3.5 Droplet size distribution

The droplet size distribution of the NEs was determined using a static laser diffraction particle size analyzer (Mastersizer 2000, Malvern Instruments, Montreal, QC, Canada) in accordance to the standard ISO 13320 with a relative refractive index of the dispersed to continuous

phases of 1.465. Drops of NE was added to the sample dispersion unit until the obscuration index reached about 15% and the droplet size distribution and the surface mean diameter (d_{32}) was measured. As the NEs displayed creaming, a uniform sample was drawn by gently mixing them before the experiment.

3.3.6 Creaming index

Creaming of NEs was visually observed and recorded using a digital camera from the samples stored in transparent glass vials and quantified by calculating creaming index (CI), defined as the ratio of the height of the bottom serum layer (H_S) to the total height of the emulsion (H_E) (McClements, 2007). A creaming index of 1 signifies stable, non-creamed emulsion and the values decrease with increase in creaming.

3.3.7 Microscopy

Optical microscopy: An optical microscope (Eclips E400, Nikon Mississauga, ON, Canada) was used to capture microstructure of the NEs and its cream and serum layers. All experiments were carried out at magnifications of 100 \times and 400 \times . Samples from cream and serum phases were drawn without disturbing the layers. A drop of the sample was placed on a microscope slide (Fisher Scientific, Nepean, ON, Canada) covered with a coverslip (VWR International, AB, Canada) and observed under the microscope.

Confocal microscopy: The structure of the freshly prepared NEs was also analyzed by confocal laser scanning microscope (CLSM). For this, emulsions were separately prepared using 0.01 wt% Nile red dye (Sigma Aldrich, Oakville, ON, Canada) in the oil phase. Samples were examined with a Nikon C2 CLSM microscope (Nikon, Mississauga, ON, Canada) using a 543 nm laser using a 60 \times Plan Apo VC (N.A. 1.4, Nikon) oil immersion objective lens.

3.3.8 Centrifugal separation analysis

The multi-sample photocentrifuge - LUMiSizer LS650 (LUM GmbH, Berlin, Germany) was used to understand the accelerated storage stability of the NEs. This equipment employs the STEP (Space and Time resolved Extinction Profiles) technology, which measures the intensity of transmitted light as a function of time and position over the entire sample length in a cuvette during centrifugation (Lerche, 2002). It displays data in the form of transmission profiles of emulsions as a function of sample height in the cuvette. 350 μ L of sample was placed in rectangular

polycarbonate cuvettes (2×8 mm) (LUM GmbH, Berlin, Germany) and centrifuged at a speed of 4000 rpm (2266×g) at 25 °C to capture 1000 transmission profiles at an interval of 60 s (total run time was 16 hours 40 minutes) using a laser wavelength of 865 nm. The progression of the transmission profiles contained information on the kinetic stability of the emulsions and allowed characterization of droplets using SEPView software v 4.1 (LUM GmbH, Berlin, Germany). The instability or separation index, a factor calculated by the software and whose derivation and calculations can be found elsewhere in detail (Detloff et al., 2013), was used to compare the stability of NEs. Briefly, instability index quantifies the clarification in transmission based on particle size and separation at a given time in the presence of accelerated gravitational force, divided by the maximum clarification possible. The clarification is due to increase in transmission or decrease in droplet concentration due to movement of nanodroplets towards the cream layer. It is a dimensionless number between 0 and 1, where 0 indicates no separation or no change in NEs' transmission and hence highest stability, and 1 represents complete segregation of phases and hence lowest stability under the centrifugal field. Comparing instability indices of NEs under accelerated gravitational field ultimately aids in a quick comparison of their shelf-life instead of waiting long-time at earth gravitation.

3.3.9 Statistics

Samples were prepared, and experiments were performed with at least three replicates. Student's T test for independent samples was applied to determine the statistical significance at a 95% confidence level using SPSS software (SPSS Inc., ver. 22, 2013, Chicago, IL).

3.4 Results and discussion

3.4.1 Droplet Size Distribution

Droplet size distributions of the NEs are reported in Figure 3.4.1. All NEs have a monomodal distribution ranging from 30 nm to less than 1 µm. To understand the change in droplet size distributions as a function of time, comparisons were made with freshly prepared (Figure 3.4.1a) and 24 weeks (6 months) old samples (Figure 3.4.1b). No change in the distribution of these NEs was visible over the period of 6 months. It should be noted that the effect of depletion flocculation was not seen in the droplet size distribution as during the light scattering measurements the samples were diluted to a great extent (few drops added to the reservoir of 150

mL in the instrument) thereby the concentration effect of excess SC submicelles were cancelled. Absence of flocculation was also confirmed by measuring the droplet size after gently mixing the NEs with 0.1 wt% SDS solution (1:5 ratio) where no change in droplet size distribution was observed (data not shown).

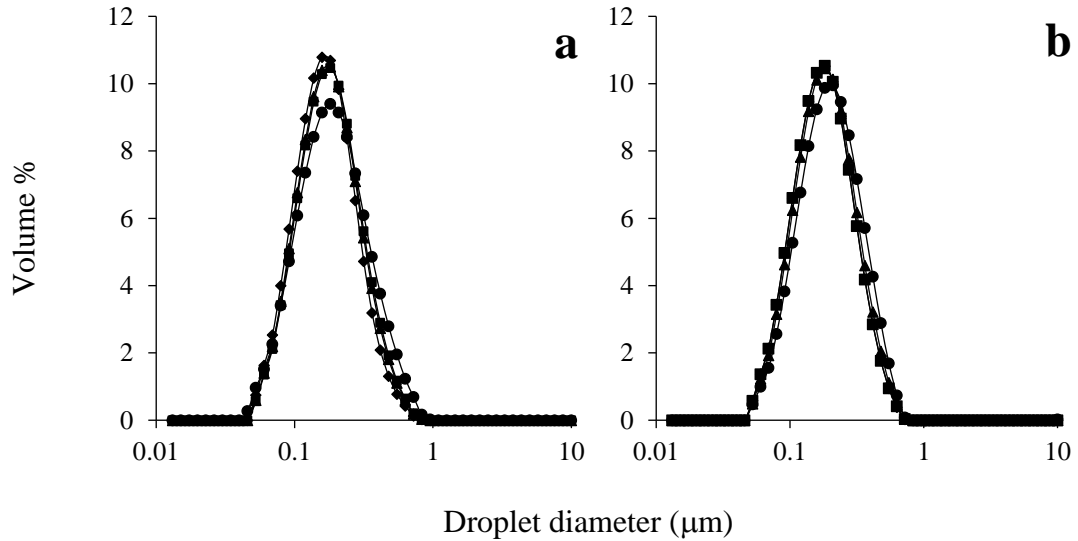


Figure 3.4.1 Droplet size distribution of 5 wt% canola oil-in water nanoemulsions stabilized by various concentrations of sodium caseinate for (a) freshly prepared and (b) 24 weeks old samples. Nanoemulsions prepared with protein concentrations of 2.5 wt% (●), 5 wt% (▲), 7.5 wt% (■), 10 wt% (◆) are compared.

The surface average droplet diameters (d_{32}) of all NEs were plotted as a function of time in Figure 3.4.2. The d_{32} values of all NEs were in the range of 155-170 nm, which falls in the below 200 nm definition of NEs proposed by McClements (2012). Moreover, the NEs in the present case did not show any significant change in their d_{32} values over a period of 24 weeks ($p > 0.05$). Among the different NEs, only the average d_{32} values of 2.5 wt% samples were higher than all other NEs although not statistically significant ($p > 0.05$).

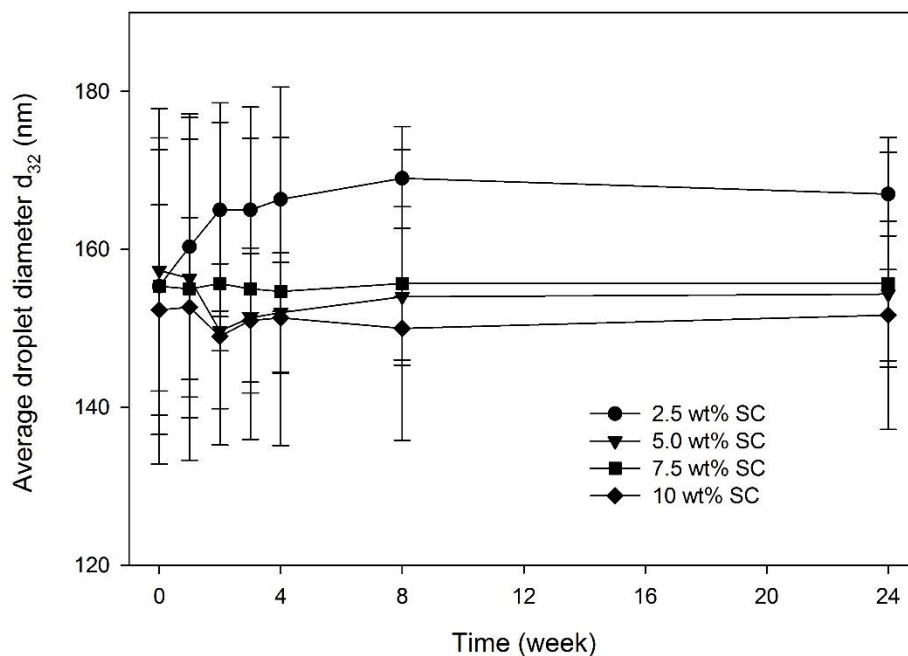


Figure 3.4.2 Surface average mean droplet diameter (d_{32}) of oil-in-water nanoemulsions stabilized with various concentrations of sodium caseinate (SC) as a function of time. 2.5 wt% (●), 5 wt% (▼), 7.5 wt% (■), 10 wt% (◆). Error bars represents \pm standard deviation of the average data (n =3).

3.4.2 Creaming behavior

Visual observation: Visual observation of the NEs was recorded to understand the extent of creaming and its influence on the overall stability of the NEs. Figure 3.4.3 shows images of undisturbed NEs in vials after 8 weeks and 24 weeks of storage. Although the NEs remain stable (no change in average droplets size) over a period of 6 months, they showed distinct cream layer formation, which increased with protein concentration. As a function of time the cream layer contracted and upon 24 weeks of storage, distinct compaction of the cream layer can be observed. This type of creaming in SC-stabilized emulsions has previously been observed when excess protein concentration in the continuous phase induced depletion flocculation (Dickinson & Golding, 1997; Dickinson et al., 1997; Liang et al., 2014). We, however, noticed that the creaming is weak and reversible and can be avoided by regular gentle mixing of the NEs. In fact, for the samples used for droplet size and bulk microscopy, gently mixed on a regular basis, we did not

observe any creaming (data not shown). In this case, the weak droplet network formed by only 5 wt% oil can be re-dispersed by gentle mixing. For conventional emulsions with larger droplets and higher oil concentration, however, depletion flocculation of oil droplets could lead to stable droplet network, which upon compaction and rearrangement expulse aqueous phase as bottom serum layer. This type of serum layer separation was measured by Dickinson and co-workers using ultrasonic scanning technique (Dickinson & Golding, 1997; Dickinson et al., 1997). Golding and co-workers investigated creaming of 30 wt% O/W emulsions stabilized with different concentration of SC. The authors prepared a stock 60 wt% O/W emulsions with 3 wt% SC in the aqueous phase ($d_{32} = 0.7 \mu\text{m}$) followed by dilution with various SC solutions to develop different final emulsions. In this case, the large droplets flocculated faster and formed a network of clusters which led to the creaming of the whole emulsion phase leaving a clear serum layer at the bottom. The advantage of NEs is that they are inherently very stable against flocculation due to their small droplet size (Tadros et al., 2004). Therefore, although depletion interaction due to unadsorbed SC in the continuous phase is present, nanodroplets' inherent stability against flocculation made them easily re-dispersable by gentle mixing. Also, the fact that we had only 5 wt% oil played a significant role in the inability to form strong clusters of flocculated droplets.

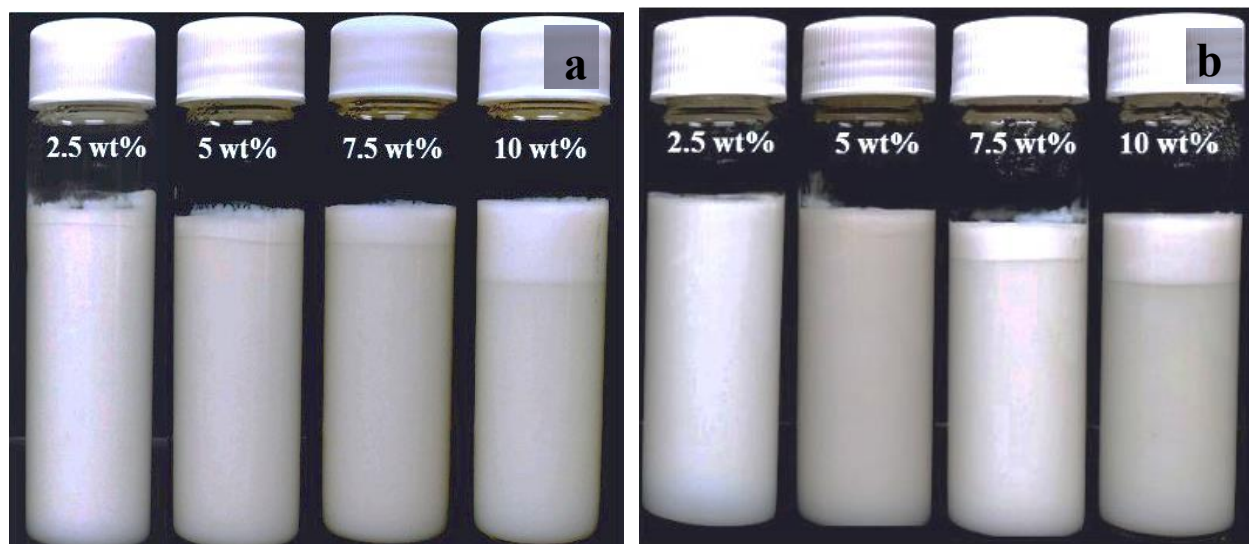


Figure 3.4.3 Visual observation of oil-in water nanoemulsions stabilized by various concentrations of sodium caseinate after (a) 8 weeks and (b) 24 weeks of storage at 4°C.

Creaming Index (CI): In order to quantify creaming in undisturbed NEs, the height of the cream layer was measured, and average creaming indices were plotted as a function of time (Figure 3.4.4). It can be observed that after a week of preparation, all NEs showed creaming as CI decreased from its initial value of 1. The formation of the cream layer from freshly made NEs was very rapid, and a discernable cream layer was visible within few hours after preparation. After 1 week there was a drop in CI and the extent of creaming increased with protein concentration. However, after this initial drop for the NEs with 2.5 and 5 wt% SC the change in CI with time was not significant for the rest of the 24 weeks of storage ($p > 0.05$), while for 7.5 wt% and 10 wt% NEs, a significant change in CI was observed ($p < 0.05$). For 7.5 wt% NE, the CI remained unchanged from 1 to 4 weeks, thereafter increased (due to compaction of the cream layer) until 8 weeks and remained unchanged for the rest of the 6 months. For 10 wt% SCE similar behavior was observed, except that the compaction of the cream layer began after 2 weeks of storage. From the CI data it is apparent that the full extent of creaming takes about a week to form, thereafter compaction of cream layer begins which stopped when no more oil droplets and proteins can be packed in the top cream layer.

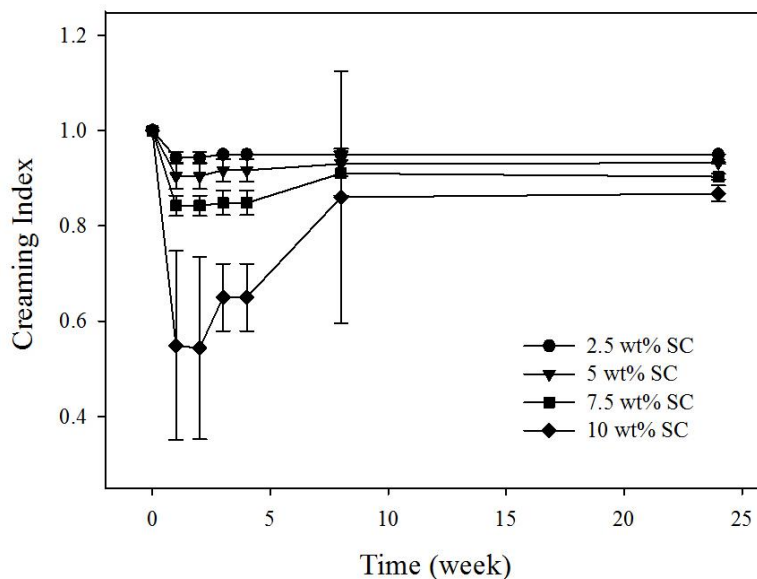


Figure 3.4.4 Change in creaming index for sodium caseinate (SC)-stabilized oil-in-water nanoemulsions as a function of time and protein concentrations: 2.5 wt% (●), 5 wt% (▼), 7.5 wt% (■), 10 wt% (◆). Error bars represent \pm standard deviation of the average data ($n=3$).

Similar behavior of compaction/compression of cream layer was observed in emulsions with excess unadsorbed polymers in the continuous phase (Fillery-Travis et al., 1993; Newling et al., 1997). It was proposed that the droplets in the cream layer underwent compression/compaction under the influence of gravity by gradually re-arranging with time leaving the serum layer squeezed out (Newling et al., 1997). The weak attractive force among the droplets in the cream layer also allowed them to re-arrange under the influence of gravity (McClements, 2007). To understand the changes brought about by the compaction of the cream layer, we also looked into the evolving microstructure of these systems.

3.4.1 Microstructure

Figure 3.4.5 shows the confocal micrographs of the NEs taken one day after preparation. The sample tubes were gently mixed to re-disperse the cream layer before taking it for microscopy. All NEs contained numerous small oil droplets in a flocculated state. The extent of flocculation appeared more with the increase in protein concentration, which is in accordance with higher cream layer thickness seen during visual observation (Figure 3.4.3). The extremely small droplet size of the NEs made it difficult to capture clear images of droplet flocculation with the present set up of the confocal microscope. In order to clearly visualize the floc structure, one image of 2.5 wt% SCE was captured with 5 times digital zoom of the 60 X objective lens (Figure 3.4.5e). It can be observed that nearly monodisperse nanodroplets are flocculated forming large clusters. Numerous small clusters of droplets can also be seen in the background. The microstructure of the NE is distinctly different from conventional emulsions with large droplet sizes and higher oil volume fractions seen by other researchers. For example, Dickinson and co-workers (Dickinson & Golding, 1997), in their pioneer work on creaming and flocculation of SC-stabilized O/W emulsions, found flocculated droplet network throughout the emulsion micrographs. For their microscopy work, the authors used 10 vol% O/W emulsions stabilized with various concentration of SC. For these emulsions, a distinct cream layer was observed when SC concentration reached 2.4 wt%. At 3 wt%, highly flocculated droplet clusters formed a network throughout the emulsion which prevented further creaming. Liang and co-workers (Liang et al., 2014) used a confocal microscope to record microstructure of SC-stabilized conventional emulsions containing 30 wt% oil. The authors also observed extensive flocculation of oil droplets throughout the emulsions. In

the present case, only 5 wt% oil was used which was not enough to form a network of droplet clusters (Figure 3.4.5e).

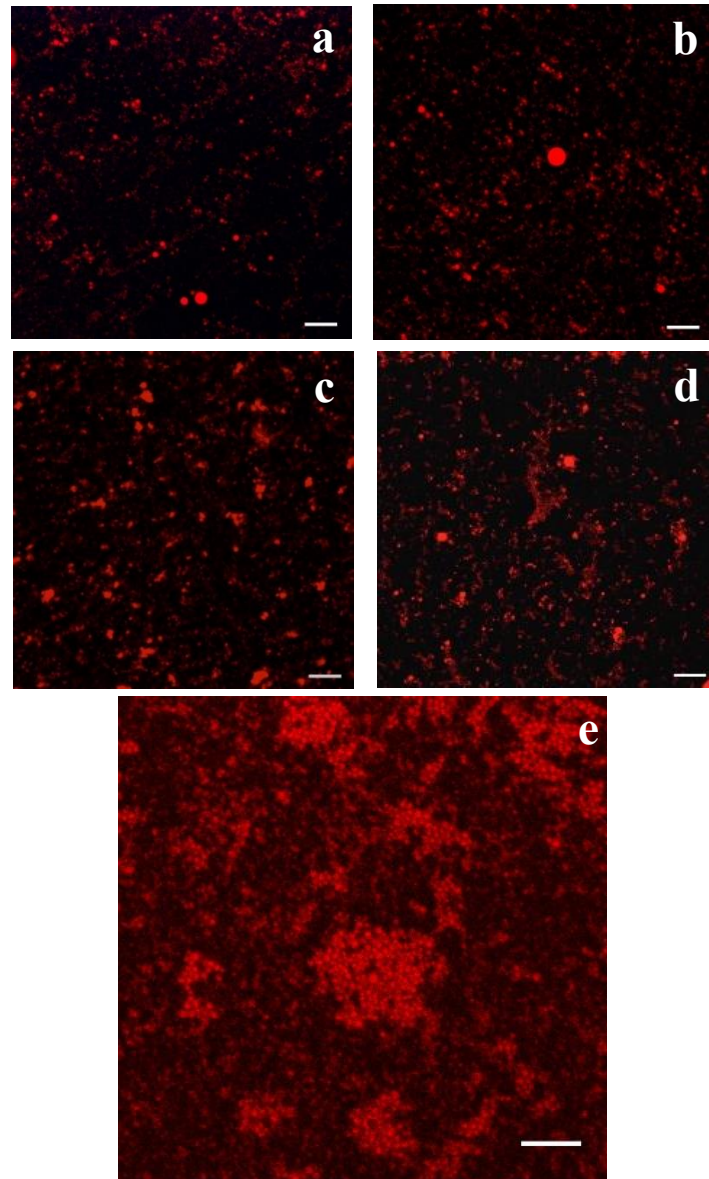


Figure 3.4.5 Confocal micrographs of 5 wt% canola oil-in-water nanoemulsions stabilized by various concentrations of sodium caseinate (a) 2.5 wt%, (b) 5 wt%, (c) 7.5 wt% and (d) 10 wt% (scale bar 20 μ m). The nanodroplet flocs are clearly visible in (e) which was captured by 5 times digital zooming on a 2.5 wt% sodium caseinate-stabilized nanoemulsion sample (scale bar 5 μ m). For a clear view of droplet flocculation an enlarged view of image (e) is shown.

Also, as discussed in the following section, NEs are more stable against depletion flocculation compared to conventional emulsions, which manifested as less aggregated droplets visible in the confocal micrographs. However, a different observation of flocculated nanodroplet structure was obtained when the undisturbed cream layer of the NEs were recorded as a function of time (Figure 3.4.6). It can be seen that in 2.5 wt% SCE cream, the droplet aggregates formed clusters, however, the clusters could not form a network. With the increase in protein concentration (5 to 10 wt% SC), the clusters of droplets formed an extensive network. As a function of time and at higher protein concentration as the cream layer compacted, the entire micrographs became filled with the nanodroplet network. The continuous aqueous phase expelled from the network (no gap can be seen) leaving a solid-like state made up mostly of packed nanodroplets. Packing of droplets was more evident after 6 months of storage compared to 8 weeks. The 2.5 wt% SCE, however, behave differently after 6 months of storage. As discussed below, due to very weak depletion interaction at 2.5 wt% SC, a very fine cream layer was formed after 6 months (Figure 3.4.3b) and its micrograph with much less cluster formation appeared different from the rest of the NEs.

3.4.2 Centrifugal separation analysis

The centrifugal separation analysis using a photocentrifuge is a novel means of comparing emulsion stability in an accelerated gravitational field. We have used this analytical technique as a supplemental method to the conventional creaming index measurement. Figure 3.4.7 shows the change of instability index with time for all NEs. Instability index aided ranking of our samples in terms of stability against phase separation. It can be observed that instability index decreased with increase in protein concentration, indicating the 10 wt% SCE was the most stable one. Statistically, 2.5, 5 and 7.5 wt% SCEs are not significantly different in terms of instability index ($p > 0.05$) which was indeed the case for CI measurement under 6 months storage (Figure 3.4.4). From Figure 3.4.7 it can also be seen that the 10 wt% SCE was significantly more stable than 2.5 and 5 wt% ($p < 0.05$), while no significant difference was observed with 7.5 wt% SCE ($p > 0.05$). As a function of time, no significant difference in instability indices was observed for all NEs ($p > 0.05$), although for 10 wt% NE the values of instability indices increased after 6 months of storage (from 0.65 for fresh NE to 0.82 after 6 months).

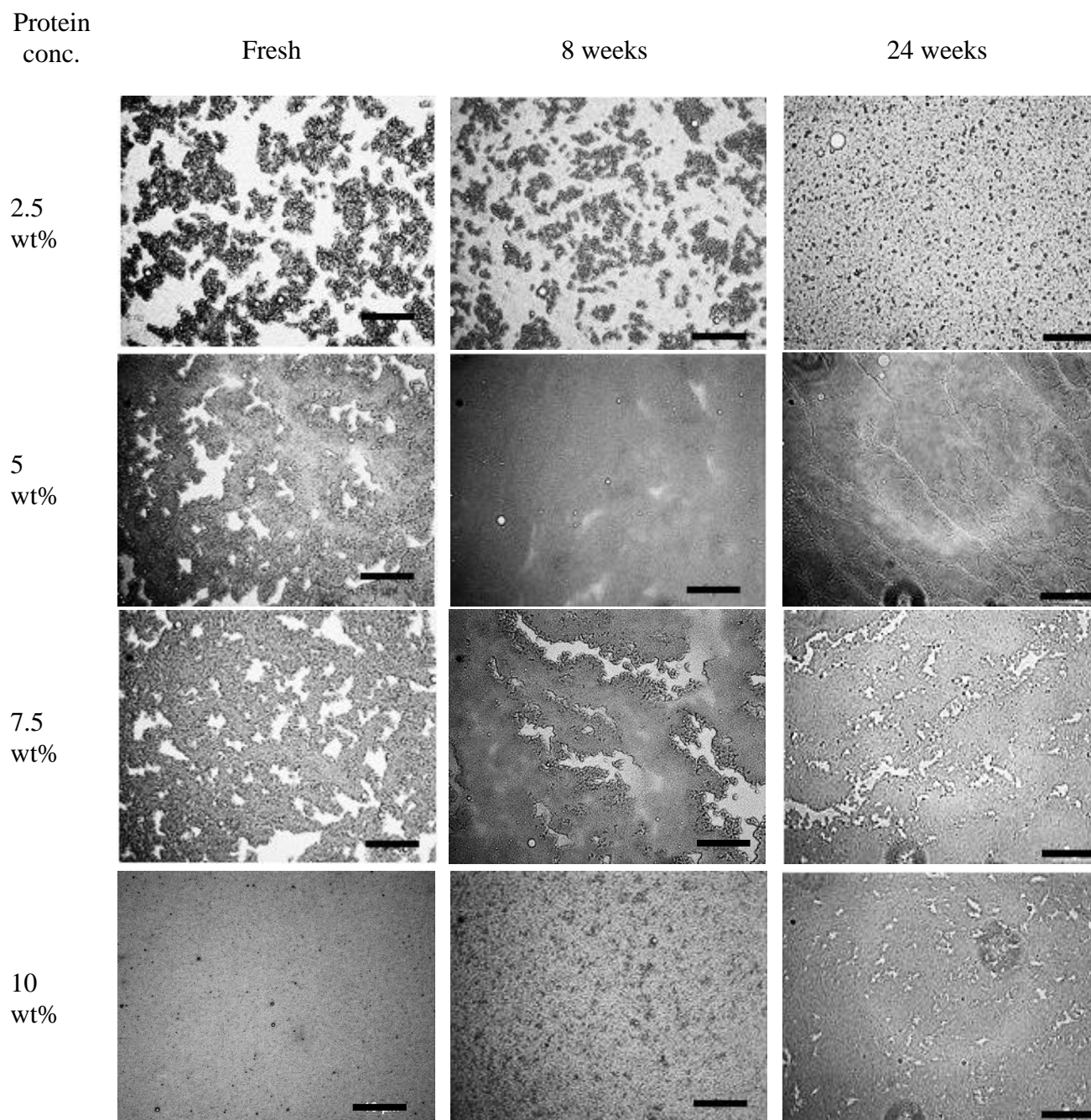


Figure 3.4.6 Optical micrographs of the cream layer from 5 wt% canola oil-in-water nanoemulsions stabilized by sodium caseinate at various concentrations on the day of preparation and after 8 and 24 weeks of storage. A working magnification of 400× was used. Scale bar represents 5 μm .

The results for NE stability under accelerated gravitation appears to contradict what we have seen in creaming behavior of undisturbed sample under gravity (Figure 3.4.4), where extent of creaming increased (stability decreased) with increase in protein concentration due to depletion flocculation. This could be due to the oversaturation of the instrument detector at high protein concentration where a large number of casein submicelles and droplet flocs prevented it to clearly detect droplet movement and hence the NEs appeared more stable. This showed a limitation of the centrifugal separation method, and may be overcome by suitable dilution of the system.

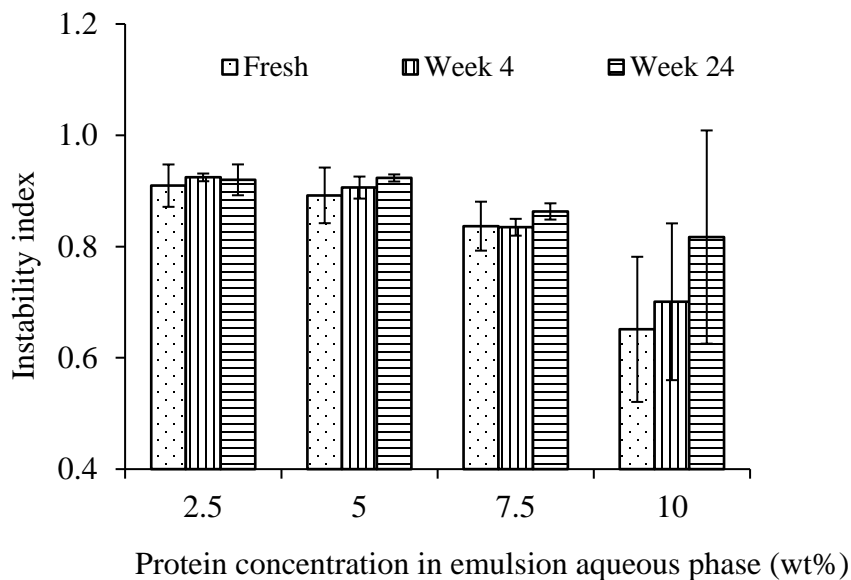


Figure 3.4.7 Instability index calculated from centrifugal separation analysis transmission profiles of the nanoemulsions prepared with various concentrations of sodium caseinate for freshly prepared, 4 weeks and 24 weeks old samples.

3.4.3 Calculation of depletion interaction energy

Dickinson and co-workers have proposed depletion flocculation as a possible mechanism of destabilization in casein sodium salt (SC)-stabilized emulsions (Dickinson & Golding, 1997; Dickinson et al., 1997). Attempts have also been made by the researchers to bring in stronger evidence to prove Dickinson hypothesis (Liang et al., 2014). Three different stages of emulsion stability have commonly been observed: the regime with no creaming and droplet flocculation was observed at a SC concentration sufficient for nearly saturation coverage of the droplets. At a lower protein concentration than this there were insufficient proteins for complete coverage of the droplet

surface, and hence, protein molecules adsorbed on one droplet may be shared with other droplets leading to emulsion destabilization due to bridging flocculation. On the other hand, the presence of excess unabsorbed protein resulted in reversible droplet flocculation due to depletion interaction, where saturation coverage of droplets by proteins was able to prevent any further coalescence. In this case depletion interaction energy (ΔG_{dep}) was calculated from equation 3.1, in congruence with the work from Radford & Dickinson in 2004 (Radford & Dickinson, 2004) :

$$\Delta G_{dep} = -VP_{osm} \quad (\text{eq. 3.1})$$

where, V is the volume of the emulsifier depleted layer in between two approaching droplets and P_{osm} is the osmotic pressure created by the presence of excess proteins in the emulsion continuous phase (Dickinson & Golding, 1997; McClements, 1994). Here we considered maximum depletion interaction when the droplet surfaces touch in which case the volume of the depleted layer could be estimated by

$$V = 2\pi r_m^2 \left(r_d + \frac{2r_m}{3} \right) \quad (\text{eq. 3.2})$$

where, in the present case, r_d and r_m can be considered as the radii of nanoemulsion droplets and casein submicelles, respectively. The osmotic pressure can be calculated using a thermodynamic model, which assumes that all SC submicelles are spherical, and they exhibit uniform molecular weight

$$P_{osm} = nK_B T \left(1 + \frac{C_{aq}}{\rho} \right) \quad (\text{eq. 3.3})$$

where n is the number density of the SC submicelles ($n = C_{aq} N_A / M$), C_{aq} the aqueous phase excess protein concentration, N_A the Avogadro number, M the effective molecular weight, and ρ the density of the sub-micelle particles ($\sim 1050 \text{ kg/m}^3$). $K_B T$ is the thermal energy of the system. The molecular weight of the SC submicelle was estimated as a function of its radius

$$M = \frac{4}{3} \pi r_m^3 \rho N_A \quad (\text{eq. 3.4})$$

From equations 3.3 and 3.4 it can be seen that the osmotic pressure and hence the depletion interaction energy is inversely proportional to the SC submicelle size and molecular mass.

Therefore, the smaller the caseinate sub-micelle, the strongest will be the depletion attraction although the range of depletion interaction is directly proportional to the sub-micelle size. Taking the range of attraction in consideration Redford & Dickinson in 2004 (Radford & Dickinson, 2004) showed that the smallest nanoparticle produced the strongest attraction, but they were very short-range where the attraction could be dominated by electrostatic or steric repulsion. On the other hand, larger sub-micelles, although produce weak depletion attraction, were long-range, and the overall interaction potential was dominated by attraction. In order to understand how SC submicelle size influence attraction when the droplet surfaces touch, we have calculated depletion interaction in terms of $K_B T$ for a range of sub-micelle size (5 nm, 10 nm and 20 nm) (Figure 3.4.8a) for the four nanoemulsions with increasing unadsorbed aqueous phase protein concentration (C_{aq}). The values of C_{aq} was calculated from the surface load analysis where NEs were ultracentrifuged to separate the cream layer from the serum layer and the protein concentration in the serum layer was determined by Dumas method (quantitative method to determine nitrogen content) (data not shown). It can be observed that depletion attraction increased with increase in un-adsorbed protein in the aqueous phase. This was also reflected by the visual observation and creaming index values for all NEs where the extent of creaming (driven by depletion flocculation) increased with increase in protein concentration. It should also be noted that the maximum attraction values fall within 2 $K_B T$ for the smallest sub-micelles size (5 nm) indicating very weak attraction among the droplets. Therefore, the flocs formed due to depletion are weak and will tend to break apart with a mere influence of thermal motion. This was reflected from the droplet size, creaming and visual observation results of all our NEs. As stated previously, the cream layer formed was so weak that a mere shaking of the vials containing NEs re-dispersed the flocs, thereby having no effect on the droplet size behaviour.

Nevertheless, for a sub-micelle size of 10 nm, reported by a vast majority of researchers (Liang et al., 2014) oil droplet size can also have a significant influence on depletion attraction. It can be seen from Figure 3.4.8b, that depletion attraction increased with increase in emulsion droplet size. For NEs with an average droplet radius ~ 78 nm (as in the present case) depletion attraction ranged from 0.4 to 1.9 times $K_B T$, while for a conventional emulsion with 500 nm droplet radius it varies from 1.3 to 6.4 times $K_B T$ with increase in protein concentration. This explain why our NEs even with high unabsorbed protein load showed very weak depletion attraction while conventional emulsions prepared by Liang et al (Liang et al., 2014) (average droplet radius 365

nm) showed extensive depletion flocculation in the range of 1.0 to 15.6 times $K_B T$ for protein concentration of 1.5 to 10% wt% . This inherent advantage of NEs against depletion-induced destabilization makes them more suitable for applications where creaming stability is important.

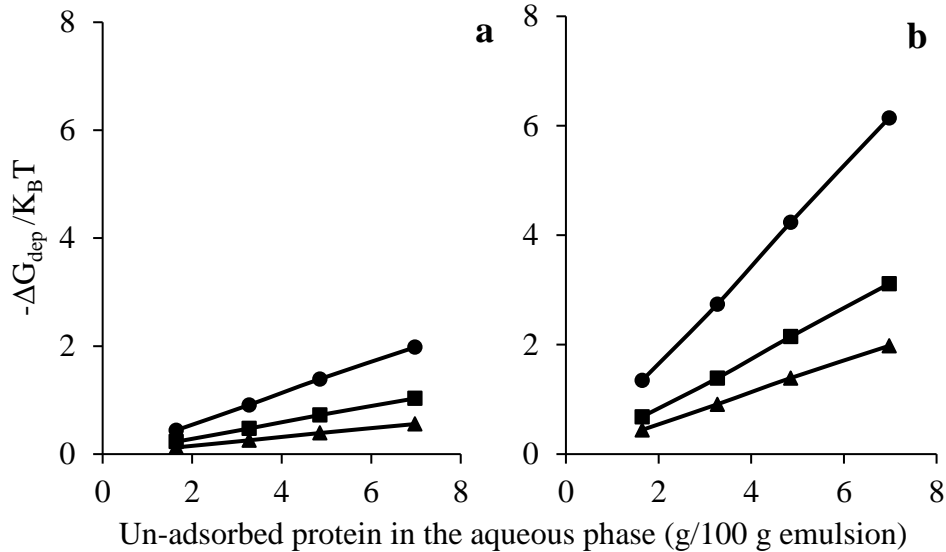


Figure 3.4.8 Calculated values of depletion interaction energy ΔG_{dep} (units of $K_B T$) as a function of unadsorbed protein concentration in the aqueous phase of the nanoemulsions for (a) different caseinate submicelle radii: 5nm (●), 10nm (■), 20nm (▲) for 78 nm average droplet diameter of nanoemulsion, and (b) different average droplet radii: 500 nm (●), 250 nm (■), 78 nm (▲) for 10 nm caseinate submicelle.

3.5 Conclusion

Stable 5 wt% O/W NEs were developed with various concentrations of SC as a sole emulsifier. All NEs remained stable to coalescence over 6 months storage period with no change in droplet size, although, excess un-adsorbed protein in the continuous phase induced reversible depletion flocculation and creaming of nanodroplets. The nanodroplet flocs broke apart upon gentle mixing and had no effect on droplet size measurement using a static light scattering instrument. The formation of the cream layer from freshly made NEs was very rapid, and a discernable cream layer was visible within few hours after preparation. The thickness of the cream layer increased with increase in protein concentration and was quantitatively analyzed by calculating the creaming index. The full extent of creaming took about a week to form, thereafter

compaction of cream layer began which stopped when no more oil droplets and associated proteins can be packed. In contrast to visual observation, stability analysis under accelerated gravitational field in a photocentrifuge revealed that the NEs with 10 wt% SC was the most stable with least separation. However, it could be due to oversaturation of the instrument detector at high protein concentration, which prevented clear detection of droplet movement. The microstructure of the flocculated nanodroplets was confirmed using confocal microscopy while the structure of the undisturbed cream layer and its compaction was recorded using an optical microscope. It was observed that at higher protein concentration, as the cream layer compacted, the entire micrograph became filled with nanodroplet network leaving continuous aqueous phase out of the packed structure.

Quantitative estimation of depletion interaction energy was done using the theory proposed by Dickinson and co-workers (Dickinson et al., 1997; McClements, 1994). It was found that depletion attraction significantly decreased with decrease in droplet size and for our NEs with an average droplet radius ~80 nm depletion attraction ranged from only 0.4 to 1.9 times $K_B T$ as a function of protein concentration demonstrating inherent advantage of NEs against depletion induced destabilization which make them more suitable for applications where creaming stability is important. The knowledge developed from this work could be useful in understanding the effect of protein concentration on the long-term stability of NEs and can be applied in food and beverages as well as for pharmaceutical and cosmetics industries.

3.6 Connection to next study

In this current study, the long-term stability of SCEs was studied for a period of 6 months. It was seen that at all concentrations of SC, it was possible to successfully develop NEs with droplet radii less than 200 nm, which also remained unchanged for a period of 6 months. However, they displayed rapid creaming due to depletion flocculation caused by excess un-adsorbed protein. In order to utilize a pulse based protein, in the next study, pea protein isolate (PPI) was incorporated by partial replacement of SC partially (in 1:1 ratio) forming, mixed protein stabilized NEs were developed. The efficacy of PPI in stabilizing the mixed protein NE and their long term stability was studied in detail.

4 IMPROVED STABILIZATION OF NANOEMULSIONS BY PARTIAL REPLACEMENT OF SODIUM CASEINATE WITH PEA PROTEIN ISOLATE²

4.1 Abstract

In this research, pea protein isolate (PPI) was used to partially replace sodium caseinate (SC) in order to investigate its efficacy in the formation and long-term stabilization of nanoemulsions (NEs). 5 wt% oil-in-water NEs were prepared by both SC and PPI and their 1:1 mixtures, with a total aqueous-protein concentration of 5, 7.5 and 10 wt%. As reported in chapter 3, all sodium caseinate-stabilized NEs (SCEs) (average droplet diameter <200 nm) displayed weak re-dispersible creaming behaviour (due to depletion flocculation by excess protein). In contrast, PPI failed to produce stable flowable NEs (PPIEs) (average droplet diameter > 200 nm) displaying excessive droplet and protein aggregation. At higher concentrations of PPI, these emulsions transformed into viscoelastic gels which could have numerous applications in food. Interestingly, the mixed SC and PPI-stabilized NEs (MPEs) did not display any creaming or aggregation. Although the MPEs displayed slight protein sedimentation over one-month period (indication of un-adsorbed protein in the aqueous phase), they remained stable throughout the experimental timeframe of 24 weeks with average droplet diameter <200 nm. Results from interfacial protein composition showed that, in NEs stabilized by individual proteins, the surface load was highest for PPI and least for SC. In the MPEs, it ranged between the two individual protein-stabilized NEs with values closer towards SC, indicating mutual presence of PPI at the interface along with SC on, confirmed from SDS-PAGE analysis of interfacial and serum layer protein. It was hypothesized that in presence of excess SC and PPI under high-pressure homogenization, denaturation of PPI (confirmed with complimentary results from FT-IR, intrinsic fluorescence and surface hydrophobicity) may lead to interactions between the two proteins which prevented depletion flocculation effect of SC and interfered with PPI aggregation thereby preventing both the destabilizing mechanisms seen in individual protein-stabilized NEs.

² Submitted to Food Hydrocolloids on 13th May, 2016

4.2 Introduction

Proteins have been widely used to stabilize oil-in-water emulsions. During the process of emulsification, proteins tend to re-orient and adsorb at the oil/water interface (McClements, 2005; Walstra, 2002). Flexible proteins (e.g., casein) adopt an arrangement at the interface such that the hydrophilic segments stay in the aqueous phase while the hydrophobic amino acids protrude into the oil phase and neutral segments lie flat at the interface. Globular proteins (e.g. soy protein, whey protein, pea protein) due to its specific orientation and larger size produce a thicker membrane compared to flexible proteins (Dickinson, 1992b). Proteins also form a thick viscoelastic membrane around the oil droplet surface which acts as a protective coating and retards droplet coalescence and flocculation by both electrostatic and steric stabilization (Walstra, 2002). The electrostatic repulsion of protein-stabilized membrane originates from the charge carried by some amino acids on protein's primary structure. Consequently, emulsifying capacity of proteins is sensitive to pH and ionic strength. Droplets stabilized with proteins tend to flocculate at pH values closer to its isoelectric point (Dickinson, 1992b). Therefore most proteins require pre-treatments (for example, enzymatic modification, alteration of pH etc., to tailor the structure of the protein) in order to improve their suitability as emulsifier (Barac et al., 2010; Donsi et al., 2010; He et al., 2011a). Additionally, proteins also contribute to an increase in the viscosity of the continuous phase, which contributes to emulsion stability by decreasing the rate of droplets movement (Sikorski, 2001).

However, when compared to small-molecular weight emulsifiers, proteins are less readily available (take longer time) to adsorb on freshly created interfaces during homogenization, giving rise to larger droplet size (Qian & McClements, 2011). Also, as larger quantities of protein are generally required to form nanoemulsions (NEs), where extremely high droplet surface area needs to be covered in order to provide long-term stability, free unabsorbed protein molecules in the continuous phase may also promote depletion flocculation of oil droplets (Dickinson, 1992b; Dickinson & Golding, 1997; Dickinson et al., 1997). Excess proteins in the continuous phase might also form aggregates leading to significant changes in emulsion behaviour (Dickinson, 1994). Therefore, it can be considered quite a challenge to prepare and stabilize NEs with desirable properties using proteins. Nevertheless, food emulsions stabilized by proteins offer the advantage of using natural products in addition to the health beneficial properties of protein themselves. Furthermore, proteins raise lesser toxicological concerns when compared to synthetic emulsifiers

for long-term food-based applications and are safer alternatives, hence promoting researchers to take up this challenge of developing protein-stabilized emulsions and NEs (Donsi et al., 2010; He et al., 2011a).

In spite of its importance, the use and application of plant proteins (e.g., proteins from soy, pea, lentil, canola) as emulsifiers when compared to animal and dairy proteins is less understood. Nevertheless, there has been a growing interest towards utilizing plant proteins as efficient substitutes for animal-based proteins in product formulations (Can Karaca et al., 2011b). Specifically, due to the potential health benefits of pulses, consumption and utilization of pulse proteins has significantly increased over the last few years (Hu, 2003). Physicochemical and emulsifying properties of various plant proteins have been studied previously (Avramenko et al., 2013; Can Karaca et al., 2011b; Liang et al., 2014). Avramenko et al. have studied the effect of trypsin-catalysed hydrolysis on emulsification properties of lentil protein isolate (LPI). They observed that un-hydrolysed LPI was more surface active than the hydrolysed fractions (Avramenko et al., 2013). Can Karaca et al. worked on chick pea protein isolate (CPI), soy protein isolate (SPI) and LPI and found that protein isolated through isoelectric precipitation produced emulsions with smaller droplet size and better stability compared to salt extraction. Also, CPI and LPI produced emulsions with smaller droplet size compared to SPI (Can Karaca et al., 2011b). Researchers have also been successful in developing NEs with the aid of pulse proteins alone. Donsi et al. developed 6 wt% oil-in-water NEs stabilized by 4 wt% pea protein (average droplet size <200nm) and proposed that it can be used for the delivery of nutraceuticals (Donsi et al., 2010). However, the long-term stability of these pulse protein stabilized NEs has not been studied before.

The overall objective of the current research is to develop oil-in-water NEs stabilized by mixed dairy and plant proteins for long-term food applications. Recently, we studied long-term stability of sodium caseinate (SC)-stabilized NEs and found that although the droplet size remain constant over a period of 6 months, the NEs were prone to depletion flocculation-induced destabilization (discussed in detail in chapter 3) (Yerramilli & Ghosh 2016a). Similar behaviour was also reported by other researchers in case of SC-stabilized conventional emulsions (Dickinson & Golding, 1997). Therefore, attempts have been made to curb depletion flocculation in SC-stabilized conventional emulsions by partially replacing it with other components (Liang et al., 2014; Zhao et al., 2015), e.g., whey protein isolate (Hunt & Dalgleish, 1994), polysaccharides

(maltodextrin or xanthan gum) (Liang et al., 2014), various alcohols (ethanol, 1-propanol, 1-butanol) (Zeeb et al., 2014). In the present work we used pea protein isolate (PPI), a pulse protein extracted and purified from pea, to curb depletion flocculation and develop long-term stable mixed protein-stabilized NEs.

Although, its efficacy in the preparation of long-term stable NEs is less well understood, pea protein is among those plant proteins which has been drawing attention from researchers for its application in the development of emulsions. The two major components in pea protein are the 11S legumin and 7S vicilin (Donsi et al., 2010). They possess a quaternary structure, legumin being hexameric and vicilin being trimeric in nature. The legumin fraction has a beta-sheet rich structure with an average molecular weight of about 380 kDa, while the vicilin fraction is a glycoprotein with an average molecular weight of about 150 kDa (Gharsallaoui et al., 2009). Studies carried out on purified fractions of pea protein showed that in their native form vicillin fraction is more surface active compared to the legumin fraction (Gharsallaoui et al., 2009; Gueguen et al., 1988). At pH 7, both of these components exist in hexameric or trimeric forms, while at acidic or basic pH disassociate into a mixture of trimers, dimers and monomers. Dissociation and unfolding of these proteins expose buried hydrophobic amino acids thereby enhancing surface hydrophobicity and interfacial adsorption behaviour of the proteins (Gueguen et al., 1988). High pressure homogenization is one such technique where large aggregates of protein is broken down into smaller fractions, thus exposing the hydrophobic groups and enhancing the emulsifying properties. Donsi et al. (2010) showed that high pressure homogenization of pea protein isolate disrupted protein disulfide-bonds making the hydrophobic groups more available for participation in droplet formation.

In this research the efficacy of pea protein isolate to partially replace sodium caseinate as an emulsifying agent in the development and stabilization of NEs was investigated. All NEs were prepared with 5 wt% canola oil and different amount of mixed PPI and SC in a 1:1 ratio (MPEs). As controls, NEs stabilized with only SC and PPI were also examined (SCEs and PPIEs). The long-term stability of these NEs was studied for a period of 24 weeks (6 months) using droplet size, microstructure, gravitational and accelerated stability analysis. Interfacial composition of the proteins was also estimated to understand the role and behaviour of PPI and SC in a mixed environment at the interface.

4.3 Materials and methods

4.3.1 Materials

Canola oil was purchased from local grocery store. Milli-Q™ water (Millipore Corporation, MA, USA) was used for the preparation of continuous aqueous phase. Casein sodium salt from bovine milk or popularly referred to as sodium caseinate (SC) was purchased from Sigma Aldrich, ON, Canada. Pea protein isolate (PPI) was a generous gift from Nutri Pea Limited (Manitoba, Canada). Sodium dodecyl sulphate (SDS) was purchased from Fisher Scientific (Nepean, ON, Canada). All the other chemicals were purchased from Sigma Aldrich (ON, Canada).

4.3.2 Preparation of aqueous phases

SC and PPI solutions: 10 wt% protein stock solutions were prepared by dispersing proteins in Milli-Q™ water and left overnight stirring on a bench top magnetic stirrer (VWR international, AB, Canada) at room temperature. 0.01 wt% sodium azide was added to the protein solution to avoid microbial contamination. This stock solution was serially diluted to obtain 5 and 7.5 wt% protein solutions.

Mixed protein solution: The mixed protein (MP) solution was prepared with a 1:1 mixture of SC and PPI solutions. For example to prepare a 5 wt% MP solution equal quantities of 5 wt% SC and 5 wt% PPI solutions were mixed using the bench top magnetic stirrer.

The pH of all protein solutions ranged between 6.8 and 7.2 (measured using Orion star A215 pH meter, Thermo scientific, Nepean, ON, Canada).

4.3.3 Preparation of nanoemulsions

Oil phase (5 wt%) and aqueous phase (95 wt%) containing either SC, PPI or MP were coarsely mixed on a benchtop stirrer. An oil-in-water coarse emulsions was initially prepared using a rotor/stator mixer (Polytron, Brinkmann instruments, ON, Canada) for 2 minutes at 20,000 rpm. NEs were then prepared by passing these coarse emulsions through a high-pressure homogenizer (EmulsiFlex-C3, Avestin Inc., Ottawa, ON, Canada) at a pressure of 20,000 psi (137.9 MPa) for 6 cycles. As PPI was quite insoluble in water, it frequently clogged the homogenizer valves at a very high pressure. To avoid this, protein solutions with PPI were pre-homogenized in the high-pressure homogenizer at a pressure of 5,000 (34.5 MPa) psi for 6 cycles before using them for emulsification. It was hypothesized that homogenization aided in solubilization of PPI by breaking

large protein aggregates into smaller ones. Similar observation of reduction in protein aggregate size by high-pressure treatment was also reported by researchers in the past (Bouaouina et al., 2006; Donsì et al., 2010).

4.3.4 Emulsion storage stability

The freshly prepared NEs were stored in 40 mL clear glass vials (VWR international, AB, Canada) for creaming index and long-term stability analysis through visual observation for 24 weeks (6 months). For all the other experiments 50 mL clear polypropylene tubes (VWR international, AB, Canada) were used. Specifically, two separate polypropylene tubes, one exclusively for microscopy (to understand the microstructure of the cream layer and the serum layer without disturbing the sample) and the other for the rest of the experiments (droplet size, bulk microscopy and accelerated stability analysis), were used. All sample vials were stored in a refrigerator at 4°C.

4.3.5 Droplet size distribution

The droplet size distribution of the NEs was determined using a static laser diffraction particle size analyzer (Mastersizer 2000, Malvern Instruments, Montreal, QC, Canada) in accordance to the standard ISO 13320 with a relative refractive index of the dispersed to continuous phases of 1.465. Drops of NEs were added to the sample dispersion unit until the obscuration index reached about 15% and the droplet size distribution and the surface mean diameter (d_{32}) was measured. As the NEs displayed creaming, a uniform sample was drawn by gently mixing them before the experiment.

4.3.6 Apparent viscosity

All rheology experiments were performed using an AR G2 rheometer (TA Instrument, Montréal, QC, Canada) at room temperature. The apparent viscosities of the samples was measured by rotational experiments with an applied shear rate ranging from 0.01 to 1000 s⁻¹. Samples was gently transferred by a pipette on the lower plate of the rheometer. A 40 mm acrylic parallel plate was used to apply shear on the samples using a geometry gap of 500 µm. The geometry was equilibrated for 30 seconds before applying any shear on the sample and measurements were taken.

4.3.7 Creaming index

Extent of creaming in the prepared NEs was visually observed from the samples stored in transparent glass vials). After they creamed, two phases could be visually observed; a droplet rich cream layer and a lower emulsion layer. The extent of creaming was quantified by creaming index (CI) (McClements, 2007), which is defined as the ratio of the height of the bottom serum layer (H_s) to the total height of the emulsion (H_E). A creaming index of 1 signifies stable, non-creamed emulsion and its value decreases with increase in creaming.

4.3.8 Confocal laser scanning microscopy

The structure of the freshly prepared NEs and protein solutions were analyzed by a confocal laser scanning microscope (CLSM). NEs were prepared using 0.01 wt% Nile red dye (Sigma Aldrich, Oakville, ON, Canada) in the oil phase. For staining the aqueous phase 0.01 wt% fast green (Sigma Aldrich, Oakville, ON, Canada) was added to the NEs right before microscopy. Samples were examined by a Nikon C2 CLSM microscope (Nikon, Mississauga, ON, Canada) using a combination of 543 and 633 nm lasers using a 60× Plan Apo VC (numerical aperture 1.4) oil immersion objective lens and a 60× objective lens. A drop of the sample was placed on a microscope slide (Fisher Scientific, Nepean, ON, Canada) covered with a coverslip (VWR International, AB, Canada) and observed under the microscope.

4.3.9 Determination of protein surface load

Separation of free protein: NEs were centrifuged (Discovery 90 ultracentrifuge, Sorvall, Canada) at 30,000 rpm (equivalent to $1.08 \times 10^5 g$) to separate them into two distinct phases, a cream layer containing oil droplets with adsorbed proteins and the continuous phase with free unadsorbed proteins. Specially designed Beckmann Coulter (ON, Canada) poly-allomer centrifuge tubes (13×51mm) filled with 3.5 g of NEs were transferred into a Sorvall SW 50.1 rotor and centrifuged for 1 hour at 25°C. The cream layer from the centrifuged samples were removed carefully with the help of a spatula and stored in glass test tubes (VWR international, AB, Canada). This was treated with 0.05 wt% SDS solution in 1:10 ratio and subjected to gentle mixing on a benchtop mixer. This process made sure that the interfacial protein was replaced by SDS leaving the protein back in solution. Then the supernatant serum layer containing free unadsorbed proteins were filtered sequentially through a 0.45 μm and 0.2 μm syringe filter (VWR international, AB, Canada) to

make sure there were no oil droplets present in that phase. In case of PPIEs, there was pea protein sediment at the bottom of the centrifuge tubes, which was recovered quantitatively and stored in separate glass test-tubes.

Protein surface load: The nitrogen content of the separated aqueous phase was determined by combustion using a Dumas nitrogen analyzer (Flash 2000, Thermo scientific, Canada). A Kjeldahl factor of 6.25 was used to calculate crude protein content from the nitrogen measurement. Protein surface load (Γ) corresponds to the amount of emulsifier that covers a unit area of droplet surface (expressed in milligram per meter squared) (Dickinson 1992, McClements 2007). The mass of emulsifier adsorbed per unit volume of the emulsion (C_a) equals the initial emulsifier concentration (C_i) minus the excess protein remaining in the aqueous phase (C_e). The total droplet surface area covered by the adsorbed emulsifier is given by $S = 6\phi V_e / d_{32}$, where, ϕ is the dispersed phase volume fraction, V_e emulsion volume and d_{32} is surface mean droplet diameter. Hence, surface load was obtained by $\Gamma = C_a V_e / S$ (Dickinson 1992, McClements 2007).

4.3.10 Identification of surface protein using SDS PAGE

To identify the type and kind of proteins adsorbed at the interface of the oil droplets, the aqueous phase protein and the interfacial protein were separately analyzed by sodium dodecyl sulfate polyacrylamide gel electrophoresis (SDS-PAGE). The serum phases collected from the NEs were freeze dried (Flexi Dry, Microprocess control, FTS systems, ON, Canada) and evaluated by SDS-PAGE under reducing conditions (SDS extraction buffer with β -mercaptoethanol) (Laemmli, 1970) using precast 8-25% T gradient gels adapting the protocol of Wanasundara & co-workers (Wanasundara et al., 2012). Briefly, samples were prepared in 1.5 mL microcentrifuge tubes using SDS extraction buffer (5% w/v SDS in 0.05 M Tri-HCl buffer at pH 8). The final concentration of protein in the SDS extract was between 1-2 mg/mL. Since the gels were ran under reducing conditions, β -mercaptoethanol was added to make a 5% (v/v) concentration level. An Eppendorf Thermomixer (Eppendorf Canada, Mississauga, ON) at 99°C, 1300 rpm for 10 minutes was used to vigorously mix this sample followed by cooling to room temperature and centrifuged for 10 minutes at $1400 \times g$. The protein extracts were loaded on to precast gels with molecular weight standards (4.6 kDa- 170 kDa, PAGERULER™ pre-stained protein ladder, Thermo Scientific) and processed according to PhastSystem Electrophoresis System Operating procedure (Phaste system,

Pharmacia Biotech, QC, Canada). Finally, these gels were scanned on an Epson scanner (ON, Canada).

4.3.11 FTIR analysis

Fourier transform infrared (FT-IR) spectroscopy of the freeze dried protein solutions (both homogenized at 5000 psi for 6 cycles and un-homogenized) was carried out by using a PerkinElmer (Wellesley, MA, USA) Spectrum GX instrument equipped with DTGS detector (Deuterated Tri Glycine Sulfate) and a KBr beam splitter. The final spectrum was averaged over 16 scans with a resolution of 4 cm⁻¹ in the range of 375–4000 cm⁻¹ wave numbers. All data was collected at room temperature. Deconvolution of the spectra in the amide I region was carried out using the Resolution pro software (Agilent Technologies Canada Inc., Mississauga, ON).

4.3.12 Surface hydrophobicity

Surface hydrophobicity was determined according to a modified Kato and Nakai method using a fluorescent probe 8-anilino-1-naphthalenesulfonic acid (ANS) (Kato & Nakai, 1980). Proteins were dispersed (0.025 wt%) in water by stirring overnight at 4°C, and further dilutions of 0.005%, 0.010%, 0.015% and 0.020% protein were made using water. For each protein concentration, 20 µl of 8 mM ANS solution was added to 1.6 mL; vortexed for 10 s and kept in the dark for 5 min. Fluorescence intensity was measured using a spectrofluorometer (FluroMax-4, Horiba Jobin Yvon Inc., Edison, N.J., USA) with excitation and emission wavelengths of 390 and 470 nm, respectively (slit widths 1 nm). Fluorescence intensity values for the ANS and protein blanks were subtracted from the fluorescence intensity of the protein solutions containing ANS. The initial slope (S_o) of the plot of the fluorescence intensity against protein concentration was calculated by linear regression analysis and used as an index of the protein surface hydrophobicity (S_o-ANS).

4.3.13 Zeta potential

Zeta potential was determined by measuring the electrophoretic mobility (U_E) of protein solutions (0.05%, w/w) was determined using a Zetasizer Nano-ZS90 (Malvern Instruments, Westborough, MA, USA). Zeta potential (ζ) was calculated using Henry's equation (eq. 4.1):

$$U_E = 2\varepsilon \zeta f(\kappa\alpha) / 3\eta \quad (\text{eq. 4.1})$$

where, ϵ is the permittivity, η is the dispersion viscosity and $f(\kappa\alpha)$ is a function related to the ratio of particle radius (α) and the Debye length (κ). For this study, the Smoluchowski approximation $f(\kappa\alpha)$ of 1.5 was considered.

4.3.14 Intrinsic fluorescence of protein solutions

A spectrofluorometer (FluoroMax-4, Horiba Jobin Yvon Inc., Edison, N.J., USA) was used to determine the intrinsic fluorescence for 0.01 wt% protein solutions. A constant excitation wavelength of 295 nm (slit width 2.5 nm) and an emission range between 300 to 450 nm (slit width 5.0 nm, increment of 0.5 nm) was used to determine the selective fluorescence spectra of aromatic amino acid tryptophan.

4.3.15 Statistics

Samples were prepared, and experiments were performed with at least three replicates. Student's T test for independent samples was applied to determine the statistical significance at a 95% confidence level using SPSS software (SPSS Inc., ver. 22, 2013, Chicago, IL).

4.4 Results and discussion

4.4.1 Droplet Size Distribution

In Figure 4.4.1 droplet size distribution of mixed-protein NEs (MPEs) prepared with 1:1 ratio of SC and PPI are compared with the NEs made with individual proteins as a function of protein type and storage time. The average droplet diameters (d_{32}) of the NEs at various total protein concentrations were also plotted as a function of time in Figure 4.4.2. From Figure 4.4.1 it can be observed that the SC nanoemulsions (SCE) have a fine monomodal distributions ranging from 30 nm to less than 1 μm at all concentrations. In accordance with this observation, their d_{32} values were in the range of 150-200 nm (Figure 4.4.2). Therefore, it can be said that using the present conditions it is possible to develop SC-stabilized NEs. However, this was not quite the case with PPI emulsions (PPIE). From Figure 4.4.1 it can be observed that these emulsions display bimodal distribution accounting for very large d_{32} values (not shown). Of the two peaks, however, the smaller one falls right within the range of 0.1-1 μm , indicating a portion of the PPIE falls within the NE range.

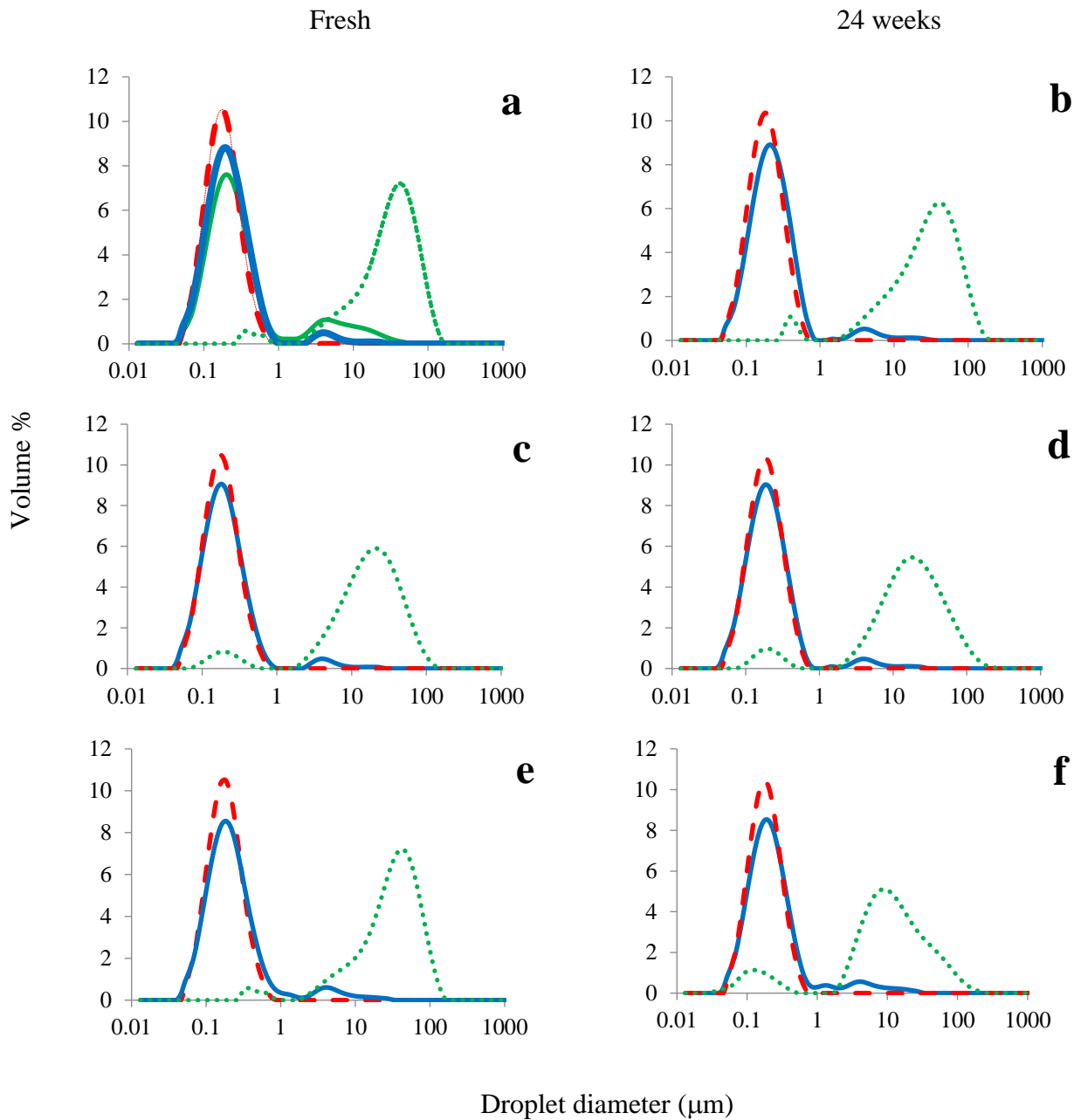


Figure 4.4.1 Droplet size distributions of 5 wt% canola oil-in-water nanoemulsions stabilized with sodium caseinate (SC) (---), pea protein isolates (PPI) (.....) and 1:1 mixture of SC and PPI (mixed protein, MP) (—). Freshly prepared emulsions (a, c, e) and at the end of 24 weeks (b, d, f) are compared with total protein concentration of 5 wt% (a) and (b); 7.5 wt % (c) and (d); 10 wt% (e) and (f). The additional curve (—) represents 5 wt% PPI emulsion diluted with SDS.

The larger peak in the range of 10 – 100 μm could be due to the presence of flocculated or coalesced oil droplets or due to the presence of aggregates of excess un-adsorbed PPI in the continuous phase. To confirm this, PPIEs were diluted 5 times with 0.1% SDS solution to deflocculate the oil droplets before measuring their droplet size distribution. It was observed that with the addition of SDS solution, the distribution shifted towards NE range with a large peak ranging between 0.1-1 μm (shown in Figure 4.4.1a) and a small peak between 1 – 10 μm due to protein aggregation. This confirmed that the initial larger second peak of PPIE was due to droplet flocculation and protein aggregation and not due to any coalescence. Therefore, the oil droplets in the PPI emulsions were actually in the range of NE but were flocculated. The droplet size distributions of the MPEs were also bimodal (similar to SDS added PPIE), with the larger peak overlapped with SCE, indicating formation of NEs with mixed proteins. The small second peak in the range of 1 – 10 μm is due to the presence of un-adsorbed aggregated PPI in the continuous phase. The d_{32} of these MPEs were calculated from the first major peak responsible for droplets alone (so that the protein aggregates do not contribute towards d_{32}) and is reported in Figures 4.4.2. It can be seen that the d_{32} for these MPEs is also well below 200 nm, indicating that the 1:1 mixture of SC and PPI was able to produce NEs. From Figure 4.4.2, it can also be observed that the NEs prepared from various concentrations of SC and MP did not show any significant change in their d_{32} values as a function of time ($p > 0.05$) making stable over a period of 24 weeks. PPIEs comparison was not included in Figure 4.4.2, due to their incorrect d_{32} values owing to the presence of large protein aggregates. The effect of protein concentration on NE droplet size can also be seen from Figure 4.4.2. For SC as the concentration increased from 5 to 10 wt%, d_{32} changed from $157.3 \pm 15.3 \mu\text{m}$ to $152 \pm 13.3 \mu\text{m}$ ($p > 0.05$).

For MPEs, d_{32} values of freshly prepared emulsions were 164.7 ± 8.2 , 155.3 ± 12.7 and $162.33 \pm 16.2 \mu\text{m}$ for 5, 7.5 and 10 wt% total protein concentrations, respectively. Overall, d_{32} values for SCEs were lower than MPEs, although no statistically significant ($p > 0.05$).

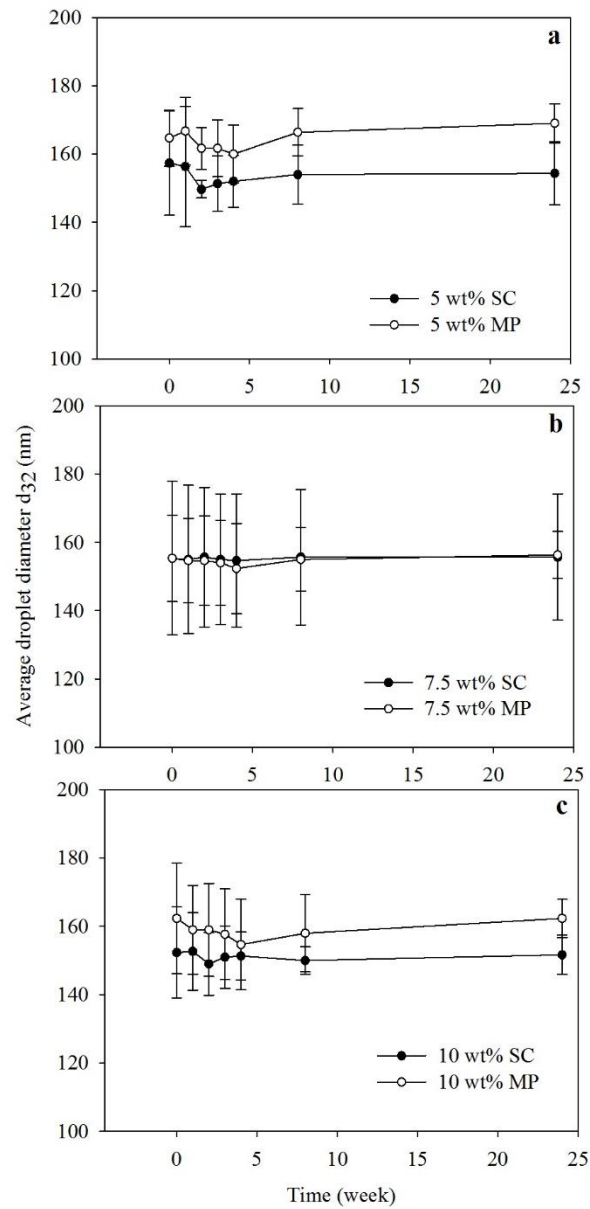


Figure 4.4.2 Change in surface mean droplet diameter (d_{32}) as a function of time for 5 wt% canola oil-in-water nanoemulsions stabilized at a total protein concentration of 5 wt% (a); 7.5 wt % (b) and 10 wt% (c) with sodium caseinate (SC) (●) and 1:1 mixture of SC and pea protein isolate (PPI) , (MP) (○). d_{32} values considered for this figure are taken from the first peak of droplet size distribution alone.

4.4.2 Visual observation of nanoemulsions

Visual observation was carried out to understand the flow behaviour and stability of the NEs. Figure 4.4.3 shows the images of MPEs in comparison with SCEs and PPIEs at a similar load after 24 weeks of storage. It can be observed that all SCEs have a distinct cream layer which increased with increase in protein concentration. Although the PPIEs did not display creaming, it was seen that these emulsions were excessively thick and formed some kind of structure throughout the tube.

The 2.5 wt% PPIE formed a thick layer leaving clear aqueous phase at the top. 7.5 wt% and 10 wt% PPIEs were very viscous and not flowable. In order to record this behaviour, the vials containing PPI emulsions were laid flat on benchtop for 30 seconds and their images were captured (Figure 4.4.3, bottom vials). It can be observed that flowability decreased with increase in PPI concentration and the 10 wt% PPIE did not flow at all. In contrast to the individual protein-stabilized NEs, the MPEs showed very little or no creaming, looked stable and flowable.

4.4.3 Viscosity

In order to obtain a quantitative estimation of the flow behavior, viscosity of the NEs was measured at 5 wt% protein concentration (Figure 4.4.4). It can be observed that the PPIE displayed maximum viscosity of the three NEs followed by SCE and MPE. As a function of shear rate viscosity of SCE and ME did not change significantly, indicating Newtonian fluid-like behaviour, while PPIE showed considerable shear thinning or pseudoplasticity indicating structure formation that broke down during application of shear. Very high viscosity of PPIE compared to the other two NEs is also consistent with the visual observation experiments (Figure 4.4.3) and their large particle size distribution owing to protein aggregation (Figure 4.4.1). No difference in viscosities of SCE and MPE was observed.

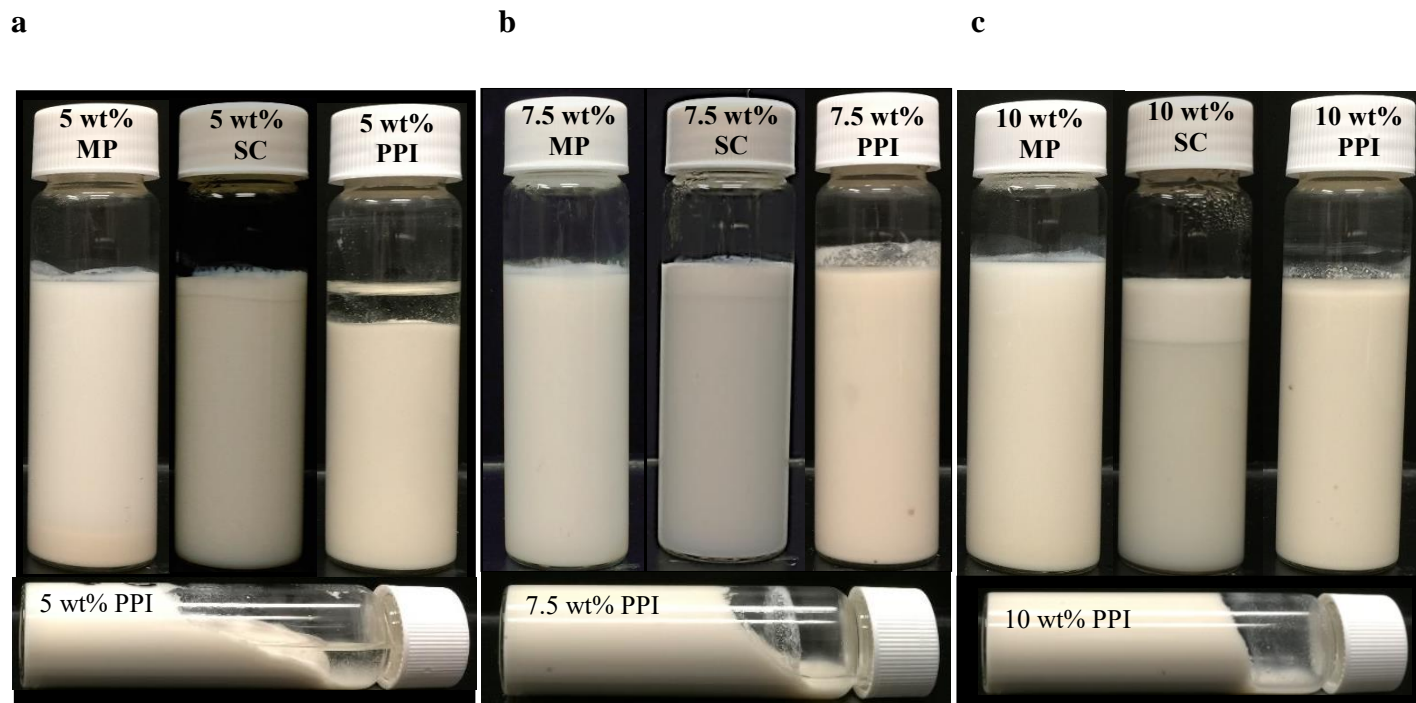


Figure 4.4.3 Visual observation of oil-in-water nanoemulsions after 24 weeks of storage. Samples of emulsions stabilized by 1:1 mixture of sodium caseinate (SC) and pea protein isolates (PPI) (mixed protein, MP), and individual proteins at (a) 5 wt%, (b) 7.5 wt% and (c) 10 wt% total protein concentrations. Horizontal vial images at the bottom indicates the flowability of PPI emulsions at various concentrations.

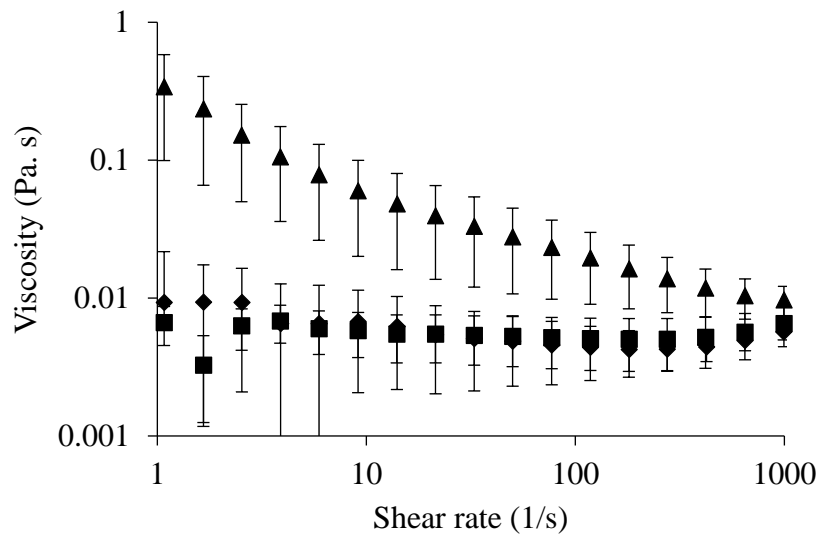


Figure 4.4.4 Viscosity of freshly prepared nanoemulsions stabilized with various concentration of sodium caseinate (SC) (■), pea protein isolates (PPI) (▲) and 1:1 mixture of SC and PPI (MP) (◆). Error bars represents \pm standard deviation of the average data (n =3).

4.4.4 Creaming Index

No creaming was observed in the case of PPIEs due to excessive flocculation and protein aggregation throughout the emulsion in the glass vials. However, some creaming was observed for both SCEs and MPEs. Creaming indices of SCEs and MPEs at similar protein load was plotted as a function of time in Figure 4.4.5. For SCEs, significant drop in creaming index was observed during the first week of storage ($p < 0.05$) and the extent of drop increased with increase in SC concentration. Nevertheless, after the initial drop, during first week the creaming indices did not change with time ($p > 0.05$) except for 10 wt% SCE ($p < 0.05$) where maximum creaming was observed after 1-2 weeks of storage, followed by a gradual increase in creaming index due to compression of cream layer with time. As a contrast, for MPEs, very little change in creaming index was observed at all protein concentrations ($p > 0.05$) and it remained constant as a function of time. Moreover, with creaming indices very close to 1 even at high protein load, it can be said that MPEs were very stable to creaming.

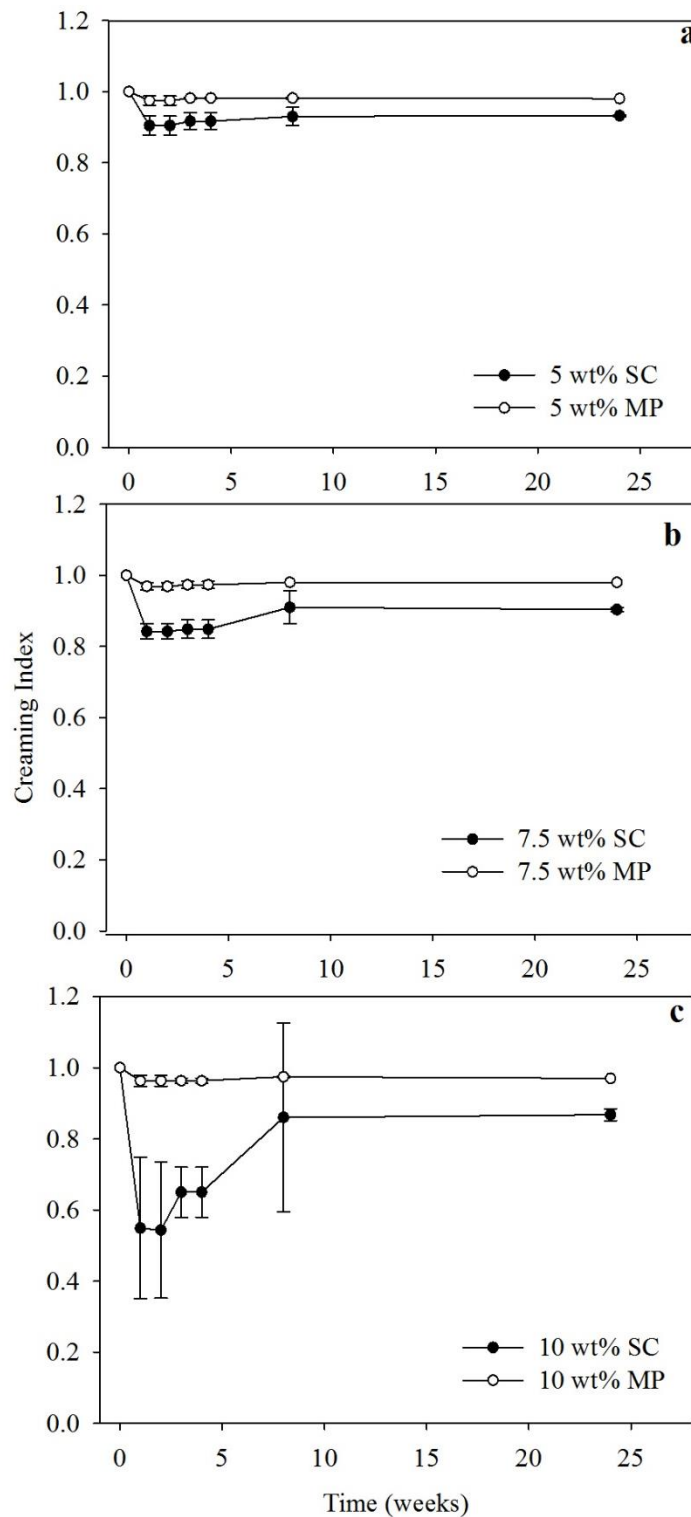


Figure 4.4.5 Change in Creaming index of nanoemulsions stabilized with a total protein concentration of (a) 5 wt%; (b) 7.5 wt % and (c) 10 wt% sodium caseinate (SC) (●) and 1:1 mixture of sodium caseinate and pea protein isolate (MP) (○).

4.4.5 Microstructure

Confocal laser scanning micrographs of freshly prepared NEs are shown in Figure 4.4.6. As a representative case, microstructure of 5 wt% MPE was compared with 5 wt % SCE and PPIE. The sample tubes were gently mixed to re-disperse any cream layer and protein aggregates before using it for microscopy. To identify the components of the nanoemulsions, 0.01 wt% Nile red and 0.01 wt% fast green was added to the oil droplets and the protein aggregates, respectively. In the micrographs, the oil droplets were tagged red and the protein green. In the case of SCE (Figure 4.4.6a), it can be observed that nanodroplets were extensively flocculated and formed clusters in a green background representative of soluble casein protein in the aqueous phase. The extensive aggregation of nanodroplets could be due to depletion flocculation by excess SC in the aqueous phase, reported previously in chapter 3 (Yerramilli & Ghosh 2016a). In contrast to SCE, the PPIE (Figure 4.4.6b) displayed large aggregates of flocculated droplet in association with pea protein aggregates. The highly viscous nature of these emulsions (Figure 4.4.4) could be due the presence of such large aggregates of proteins and oil droplets. In contrast to both SCE and PPIE, neither flocculated droplets nor any large aggregates of pea can be seen in MPE (Figure 4.4.6c).

It is possible that during high-pressure homogenization presence of SC was able to breakdown and interact with the PPI aggregates making it more soluble. In order to test this hypothesis equal volume of 5 wt% PPIE and 5 wt% SCE was mixed to create post-homogenized emulsions and its micrograph was recorded (Figure 4.4.6d). It can be seen that the microstructure of the post-homogenized mixed emulsions were very similar to the PPIE, namely, presence of large aggregates of droplets and protein particles. This highlights the critical importance of co-homogenization of PPI and SC that leads to remarkably improved stability of MPE.

4.4.6 Protein surface load and surface composition

Surface load was calculated to estimate the amount of different types of proteins adsorbed on the oil droplets. In Figure 4.4.7 surface load of all NEs were plotted as a function of total protein concentration (Figure 4.4.7). Surface load values obtained for SCEs were in accordance to that reported in the literature ($\sim 3 \text{ mg/ m}^2$) (Dickinson & Golding, 1997; Hunt & Dalgleish, 1994).

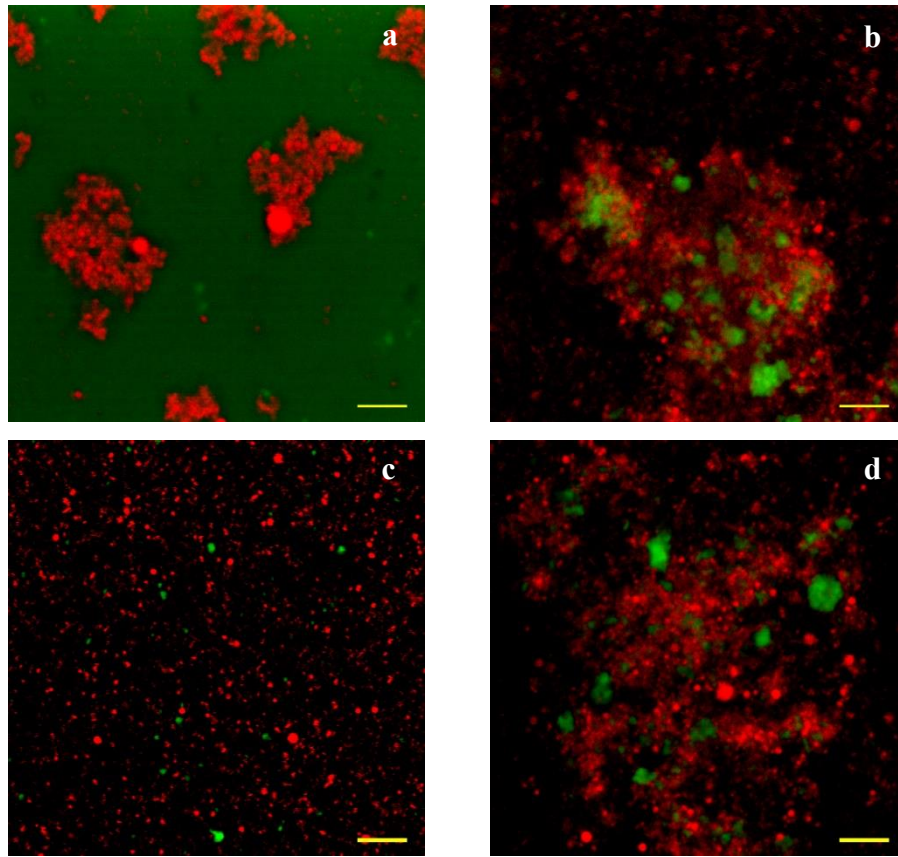


Figure 4.4.6 Confocal laser scanning micrographs of freshly prepared (a) 5 wt% sodium caseinate (SC) nanoemulsion, (b) pea protein isolate (PPI) nanoemulsion, (c) 5 wt% mixed protein (1:1 of SC:PPI) nanoemulsion and (d) emulsion made up by mixing 1:1 ratio of 5 wt% SC and 5 wt% PPI nanoemulsions. All images captured at a working magnification of 600 \times with a 5 times digital zoom. Nanoemulsions' oil phase was stained with 0.01 wt% Nile red, and the proteins were stained with 0.01 wt% fast green. Scale bars represent 5 μ m.

Overall, surface load increased with increase in protein concentration except for SCEs, which showed a plateau beyond 7.5 wt% total protein. It can also be observed that the droplets of PPIEs have the highest surface load amongst all NEs, while droplets of SCEs have the least. In case of MPEs, the surface load falls between that of SCE and PPIE, with values closer towards SCE, indicating that the interface of MPEs were composed of both SC and PPI, and it is likely richer in SC than PPI.

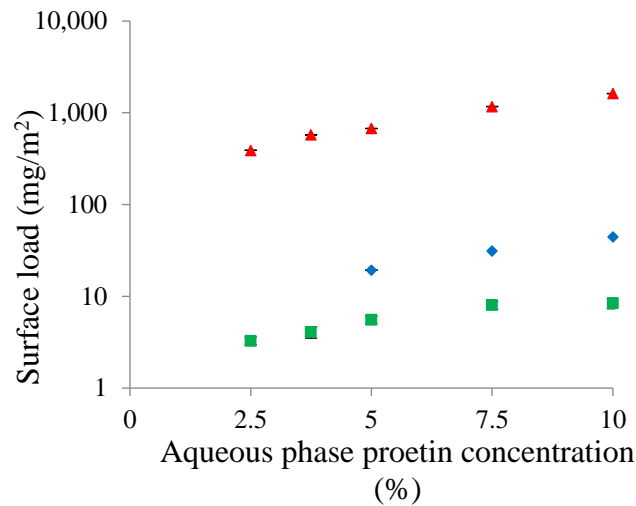


Figure 4.4.7 Surface load of freshly prepared nanoemulsions stabilized with various concentration of sodium caseinate (SC) (■), pea protein isolates (PPI) (▲) and 1:1 mixture of SC and PPI (MP) (◆). Error bars represent \pm standard deviation of the average data (n = 3).

In order to confirm whether PPI indeed took part in the nanodroplet formation in presence of SC, SDS-PAGE of the proteins separated from the interface (obtained from the cream layer) of the MPEs were analyzed (Figure 4.4.8). As a reference SDS-PAGE of the serum layer of all NEs were also performed. Lane 1 represents the molecular weight markers taken as reference for the gel. Lanes 3 and 4 represent the serum and cream phase from the MPE. Lanes 2 and 5 represent the serum phase run from PPIE and SCE respectively, taken as control. It can be seen that the cream phase from MPE (lane 4) has bands in the range of 72-95 kDa (highlighted in red), which indicate a probable presence of pea at the interface. This can also be confirmed from lane 2, where pea shows visible bands in the range of 72-95 kDa, which are otherwise not discernably present in sodium caseinate (lane 5). Also, stronger appearance of band at 23 kDa from the cream phase of MPE indicates the presence of sodium caseinate too at the interface.

The high pressure homogenization treatment applied to these proteins during the development of NEs was found to disrupt them into smaller ones (explained in detail in consequent section). Hence assignment of individual components of proteins (like pea leguminin, pea vicilin, α -casein, β -casein) is difficult, since the extent of disruption is not known through the scope of

this work. Hence, from the SDS-PAGE run, the presence of pea at the interface confirms the fact there along with SC there is some PPI that is participating in oil droplet formation and stabilization.

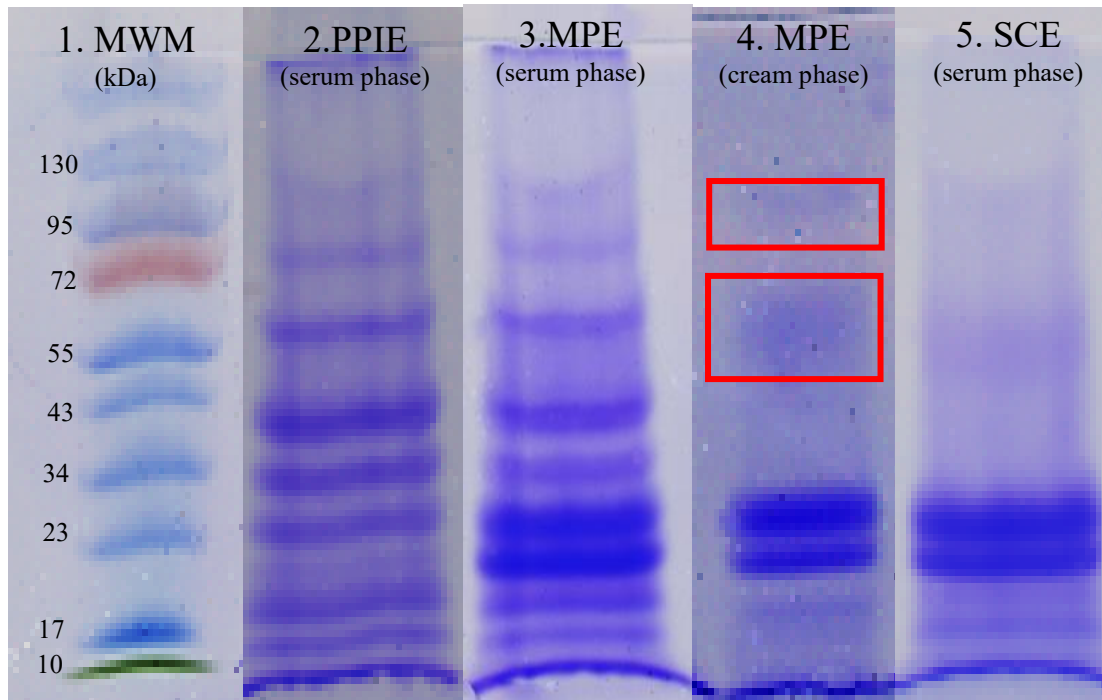


Figure 4.4.8 SDS-PAGE of separated serum phase and cream phase from the nanoemulsions. MWM on Lane 1 represents molecular weight marker, with pre-stained standards ranging from 10 kDa to 130 kDa. Lanes from left to right (2-5) represent serum phase from 5 wt % PPI nanoemulsion (PPIE), serum phase from 5 wt % mixed protein nanoemulsion (MPE), protein extracted from cream phase of 5 wt % mixed protein nanoemulsion (MPE), serum phase from 5 wt % sodium caseinate nanoemulsion (SCE).

4.4.7. Mechanism of improved stabilization of mixed-protein nanoemulsions

The MPEs developed in this research, showed overall better stability in terms of creaming behaviour, microstructure and long-term visual observation compared to their individual counterparts: SCEs (displayed depletion-induced destabilization) and PPIEs (extensive aggregation between droplet and protein that also enhanced viscosity and gel-like behaviour). Using surface

load analysis and SDS-PAGE of interfacial protein from MPE we showed that both the PPI and SC took part in stabilizing the droplets in the MPEs. However, the average oil droplet sizes of SCEs are still smaller or equal to the MPEs, indicating that it is not the droplets, but the unadsorbed proteins in the continuous phase of MPEs might played an important role in preventing the destabilizing mechanisms seen in SCEs and PPIEs. Previously, attempts have been made by researchers to develop emulsions with SC in combination with other proteins, whey protein (WP) being one of the most commonly used (Ye, 2008, 2011). Results have indicated that in a 1:1 binary system containing SC and WP, depletion interaction was unchanged with or without the presence of WP, and hence the stability and creaming rate of these emulsions were governed by the presence of unabsorbed SC in the system. Similarly, when SC was combined with xanthan and maltodextrin (Liang et al., 2014), higher viscosity of the continuous phase due to the presence of gums prevented creaming in these systems, but did not have any effect on depletion-induced droplet flocculation. In the present case, the presence of a plant-based protein (PPI) had positive influence on both the creaming stability and depletion flocculation of the MPEs. This inhibition of creaming-induced phase separation in the MPEs could be due to a number of reasons. First, presence of excess PPI could increase the viscosity of the continuous phase. However, from Figure 4.4.4, we have seen that viscosity of MPE was similar to the SCE. Second, presence of PPI could increase the depletion interaction leading to the formation of strong inter-droplet network, thereby improving the stability against creaming. However, confocal microscopy showed no flocculation in MPE, hence, this possibility is also not valid. Third, during high-pressure homogenization, large insoluble aggregates of PPI are subjected to intense shearing action leading to disintegration into small soluble particles which may improve their emulsion stabilization ability. To demonstrate this effect we used confocal microscopy to visualize the microstructure of protein solutions before and after homogenization (Figure 4.4.9). It can be seen that there is significant reduction in the size of the protein when subjected to homogenization. These results are in accordance to the previous study by (Donsì et al., 2010) also using PPI. From Figure 4.4.9, it can also be seen that the effect of particle size reduction is similar in both systems (PPI and MP). Why, then the microstructure of the two emulsions was so different? One possible reason could be re-aggregation of PPI by hydrophobic interaction in presence of oil droplets in PPIE.

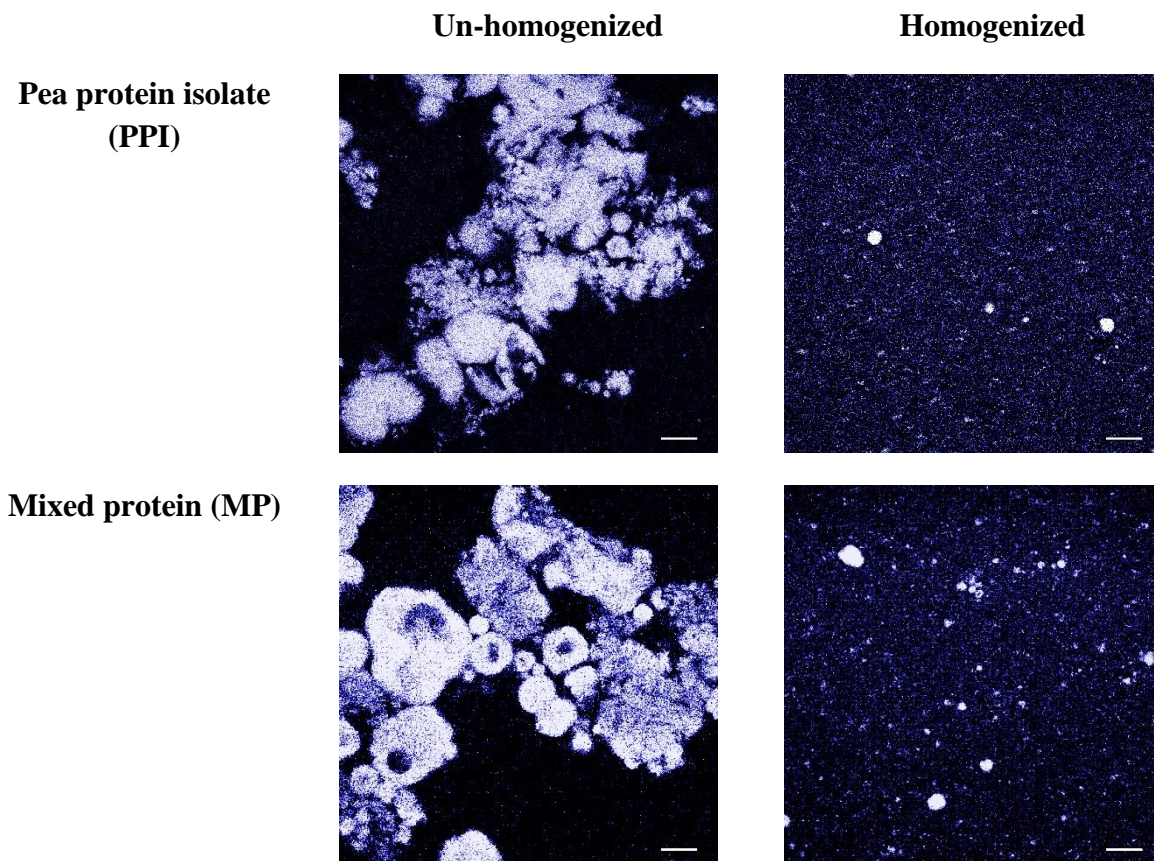


Figure 4.4.9 Confocal laser scanning micrographs of solutions (homogenized and un-homogenized) of pea protein isolate (PPI), 1:1 mixture of SC and PPI (MP). Fast green (0.01 wt%) was used to stain these protein solutions. Working magnification of 600 \times . Scale bar represents 20 μm .

In case of MPEs, mutual presence of both the proteins during homogenization might have resulted in SC stabilizing the smaller PPI particles in the continuous phase resulting in enhanced solubilisation. The soluble PPI-SC moieties prevent further aggregation of PPI seen in PPIEs. Engaging SC in the continuous phase also prevented it from inducing depletion flocculation as seen in SCEs.

It should also be noted that for depletion flocculation to happen there is an optimum size ratio of droplet to polymer in the continuous phase. Redford and Dickinson (2004) showed that strongest depletion would happen for a droplet diameter to polymer size ratio of 10:1. Anything smaller than that would lead to too close approach of droplets such that steric and electrostatic repulsion dominates. For larger size polymer depletion interaction would decrease and beyond a

critical size it may disappear which is probably the case for PPI-SC interactions. If this hypothesis is true, interaction between the two proteins should affect their original conformation, which should be detectable at secondary and/ or tertiary level.

In order to confirm whether the interactions between SC and PPI were at secondary structure level, FTIR spectroscopy was performed on these samples. FTIR spectroscopy has been widely used to determine the changes in secondary structure of proteins when subjected to high pressure homogenization and adsorbed at the oil droplet interface (Corzo-Martínez et al., 2015; Fang & Dalgleish, 1997; Lee et al., 2009; Subirade et al., 1998). Subirade et al. (1998) were the first to use the deconvoluted amide I FTIR spectra to study the changes in beta-lactoglobulin conformation under dynamic high pressure treatment (0-1400 bar) using a homogenizer. When deconvoluted, changes in intensity or shift in the individual components of α -helix, β -sheets or random coil structure in the amide I region (1600 to 1700 cm^{-1}) indicates a possible modification or change in the protein conformation. The authors found that β -sheet was the major structural element at all pressures and overall high pressure had no significant effect on the structure of β -lactoglobulin. However, when whey protein adsorbed on emulsion droplet interface, higher homogenization pressure led to decrease in α -helix and increase in β -sheet, indicating more interactions with protein molecules rather than with lipids (Lee et al., 2009). In the present work, as we are mostly interested in SC and PPI interactions in the continuous phase, hence these proteins were mixed, homogenized (similar to the making nanoemulsions) and freeze-dried to preserve their conformation before collecting the FTIR spectra (Figure 4.4.10). The assignment of the deconvoluted amide I spectral bands was established based on previous studies on proteins (Subirade et al., 1998). It can be seen that amide-I bands for homogenized mixed protein are located at positions very close to those observed for un-homogenized protein, although the intensity of β -sheet at 1630 cm^{-1} , random coil and α -helix bands have significantly decreased in the homogenized mixed protein. Some shift in peaks in the β -turn region (1775-1688 cm^{-1}) was also observed. Therefore, it can be inferred that high-pressure homogenization, although did not create any new conformation, certainly suppressed the structural features when SC interacted with PPI.

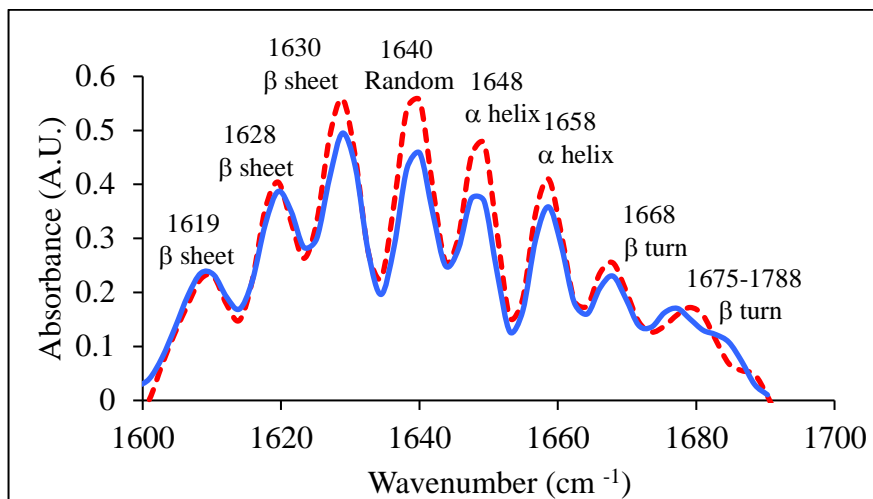


Figure 4.4.10 Deconvoluted amide I region of FT-IR spectra of freeze dried protein solution containing mixed protein (1:1 mixture of SC and PPI) mixed protein un-homogenized (---) and homogenized (—).

If the two proteins interacted and formed a new entities their overall molecular organization and exposure of hydrophobic amino acid should also be affected. In order to confirm we measured their surface hydrophobicity and intrinsic fluorescence at 5 wt% level with or without high-pressure homogenization. As a control, individual proteins solutions were also taken into consideration. Surface hydrophobicity is a measure of exposure of hydrophobic amino acids in the protein chain, which were otherwise buried within the interior (Avramenko et al., 2013). From Figure 4.4.11a, it can be seen that surface hydrophobicity (expressed in arbitrary units of S_0 -ANS) significantly increased upon high-pressure homogenization of the protein solution. PPI had highest surface hydrophobicity of all and it increased from 93.96 ± 2.94 to 111.11 ± 4.03 ($p < 0.05$), while for SC, it increased from 23.36 ± 1.70 for un-homogenized to 38.13 ± 2.56 for homogenized solution ($p < 0.05$). For mixed protein solution, the values are in between SC and PPI and increased from 44.09 ± 4.77 to 74.42 ± 3.20 upon homogenization. Similar increase in surface hydrophobicity with homogenization pressure was also seen by others (Bouaouina et al., 2006; Smith et al., 2000). It was proposed that high-pressure homogenization did not change the native protein structure, as we have seen using FTIR spectra (Figure 4.4.10), rather, the increase in surface hydrophobicity could be due to the disruption of large aggregates into smaller ones leading to exposure of buried hydrophobic amino acids. Zeta potential of the protein solutions was also

measured in order to determine the effect of homogenization on protein molecules overall charge (Figure 4.4.11b).

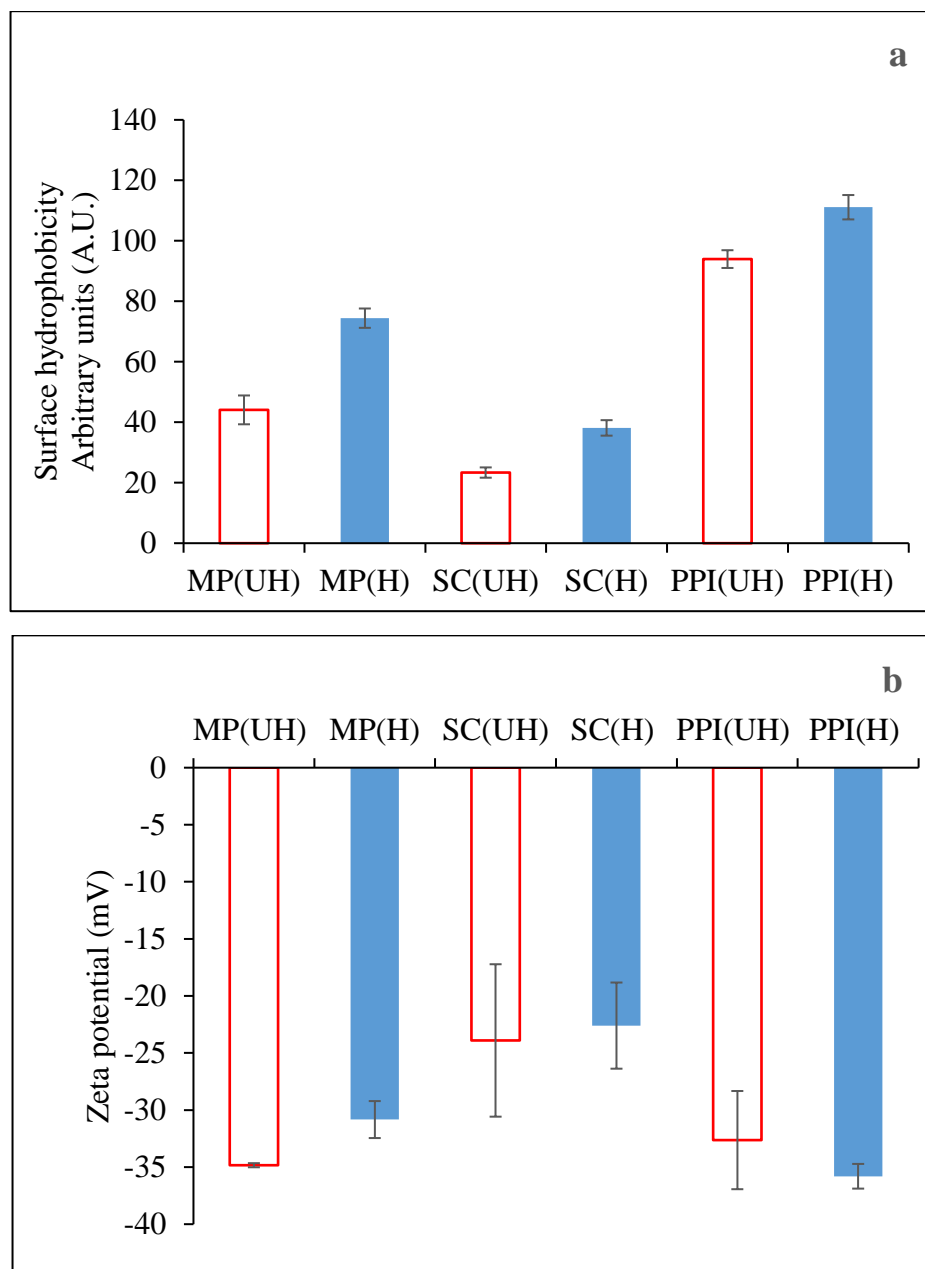


Figure 4.4.11 (a) Surface hydrophobicity expressed in arbitrary units at an excitation and emission wavelengths of 390 nm and 470 nm, respectively and (b) Zeta potential expressed in mV of mixed protein (MP), sodium caseinate (SC) and pea protein isolate; un-homogenized (UH) □ and homogenized (H) ■.

It can be seen that zeta potential did not change for SC as it is already in a random coil state while for PPI, it was higher than SC although did not change significantly due to homogenization ($p > 0.05$). For MP, high-pressure homogenization significantly decreased the zeta potential ($p < 0.05$) meaning that the charge on PPI particles are somewhat neutralized by their interaction with SC.

If the hydrophobic amino acids of the proteins are exposed due to high pressure homogenization, their fluorescence spectra might also be affected, which was tested by measuring the intrinsic fluorescence of the protein solutions. In proteins, the three aromatic amino acids, phenylalanine, tyrosine and tryptophan, give rise to distinctive fluorescent spectra, which can be used to determine structural changes in proteins. Of the three, tryptophan is the most dominant fluorophore, and its fluorescence emission is affected by changes in protein's tertiary conformation, subunit association, substrate binding, and solvent polarity (Lakowicz, 2010). Tryptophan emission is also very sensitive to collisional quenching where its fluorescence intensity is significantly reduced due to physical contact with extrinsic molecules in solvent that leads to transfer of energy from the excited indole group. In the present case, the intrinsic fluorescence of only tryptophan from the native state and homogenized protein solutions were measured at an excitation wavelength of 295 nm (Figure 4.4.12). For mixed proteins and both individual proteins, significant quenching of fluorescence intensity upon homogenization was observed, indicating exposure of tryptophan towards the surface of the protein where quenchers from the solution decrease the fluorescence intensity. Decline in fluorescence intensity upon protein hydrolysis, which exposes the tryptophan residue more towards the solvent was also seen previously (Avramenko et al., 2013). A similar phenomenon was also observed from surface hydrophobicity results (Figure 4.4.11a). In contrast, Shen et al. (2012) reported a small increase in fluorescence intensity upon microfluidization of unheated soy protein isolate although their surface hydrophobicity increased by a narrow margin. The authors proposed that initial exposure of hydrophobic domain followed by re-aggregation, although the time scale of these two processes and when the data was captured is not clear. In the present case, the extent of quenching for different protein solutions is also noted. In the present case, majority of the SC is in disordered state, hence upon homogenization not much change in protein conformation is expected, so its fluorescence quenching is also the least (Figure 4.4.12). PPI, on the other hand, is a large protein with many subunits, which was disrupted due to homogenization and the buried tryptophan

residue, become most exposed leading to the largest quenching in its intrinsic fluorescence. For mixed SC and PPI, the quenching of tryptophan emission upon homogenization is less than PPI. Here the exposed tryptophan residue from PPI is less exposed to the quenchers from the solvent due to its interaction with casein molecules. Therefore, we postulated that under high-pressure homogenization flexible and disordered casein molecules formed a layer around the disrupted PPI subunits thereby increased their dispersibility in solution (as also seen from the confocal micrograph, Figure 4.4.6).

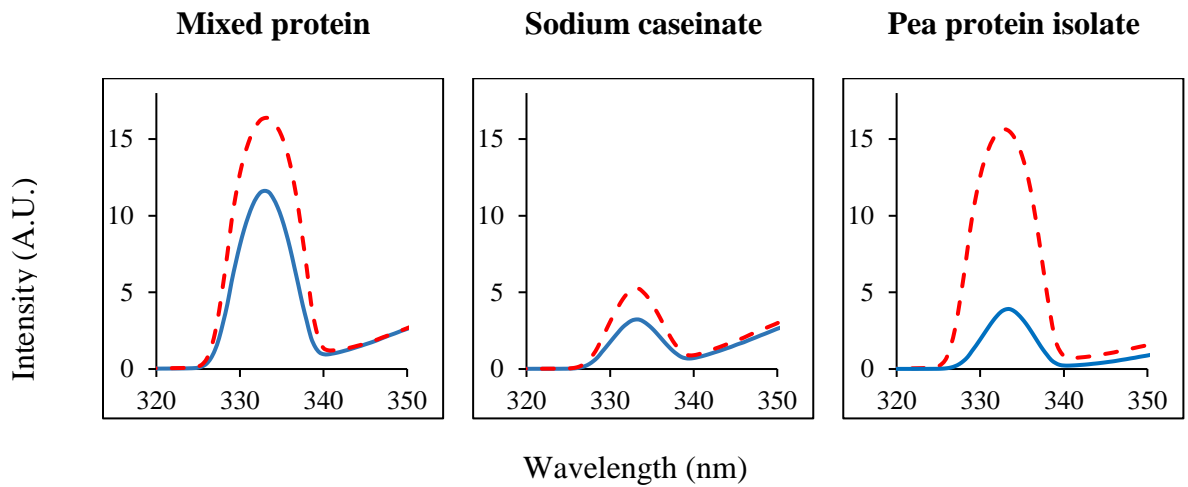


Figure 4.4.12 Fluorescence spectra of protein solutions carried out at constant excitation wavelength of 295 nm. Fluorescence is given as arbitrary units (AU) as a function of wavelength (nm). Spectra of un-homogenized (-----) and homogenized (—) protein solutions.

4.5 Conclusion

In this research, O/W NEs (MPEs) were developed with various concentrations of mixed SC and PPI as emulsifiers in 1:1 ratio. NEs prepared with SC and PPI alone were also developed and used as control. The MPEs displayed better stability when compared to their individual counterparts (SCEs and PPIEs). They remained stable over the 6 months storage period with no change in droplet size. While the SCEs displayed depletion-induced destabilization, the PPIEs displayed extensive aggregation and enhanced viscosity. Surface load analysis and SDS-PAGE of interfacial protein from MPE showed that both the PPI and SC took part in stabilizing the droplets in the MPEs. It was hypothesised that the mutual presence of PPI and SC in the case of MPEs,

resulted in their stability. Confocal microscopy confirmed that, high-pressure homogenization resulted in significant reduction of larger PPI aggregates to smaller ones.

It was hypothesised that PPI-SC aggregates present in the continuous phase of these MPEs, prevent further aggregation of PPIs, as observed in the PPIEs. Also, the size of the mixed protein aggregate is such that it does not induce depletion as observed in the case of SCEs.

To test for any possible interactions between the SC and PPI (during high-pressure homogenization) that would possibly induce structural changes at secondary level, FTIR spectroscopy was performed on these samples. It was seen that high-pressure homogenization did not alter the secondary structure of these proteins. However, surface hydrophobicity confirmed that the hydrophobicity of the protein was enhanced when subjected to homogenization. The buried hydrophobic moieties were unravelled during homogenization that facilitated in better emulsification. With the help of results from intrinsic fluorescence, we postulated that flexible and disordered casein molecules formed a coating around the disrupted globular protein, PPI thereby increased their dispersibility in the continuous phase. From the scope of this work it can be concluded that MPEs are a novel way of utilizing plant based protein. The knowledge developed from this work could be useful in understanding the effect of pre-homogenization on proteins interactions and functionality in terms of emulsification. The long-term stable MPEs can find numerous applications in food and pharmaceutical industries.

4.6 Connection to the next study

In this chapter, mixed SC and PPI-stabilized NEs was developed and their long-term stability was studied for a period of 6 months. When mutually present, SC and PPI were successful in developing NEs with droplet radii less than 200 nm that remained stable for a period of 6 months. It was also seen that the mixed protein NEs did not display any destabilization due to depletion flocculation, creaming and extensive aggregation, which were otherwise observed in the individual protein-stabilized NEs. Hence, the mutual presence of PPI and SC is a benefiting combination in terms of development of long-term stable NEs. In the next study, application of these NEs in encapsulating curcumin, a bioactive component with numerous health benefit, was investigated. Its bioaccessibility from the mixed NEs was investigated through *in vitro* digestion experiments. The efficacy of the mixed protein NEs in terms of encapsulation, delivery and bioaccessibility of curcumin was examined and compared to SC NEs.

5 EFFECTS OF PARTIAL REPLACEMENT OF SODIUM CASEINATE WITH PEA PROTEIN ISOLATE IN NANOEMULSIONS ON THE STABILITY, DELIVERY AND BIOAVAILABILITY OF CURCUMIN

5.1 Abstract

Oil-in-water nanoemulsions (NEs) containing curcumin, a polyphenolic bioactive compound were prepared using mixture of sodium caseinate (SC) and pea protein isolate (PPI) and SC as sole emulsifier and its bioaccessibility was assessed. Curcumin, a polyphenolic compound derived from the dietary spice, turmeric (*Curcuma longa*) and is known for its beneficial effects on human body including anti-tumor, anti-oxidant, anti-carcinogenic, anti-microbial, anti-inflammatory properties. Due to its poor water solubility, its bioavailability remains poor. Studies have shown that NE based delivery systems not only successfully encapsulate curcumin but also show enhanced bioavailability when compared to conventional systems. In this study, stability of curcumin in SC and mixed protein-stabilized NE was investigated for a period of 8 weeks. *In vitro* digestion studies were performed on these NEs to evaluate the bioaccessibility of curcumin through these systems. Structural changes in droplet behaviour during the course of digestion was examined through particle size measurement and confocal laser scanning microscopy. Results show that increase in droplet size during simulated digestion is a combined effect of the NEs being subjected to digestive enzymes and rapid changes in pH. Also, results from bioaccessibility study show that the mixed protein stabilized NE is as efficient as the SC stabilized NE to successfully encapsulate curcumin and deliver it to the human gut.

5.2 Introduction

Naturally occurring bioactive compounds are part of the food chain that have beneficial effect on human health (Biesalski et al., 2009). These compounds are also known as nutraceuticals, meaning that they are present as natural constituents in food and provide health benefits beyond basic nutrition (Biesalski et al., 2009). Curcumin, a polyphenolic compound derived from the dietary spice, turmeric (*Curcuma longa*), is one such bioactive compound that has been studied extensively for its numerous health benefits (Aggarwal et al., 2003; Anand et al., 2007; Sharma, 1976). Chemically curcumin is 1,7-bis (4-hydroxy- 3-methoxyphenyl) -1,6-heptadiene-3,5-dione (C₂₁H₂₀O₆), commonly known as diferuloylmethane (Figure 5.2.1) (Anand et al., 2007). It exhibits keto-enol tautomerism having a predominant keto form in acidic and neutral solutions and enol form in alkaline solutions. It is believed to have a number of beneficial biological activities in the human body; for example, anti-tumor, anti-oxidant, anti-carcinogenic, anti-microbial, anti-inflammatory properties (Ahmed et al., 2012; Anand et al., 2007; Wang et al., 2008). Traditionally turmeric has been used in curing many health ailments, more prominently in Asian countries (Anand et al., 2007; Biesalski et al., 2009). However, its lower bioavailability is one of the biggest challenges against its widespread application. Extremely low water solubility (as low as 1 ng/mL) also makes it difficult to incorporate into foods (Anand et al., 2007; Biesalski et al., 2009). However, its oil solubility is quite high and depends on the type of oil used and the source of curcumin (Tønnesen et al., 2002). Low or reduced bioavailability of any ingredient in the body could also be due to various other reasons, like poor absorption, higher metabolism rate, inactivity or rapid elimination of metabolised products from the body. Studies involving curcumin reported extremely low serum levels when administered orally and intravenously (using rat models) and established poor absorption in gastrointestinal (GI) tract and rapid metabolism of curcumin are mainly responsible for its lower bioavailability (Anand et al., 2007; Pan et al., 1999; Shaikh et al., 2009). Researchers have come up with various ways to overcome this problem. Adjuvants are compounds that block the metabolic pathway and thus improve bioavailability. Piperin is one such compound that has proven effective for curcumin (Anand et al., 2007; Shaikh et al., 2009). Nanoparticle-based delivery systems are other novel and upcoming ways to deliver and improve bioavailability of poorly water soluble curcumin (Tiyaboonchai et al., 2007). Liposomes, micelles and phospholipid complexes are among the other routes investigated for improving curcumin bioavailability (Tiyaboonchai et al., 2007).

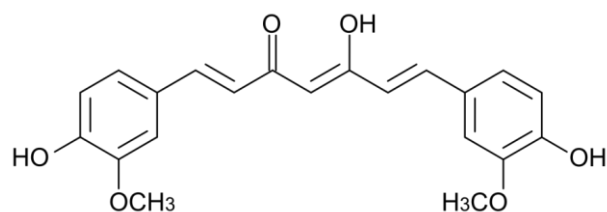


Figure 5.2.1 Chemical structure of curcumin (adapted from Anand et al., 2007)

Oil-in-water emulsion-based encapsulation techniques have been widely used to deliver and enhance the bioavailability of curcumin (McClements et al., 2007; Sari et al., 2015). A kinetically stable emulsion not only protects curcumin from light and chemicals but also successfully delivers it to the human gut (McClements et al., 2007; Sari et al., 2015). Additionally, nanoemulsion-based delivery system has been shown to further improve bioavailability when compared with conventional emulsions (Anand et al., 2007; McClements et al., 2007; Sari et al., 2015; Wang et al., 2008). A common way to determine the release of bioactives and hence their bioavailability is to use *in vitro* digestion models. However, *in vitro* release of the bioactives does not provide a real estimation of bioavailability, rather it should be taken as a measure of bioaccessibility (McClements et al., 2007). Recently, Li and coworkers (Li et al., 2012) have shown that results from *in vitro* studies were qualitatively similar when compared to *in vivo* studies. Hence, it is hypothesized that an increase in bioaccessibility should be an indication of improved bioavailability.

When designing emulsion-based delivery systems one of the most critical factors is the choice of emulsifiers and stabilizers. In this regard, food proteins have been widely utilized for their emulsification ability, innate nutritional value and general recognition as a safe ingredient (Chen et al., 2006). Proteins are also amphiphilic in nature and are regarded to be more biocompatible due to faster biodegradation by proteases (He et al., 2011b). In this regard they have been extensively used to formulate nanoemulsion-based delivery systems for poorly water-soluble bioactives (Ahmed et al., 2012; Huang et al., 2010; McClements et al., 2007). Ahmed and co-workers developed both conventional emulsions and NEs to encapsulate curcumin and study its stability using β -lactoglobulin as emulsifier (Ahmed et al., 2012). Sari and co-workers encapsulated curcumin in whey protein stabilized NEs and studied its release (Sari et al., 2015).

One of the central theme of this research is to demonstrate the application of pulse proteins

in value-added food usage. In this research the efficacy of mixed (1:1) sodium caseinate (SC) pea protein isolate (PPI) as an emulsifying agent in the development and stabilization of curcumin encapsulated NEs was investigated. All NEs were prepared with 5 wt% canola oil and 5 wt% mixture of PPI and SC in a 1:1 ratio. As a control, NEs stabilized with only SC were also examined. The release and stability of curcumin was studied for a period of 8 weeks and its bioavailability was determined using an *in vitro* digestion model.

5.3 Materials and methods

5.3.1 Material

Canola oil was purchased from local grocery store. Milli-Q™ water (Millipore Corporation, MA, USA) was used for the preparation of continuous aqueous phase. Casein sodium salt from bovine milk or popularly referred to as sodium caseinate (SC) was purchased from Sigma Aldrich, ON, Canada. Pea protein isolate (PPI) was a generous gift from Nutri Pea Limited (Manitoba, Canada). Analytical grade sodium azide, chloroform, ethyl alcohol (95%), potassium chloride (99%), sodium bicarbonate (99.5%), hydrogen chloride (99.8%), potassium phosphate monobasic (99%), magnesium chloride (98%) , bicarbonate (99%), sodium phosphate dibasic (96%), sodium phosphate monobasic (98%), sodium chloride (99.5%), calcium chloride (96%), ammonium chloride (99.5%), Nile red and fast green were purchased from the Sigma-Aldrich Chemical Company (ON, Canada). Digestive enzymes pepsin (Pepsin from porcine gastric mucosa, Product #P7000, 800–2,500 units/mg protein), pancreatin (pancreatin porcine pancreas, Product # P8096, 1 × USP specifications), lipase (lipase type II, crude from porcine pancreas, Product # L3126), and bile salt extract (B8631, porcine) were also purchased from Sigma-Aldrich Chemical Company (ON, Canada).

5.3.2 Preparation of nanoemulsions

Preparation of aqueous phases: All the protein solutions were prepared using de-ionized Milli-Q™ water at neutral pH. The pH of the prepared protein solution (ranged between 6.8 and 7.2) was measured using a pH meter (Orion star A215, Thermo scientific, Nepean, ON, Canada).

SC and PPI solution: A 5 wt% protein stock solution was prepared by dispersing the protein in Milli-Q™ water and left overnight stirring on a bench top magnetic stirrer (VWR international,

AB, Canada) at room temperature. To this, 0.01 wt% sodium azide was added to avoid microbial contamination.

Mixed protein solution: The mixed protein (MP) solution was prepared with a 1:1 mixture of 5 wt% SC and 5 wt% PPI solutions.

Preparation of nanoemulsions: The oil phase was prepared by mixing 0.3 wt% curcumin into canola oil at 60 °C by 30 min magnetic stirring and sonicating followed by centrifugation at 14,000 g for 10 min (Sorvall RC 6+ centrifuge, F18s rotor, Thermo fisher scientific Inc., Mississauga, ON) to precipitate any un-dissolved curcumin. 5 wt% of this oil phase was mixed with aqueous phase (95 wt%) containing 5 wt% of either SC or MP on a magnetic stirrer. Coarse oil-in-water emulsions were initially prepared in a rotor/stator mixer (Polytron, Brinkmann instruments, ON, Canada) for 2 minutes at 20,000 rpm. NEs were then prepared by passing these coarse emulsions through a high-pressure homogenizer (EmulsiFlex-C3, Avestin Inc., Ottawa, ON, Canada) at 20,000 psi (137.9 MPa) for 6 cycles. As PPI was quite insoluble in water, it frequently clogged the homogenizer valves at high pressures. To avoid this, mixed protein solutions with PPI were pre-homogenized in the high-pressure homogenizer at 5,000 psi (34.5 MPa) for 6 cycles before using them for emulsification. Homogenization aided in solubilization of PPI by breaking large protein aggregates into smaller ones. Similar observation of reduction in protein size by high-pressure treatment was also reported by other researchers (Bouaouina et al., 2006; Donsì et al., 2010).

5.3.3 Emulsion storage stability

The freshly prepared NEs were stored in 40 mL clear glass vials (VWR international, AB, Canada) for creaming index and long-term stability analysis through visual observation for 8 weeks (2 months). For all the other experiments 50 mL clear polypropylene tubes (VWR international, AB, Canada) were used. All the sample vials were covered with aluminum foil since curcumin is sensitive to light and stored in dark at 4°C.

5.3.4 Droplet size distribution

The droplet size distribution of the NEs and the samples drawn from digestion experiments were determined using a static laser diffraction particle size analyzer (Mastersizer 2000, Malvern

Instruments, Montreal, QC, Canada) in accordance to the standard ISO 13320 with a relative refractive index of the dispersed to continuous phases of 1.465. Drops of NE were added to the sample dispersion unit until the obscuration index reached about 15% and the droplet size distribution and the surface mean diameter (d_{32}) was measured.

5.3.5 Stability of curcumin

Stability of curcumin that has been encapsulated in the prepared NEs was measured as a function of storage time. The stored NEs were completely destabilized using ethanol to recover curcumin encapsulated within them. 200 μ L of emulsion was treated with 10 mL of ethanol. The ethanolic extract was centrifuged at 14,000 rpm for 10 min (Sorvall RC 6+ centrifuge, F18s rotor, Thermo fisher scientific Inc., Mississauga, ON). The supernatant was taken to measure the absorbance at 425 nm using a UV–VIS spectrophotometer (cuvette containing pure ethanol was taken as blank) (Beckman Life sciences DU 530, Mississauga, ON) based on the protocol developed in previous studies (Taylor & McDowell, 1992; Tikekar et al., 2013). To reconfirm, a preliminary scan of absorbance of curcumin was performed and the peak was obtained at 425 nm. Absorbance of solutions extracted from NEs was then converted into curcumin concentration by using a standard calibration curve that was prepared by using known concentrations of curcumin in ethanol.

5.3.6 *In vitro* digestion model

The *in vitro* digestion model used in this study simulated the stomach and small intestine. It was adapted from Hur et al. with slight modifications (Hur et al., 2009). The compositions of the simulated, gastric, duodenal and bile juices are listed in Table 5.3.1. To simulate the stomach 25 mL of simulated gastric juice (SGJ) (pH 2-3) was added to 10 mL of NE in a beaker and the mixture was mixed for 2 h at 37 °C in swirling motion (90 rpm) on a shaking water bath to simulate the motility of the GI tract (Model G76, New Brunswick scientific Co, Edison, NJ, USA). After that gastric emptying was done where contents from the simulated stomach were emptied into a beaker containing simulated intestinal juice (SIJ) mimicking small intestine and the contents were mixed in the same shaker for 2 h at 37 °C. The SIJ consisted of 25 mL of duodenal juice, 15 mL of bile

juice and 5 mL of bicarbonate solution (pH 6.5–7). Digestion beakers were covered with aluminum foil and the process was carried out in a dark room with minimal light exposure to the samples.

Table 5.3.1 Constituents and their concentration for simulated gastric, duodenal and bile juices used in the *in vitro* digestion model.

	Gastric juice	Duodenal juice	Bile juice
Inorganic components	15.7 mL NaCl (175.3 g/L) 3.0 mL NaH ₂ PO ₄ (88.8 g/L) 9.2 mL KCl (89.6 g/L) 18 mL CaCl ₂ ·2H ₂ O (22.2 g/L) 10 mL NH ₄ Cl (30.6 g/L) 6.5 mL HCl (37 wt%)	40 mL NaCl (175.3 g/L) 40 mL NaHCO ₃ (84.7 g/L) 10 mL KH ₂ PO ₄ (8 g/L) 6.3 mL KCl (89.6 g/L) 10 mL MgCl (25 g/L) 180 µL HCl (37 wt%)	30 mL NaCl (175.3 g/L) 68.3 mL NaHCO ₃ (84.7 g/L) 4.2 mL KCl (89.6 g/L) 150 µL HCl (37 wt%)
Enzymes	2.5 g pepsin	9 g pancreatin 1.5 g lipase	30 g bile salts

5.3.7 Determination of bioaccessibility

After *in vitro* digestion, the contents from the beaker were centrifuged at 30,000 g at 25 °C for 30 minutes in a ultracentrifuge (Sorvall RC 6+ centrifuge, F18s rotor, Thermo fisher scientific Inc., Mississauga, ON), where it was separated into three phases; an opaque sediment phase at the bottom (representing undigested matter), a clear micelle phase in the middle, and sometimes an oily phase at the top. Aliquots (5 mL) of the micelle phase (containing any dissolved curcumin) were collected using a syringe, vortexed with 5 mL of chloroform, and then centrifuged at 1200 g at 25 °C for 10 minutes (Sorvall RC 6+ centrifuge). The bottom chloroform layer was collected and the top layer was vortexed with another 5 mL of chloroform to repeat the extraction. Finally, the chloroform with curcumin was analysed by UV–VIS spectrophotometer (cuvette containing pure chloroform was used as a blank) (Beckman Life sciences DU 530, Mississauga, ON). The concentration of curcumin extracted from the micelle phase was then determined from a previously prepared calibration curve made with dissolving known amount of curcumin in chloroform.

5.3.8 Confocal laser scanning microscopy

Microstructure of the NEs during different stages of digestion was recorded by a Nikon C2 confocal laser scanning microscope (CLSM) with a 60× Plan Apo VC objective lens (numerical aperture 1.4) (Nikon, Mississauga, ON, Canada) using 488 and 543 nm lasers to excite fast green and Nile red, respectively. NEs for microscopy experiment were prepared by replacing curcumin in the oil phase with a lipophilic fluorescent dye Nile red (0.01 wt%) and fast green (0.01 wt%) was added to the emulsion after it was prepared (to stain the aqueous phase proteins). Simulated *in vitro* gastric and intestinal digestion was carried out based on the protocol discussed earlier. In order to understand the influence of enzymes (pepsin, pancreatin and lipase), digestion was carried out with and without the enzymes. Samples for microscopy were drawn at the beginning and at the end of the digestion process for both stomach and small intestine.

5.3.9 Statistics

Samples were prepared, and experiments were performed with at least three replicates. Student's T test for independent samples was applied to determine the statistical significance at a 95% confidence level using SPSS software (SPSS Inc., ver. 22, 2013, Chicago, IL).

5.4 Results and discussion

5.4.1 Droplet size and visual observation of curcumin encapsulated nanoemulsions

The droplet size distributions of freshly prepared and 8 weeks old NEs stabilized by 5 wt% SC and mixed protein (1:1 ratio of SC and PPI) are showed in Figure 5.4.1. It can be observed that there is no change in the droplet size in presence of curcumin as a function of time. Both mixed protein-stabilized nanoemulsion (MPE) and sodium caseinate-stabilized nanoemulsion (SCE) have a fine monomodal distributions ranging from 30 nm to less than 1 μm . The average droplet diameters (d_{32}) of the MPE and SCE was plotted as a function of time in Figure 5.4.2. In accordance with their distribution, their (d_{32}) values were also less than 200 nm making them nanometric in range. The NEs did not show any significant change in their d_{32} values ($p > 0.05$) as a function of time making them stable over a period of 8 weeks. It should also be noted that average droplet size of MPEs (158.6 ± 12.42 nm) were smaller compared to SCEs (190 ± 26.96 nm) ($p < 0.05$). Visually, these NEs had a yellow shade attributing to the presence of curcumin (Figure 5.4.3). SC stabilized

NEs developed a cream layer due to depletion flocculation in these systems (discussed in detail in chapter 3) (Yerramilli & Ghosh 2016a) while mixed protein-stabilized NEs showed sedimentation of PPI after 8 weeks of storage (discussed in chapter 4) (Yerramilli & Ghosh 2016b).

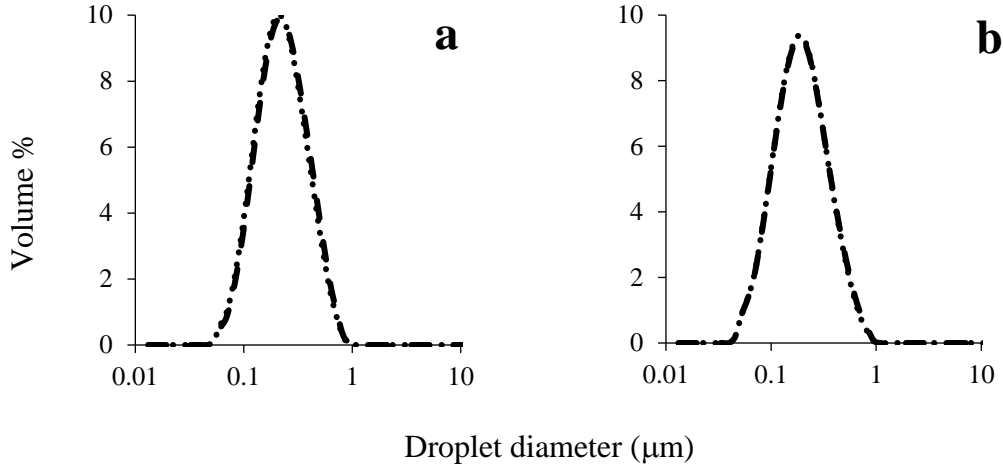


Figure 5.4.1 Droplet size distribution of 5 wt% canola oil-in water nanoemulsions with curcumin encapsulated in the oil phase and stabilized by (a) 5 wt% sodium caseinate (b) 5 wt% mixed protein (1:1 ratio of sodium caseinate and pea protein isolate). Data for freshly prepared (----) and 8 weeks old (....) samples are shown.

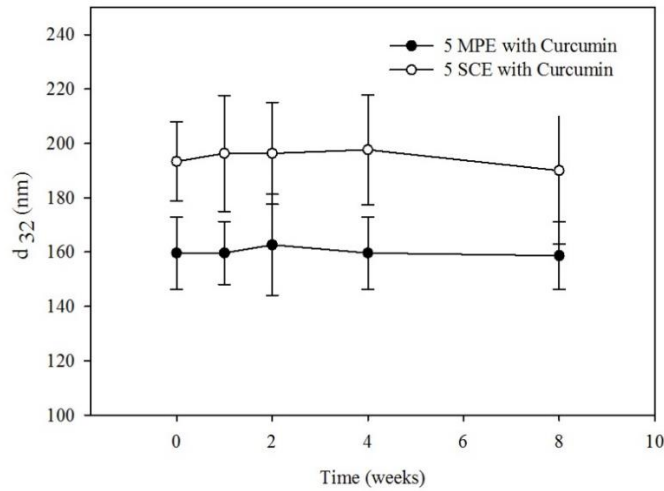


Figure 5.4.2 Change in surface mean droplet diameter (d_{32}) as a function of time for 5 wt% canola oil-in-water nanoemulsions containing curcumin and stabilized by 5 wt% mixed protein (1:1 ratio of sodium caseinate and pea protein isolate) (5 MPE) (●) and 5 wt% sodium caseinate (5 SCE) (○).

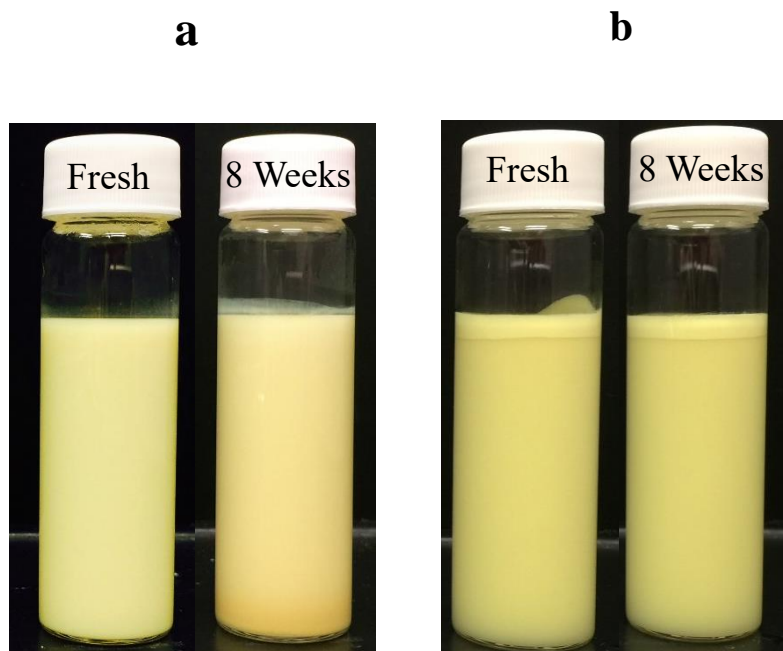


Figure 5.4.3 Visual observation of fresh and 8 weeks old oil-in-water nanoemulsions containing curcumin and stabilized by (a) 5 wt% mixed protein (1:1 ratio of sodium caseinate and pea protein isolate) and (b) 5 wt% sodium caseinate.

5.4.2 Curcumin stability in nanoemulsions

Curcumin is practically insoluble in water at acidic or neutral pH. However, it is relatively soluble at alkaline pH (Tønnesen & Karlsen, 1985) where it undergoes rapid hydrolytic degradation, giving rise to decomposition products identified as feruloyl methane, ferulic acid other minor components (Tønnesen & Karlsen, 1985; Tønnesen et al., 2002). When present in oil or other organic solvents (e.g., ethyl alcohol), curcumin was found to undergo light-induced degradations leading to discoloration (Tønnesen & Karlsen, 1985; Tønnesen et al., 2002). Hence, encapsulating it in an emulsion would expose curcumin to light to a lesser extent when compared to curcumin dispersed in oil. The emulsion droplets with their interfacial emulsifier layer would scatter light and hence curcumin would be available in active (non-degraded) form. Figure 5.4.4 shows the stability of curcumin encapsulated in SCE and MPE as a function of time. It can be seen that, although both the NEs start with the same wt% of curcumin, the amount of active curcumin in freshly prepared NEs is more in the MPE compared to SCE. This indicates that in freshly-prepared state encapsulation efficiency of the MPE was superior compared to SCE. However, over a period of 8 weeks, curcumin encapsulated in the NEs degraded (although the NEs were covered

in aluminum foil to prevent any possible exposure to light), thereby significantly reducing the active form present in the NEs. Interestingly, rate of degradation was higher for MPE (~54% reduction over 8 weeks) compared to SCE (~42% reduction). Curcumins stability in conventional emulsions and NEs has previously been investigated, however, not for a long time-frame as in this study (Ahmed et al., 2012; Tikekar et al., 2013). Although, our research showed some stability of curcumin in NEs, the amount retained in this work may not be enough to fulfil food or pharmaceutical industry's need.

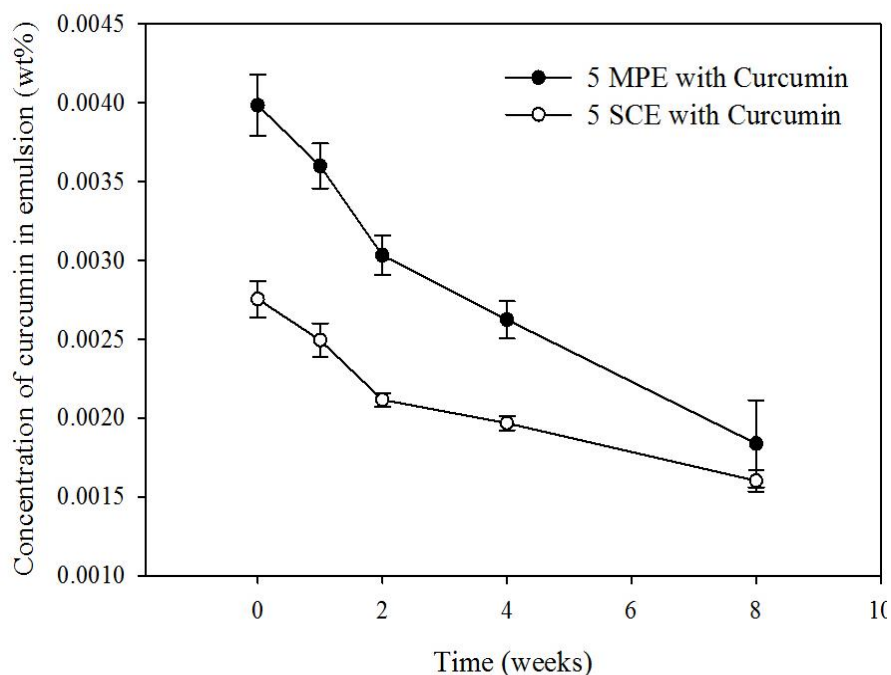


Figure 5.4.4 Stability of curcumin encapsulated in 5 wt% oil-in-water nanoemulsions stabilized by 5 wt% mixed protein (1:1 ratio of sodium caseinate and pea protein isolate) (5 MPE) (●) and 5 wt% sodium caseinate (5 SCE) (○) and as a function of time. Theoretically the NEs should have a curcumin concentration of 0.005 wt%.

5.4.3 Droplet size and microstructure of nanoemulsions during *in vitro* digestion

We characterized the change in particle size distribution of the NEs as a function of digestion steps (stomach/ small intestine) and time (Figures 5.4.5 and 5.4.6). Before entering the *in vitro* digestion system both the NEs had a fine monomodal distribution. However, as soon as they were placed in the stomach and subjected to simulated gastric juice (SGJ), the distribution becomes bimodal with a large second peak between 10 to 100 μm .

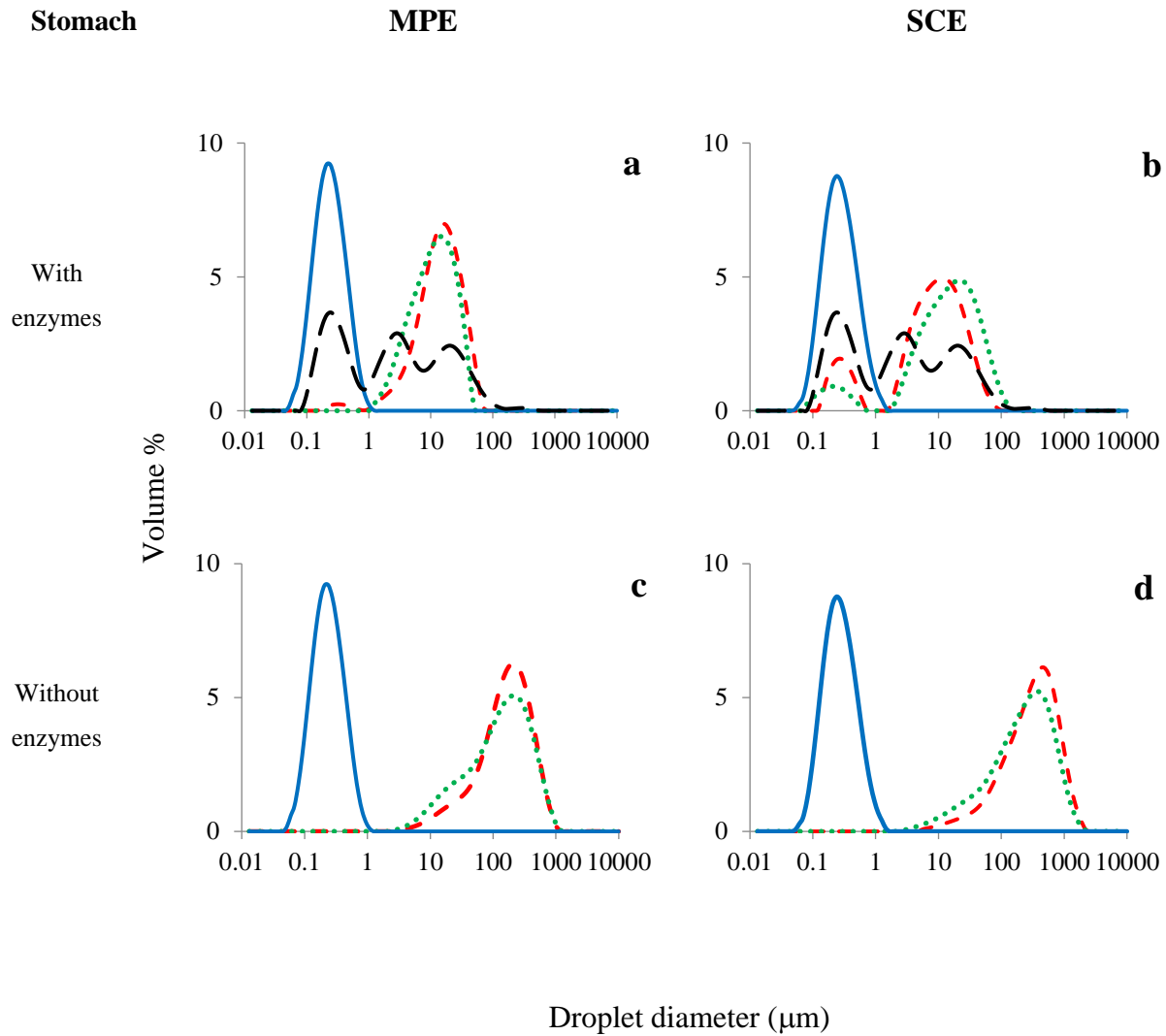


Figure 5.4.5 Change in droplet size distribution of curcumin encapsulated oil-in-water nanoemulsions stabilized by 5 wt% mixed protein (1:1 ratio of sodium caseinate and pea protein isolate) (MPE) (a, c) and 5 wt% sodium caseinate (5 SCE) (b, d) as a function of digestion time with respect to various digestion steps of stomach (with and without digestive enzymes). Distribution represented as: stomach blank (----), Fresh NE (—), at the beginning of digestion 0 hour (-----), and after 2 hours of digestion (.....).

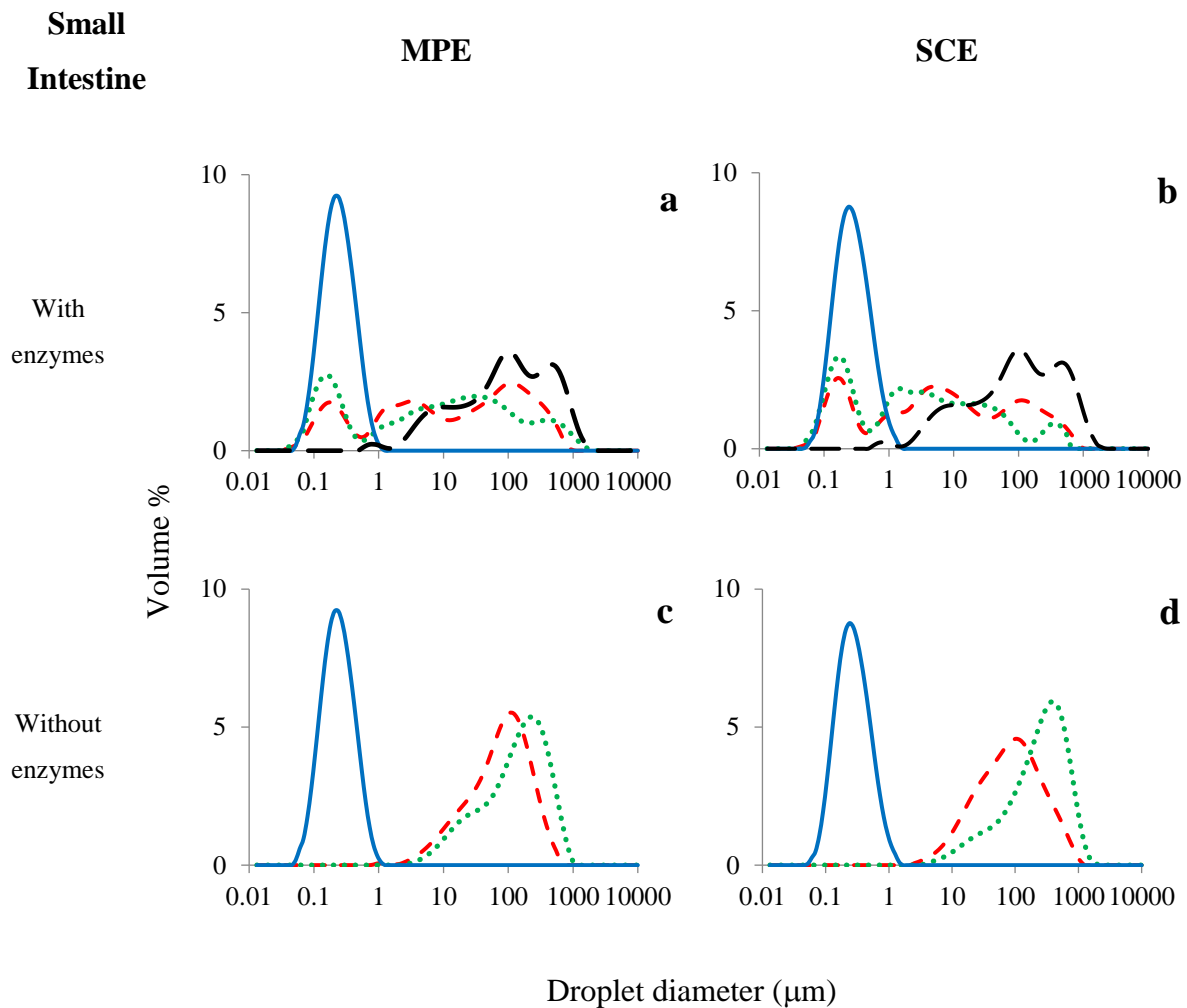


Figure 5.4.6 Change in droplet size distribution of curcumin encapsulated oil-in-water nanoemulsions stabilized by 5 wt% mixed protein (1:1 ratio of sodium caseinate and pea protein isolate) (MPE) (a, c) and 5 wt% sodium caseinate (5 SCE) (b, d) as a function of digestion time with respect to various digestion steps of small intestine (with and without digestive enzymes). Distribution represented as: small intestine blank (----), Fresh NE (—), at the beginning of digestion 0 hour (----), and after 2 hours of digestion (.....).

This increase in droplet size distribution could be due to extensive droplet aggregation as soon as the NEs were placed in the acidic condition of SGJ, which was also confirmed using CLSM (Figure 5.4.7a and b). After 2 hours of stomach digestion, the small droplets from MPE disappeared and only the large droplet peak remained (Figure 5.4.5a). For SCE, however, both peaks were observed and the second peak shifted towards larger droplet size (Figure 5.4.5b). The peak shift towards the large droplet peak indicates either droplet aggregation or increase in droplet size or both when the NEs were subjected to digestion under the acidic conditions of SGJ. Similar behavior of emulsion droplet size increase was also observed by Sarkar and co-workers (2009) during SGJ digestion of β -lactoglobulin stabilized oil-in-water emulsions. By dispersing the digested emulsions in SDS buffer to remove any flocs before measuring their droplet size distribution, the authors confirmed that the increase in droplet size was due to coalescence (Sarkar et al., 2009). Although our NEs and experimental set up were different, the impact of digestion is similar where emulsion droplets coalesced when subjected to SGJ. The pepsin present in the SGJ proteolyzed the protein adsorbed on the droplet surface and un-adsorbed in the continuous phase. The peptides generated during proteolysis are much smaller than the intact protein, therefore, the protective effect of the interfacial protein was reduced, subjecting the droplet to flocculation and eventual coalescence (Sarkar et al., 2009). The coalescence of droplets with SGJ can also be confirmed using CLSM where large droplets and protein aggregates were distinctly visible (Figure 5.4.7c and d). It should also be noted that, if present in its native form, protein is less susceptible to proteolysis caused due to pepsin (Sarkar et al., 2009). Since, the proteins present here were subjected to high pressure homogenization, there is an alteration in their tertiary structure (explained in detail in chapter 4) (Yerramilli & Ghosh 2016b), making the hydrophobic residues available for proteolysis.

Although we have seen presence of large coalesced droplets and protein aggregates in confocal micrographs, it was still not clear whether it was due to the action of the digestive enzymes or simply the effect of salts and pH of the SGJ. In order to understand the true effect of digestive enzymes, control '*in vitro* digestion' experiments were performed without the enzymes. It can be observed that the NEs 'digested' without the enzymes (Figure 5.4.5c and d) showed a large peak at even bigger droplet size compared to the samples digested with enzymes (Figure 5.4.5a and b).

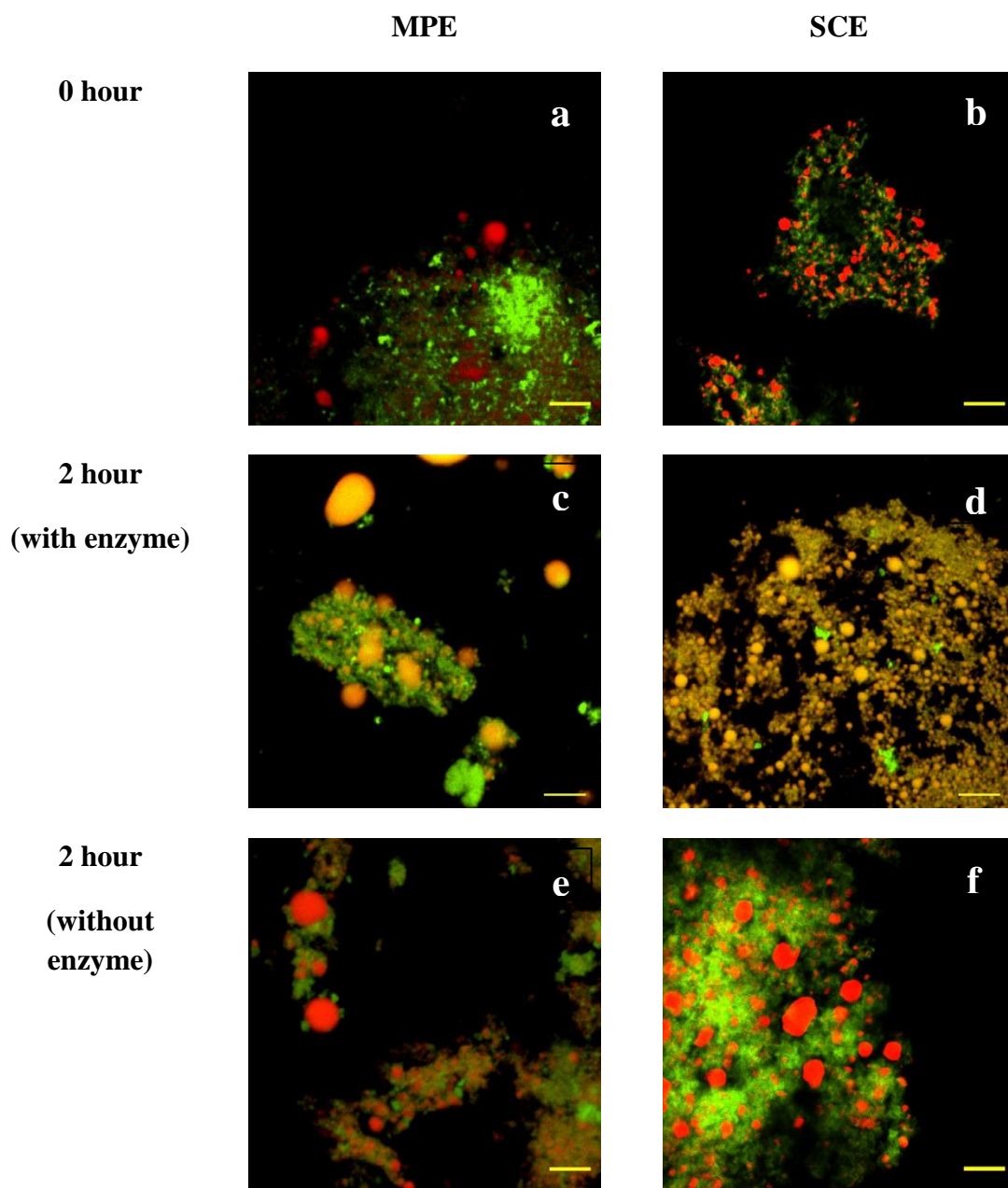


Figure 5.4.7 Confocal laser scanning micrographs from simulated gastric digestion of 5 wt% mixed protein and sodium caseinate stabilized nanoemulsions as a function of digestion time; 0 hour (a, b), after two hours of digestion (c, d), after two hours of digestion without enzymes (e, f). Micrographs captured at a magnification of 600X, with a 5 times digital zoom. Scale bar represents 5 μm .

This could be attributed to the absence of pepsin in the former, without which large protein and droplet aggregates remains in the medium, although we were not able to capture such differences in the confocal micrographs (Figure 5.4.7e and f). The results from droplet size distribution and CLSM suggest that the increase in droplet size during simulated gastric digestion is a concomitant effect of the presence of digestive enzymes and the influence of rapid changes in pH and ionic strength of the SGJ (Pinheiro et al., 2013; Sarkar et al., 2010).

The change in droplet size distribution was significant when the NEs were transferred from stomach to small intestine where they were subjected to simulated intestinal juice, SIJ). Once subjected to SIJ the droplet size distribution of both MPE and SCE became multimodal with a significant decrease in the smaller droplet size peak in the region 0.1 to 1 μm (Figure 5.4.6a and b), owing to the number of changes happened during the course of digestion where the contents of the stomach were passed to the small intestine. Interestingly the peaks at large droplet size were much smaller compared to the SGJ digested samples. From the CLSM of small intestine samples (Figure 5.4.8a and b) it can also be observed that for both MPE and SCE the aggregates of large droplets seen in stomach disappeared and while some large protein aggregates are still present at the beginning of intestinal digestion (Figure 5.4.7a and b). The decrease in the amount of lipid droplets can be partially attributed to dilution when the mixture of emulsion and the SGJ was added to the SIJ (Hur et al., 2009). Disappearance of droplet aggregation upon mixing with intestinal fluid can be due to drastic increase in pH of the system where the droplets charge changes from near zero or positive at low pH of stomach to highly negative at neural pH of intestine. Hur et al. (2009) observed that the zeta potential of emulsions stabilized with casein and whey proteins changed from near zero and positive, respectively in stomach condition to highly negative in intestine condition. After 2 hours of intestinal digestion, the droplet size distributions for both NEs shifted towards small size peaks although they still remained multimodal, indicating generation of small droplets due to lipolysis of larger ones by lipase and pancreatic lipase enzymes (Figure 5.4.6a and b).

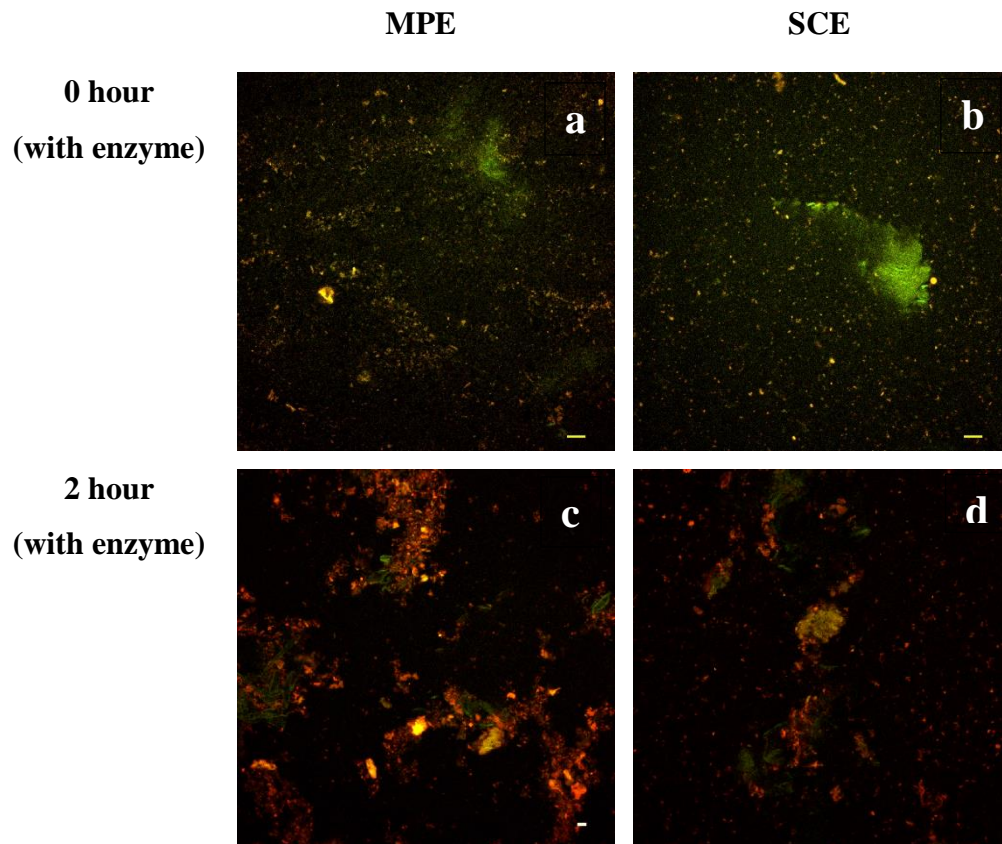


Figure 5.4.8 Confocal laser scanning micrographs from simulated intestinal digestion as a function of digestion time; 0 hour (a, b), after two hours of digestion (c, d) with enzymes. Micrographs captured at a magnification of 600X. Scale bar represents 10 μm .

The microstructure of the digested samples showed some aggregated droplets and undigested proteins and other materials while no difference between the two NEs were observed (Figure 5.4.8c and d). Similar shift in droplet size distribution was also observed by Hur et al. (2009) during *in vitro* digestion of emulsions stabilized by casein and whey proteins. Here the change in droplet size can be attributed to the action of bile salts, which are strong anionic surface active components present as mixed micelles in the aqueous phase, but rapidly adsorb to the oil droplet surface displacing interfacial proteins (Maldonado-Valderrama et al., 2008). Bile salts also promote action of lipases on lipid droplets and aid in pancreatic protease activity by altering the structure of proteins (Nik et al., 2010). Bile salts also help in the adsorption of lipid digestion products (e.g., free fatty acids, monoglycerides etc.) as well as any nonpolar bioactive presents in

the lipid droplets. It should be noted that the confocal micrographs of our samples after intestinal digestion (Figure 5.4.7c and d) appeared a bit different compared to reports from other authors. For example, many authors showed presence of perfectly spherical droplets of emulsions, although smaller and less, even after 2 hrs of gastric and 2 hrs of intestinal digestion (Li et al., 2013, Hur et al., 2009). This difference could be attributed to the nanoscale droplets in our NEs (d_{32} less than 200 nm compared to more than 350 nm in other reports) and presence of excess SC and PPI (with its impurities containing starch and dietary fibers) in the continuous phase.

Similar to the stomach ‘digestion’ without any enzyme, intestinal ‘digestion’ experiments were also carried out without enzymes in order to understand the true effect of digestion. Both the droplet size distribution and microstructure of the samples digested without enzymes showed presence of large aggregates owing to the action of salts on the droplet flocculation. The digestion steps without enzymes showed intact lipid droplets owing to the absence of lipase and bile salts (Figures 5.4.9c and d). Finally, although the initial stability of curcumin in MPE is higher compared to SCE under normal storage conditions, the behavior of the two different NEs under *in vitro* digestion is fairly similar. Additionally, blank experiments were carried out to measure the droplet size distribution of just the SGJ and SIJ (Figures 5.4.5a, b and 5.4.6a, b). This data reveals that the multimodal distribution of the digested NEs is not only an effect of mere droplet aggregation or coalescence during digestion, but also the effect of light scattering from insoluble enzymes and other salts present in these juices. In this regard it is also important to understand that the droplet size distribution from light scattering is not completely accurate for understanding the droplet behavior through complex digestion systems. Ideally, it could be suggested to filter out either the oil droplets or the other components in order to get a correct measure of oil droplet size. It is clear that better understanding of the process by utilizing better analytical methods is needed in order to confirm all of the above mentioned phenomena. In this context, it would be noteworthy to study the zeta potential of these solutions during digestion to have better insights of the process. Also, it is important to note that the substrate to enzyme ratio plays a crucial role in understanding the extent of digestion. It is difficult to select a ratio that mimics the exact conditions of human gastrointestinal systems as it varies among different persons (da Silva Gomes et al., 2003; Sarkar et al., 2009).

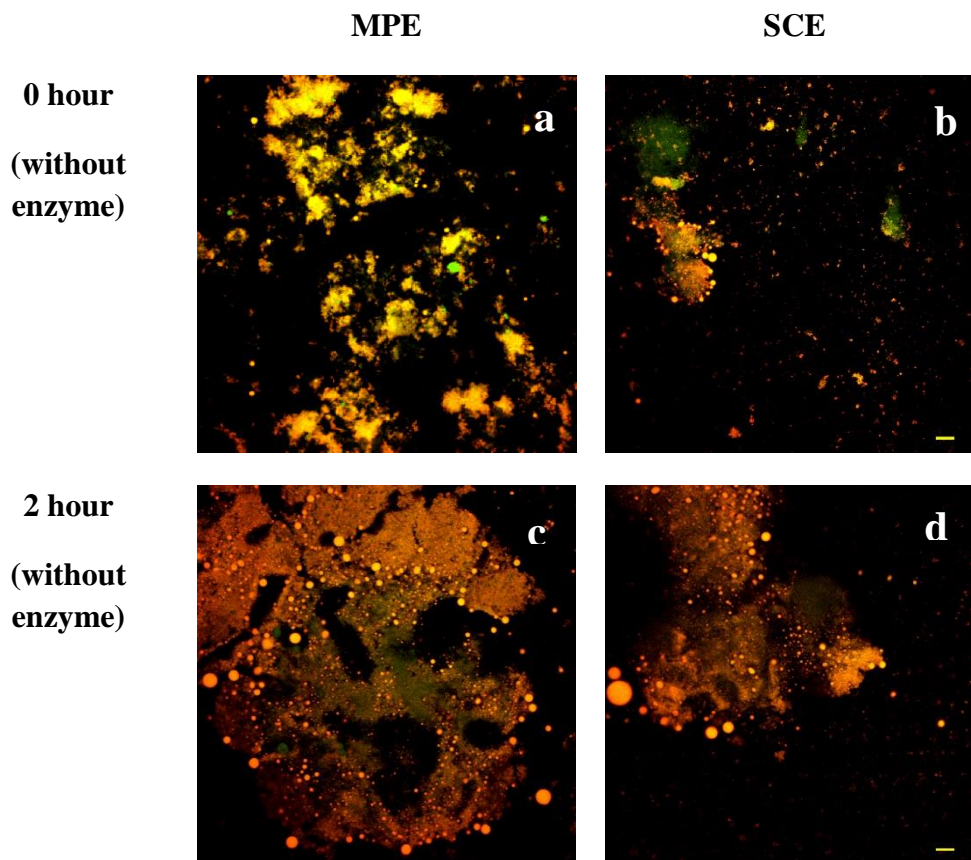


Figure 5.4.9 Confocal laser scanning micrographs from simulated intestinal digestion as a function of digestion time; 0 hour (a, b), after two hours of digestion (c, d) without enzymes. Micrographs captured at a magnification of 600X. Scale bar represents 10 μm .

Finally, the amount of lipid that gets digested through the intestine, and the interaction of the interfacial protein with bile salts and eventual replacement from the oil droplet surface depends largely on the type of bile salt and its concentration, which also differs among various models. Moreover, digestion involves complex peristaltic movements of the stomach and small intestine that cannot be mimicked by the *in vitro* systems. Overall, knowledge from this experimental set up allow us to understand the tentative behavior of the NEs when subjected to gastric and intestinal conditions in presence of two different interfacial systems.

5.4.4 Bioaccessibility

The extent of digestion of encapsulated curcumin in the gastrointestinal tract was studied through bioaccessibility from the *in vitro* model. The intestinal digest (digestion products obtained after simulated intestinal digestion) for both the MPE and SCE were collected to determine the amount of curcumin being released from the lipid droplets into the mixed micelle phase. From Figure 5.4.10, it can be observed that the bioavailability of curcumin from SCE was 52.06 ± 5.53 %, while from MPE it was 47.39 ± 1.76 % ($p > 0.05$). Although difference is not statistically significant, higher bioavailability of SCE compared to MPE could be attributed to a thicker droplet interface in the mixed protein NE (a contribution from globular protein PPI) that is less susceptible to proteolysis in the stomach as compared to SCE. Previous studies have shown that globular proteins tend to form a two-dimensional network of cross-linked molecules at the interface (Lee & McClements, 2010). This thicker interfacial layer would have consequently reduced the extent of protein displacement by bile salts in the intestine leading to less lipolysis and eventually lesser release of curcumin in the mixed micelle phase. However, it should be noted that this difference in structure was not discernable in the CLSM experiments performed in this work.

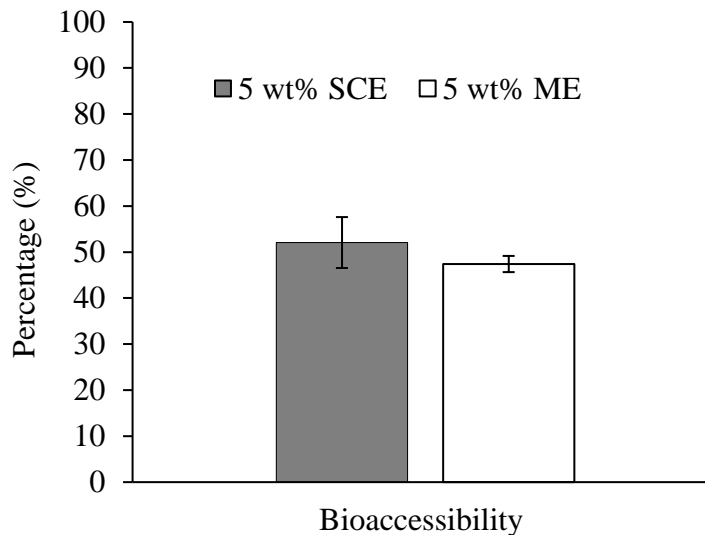


Figure 5.4.10 Bioaccessibility of curcumin from the micelle phase of 5 wt% canola oil-in water nanoemulsions after *in vitro* digestion, stabilized by 5 wt% sodium caseinate and 5 wt% mixed protein (1:1 ratio of sodium caseinate and pea protein isolate) .

Tikekar and co-workers studied the release of curcumin from silica nano particle stabilized oil-in-water pickering emulsions. They showed that about 60% curcumin was released after 3 hours of incubation in the intestine (Tikekar et al., 2013). Higher bioaccessibility of curcumin when compared to our systems could be attributed to the fact that they had higher incubation time and incomplete coverage of droplets by silica nano particles that would result in more digestion and hence release of curcumin. In another study, Pinheiro et al. (2013) used a human gastric simulator to determine the release of curcumin from 5 wt% oil-in-water NEs stabilized by 0.5 wt% of Tween 20, SDS and a cationic emulsifier DTAB. It was found that curcumin bioaccessibility was less than 20% for both Tween and SDS-stabilized NEs and while for DTAB it was insignificant due to extensive emulsion destabilization during digestion that led to oil phase separation. The lower bioaccessibility of their NEs compared to our system could be due to the presence of synthetic emulsifier that does not digest by pepsin and displaced by bile salt.

Studies carried out by Ahmed and co-workers suggest that there was no advantage in terms of bioaccessibility of curcumin encapsulated in NE (10 wt% oil), when compared to a conventional emulsion (Ahmed et al., 2012). Bigger droplet size and weaker interface leads to larger extent of digestion, consequently leading to increase bioaccessibility for conventional emulsions even with much smaller total interfacial area. Therefore, the thought of switching to NEs must be evaluated if bioaccessibility is the prime goal of the final application. However, the undue advantage of the NE systems is that they remain stable for a longer time and stay unaffected to major destabilization mechanisms as compared to conventional systems. As in our case, the emulsion remained stable for an experimental time frame of 8 weeks and showed potential to remain stable for a time period of 1.5 years were droplet size distribution remained unchanged (data not shown).

5.4.5 Conclusion

In this work, curcumin, a highly insoluble bioactive compound, was encapsulated in NEs stabilized by SC and mixed protein (SC and PPI in 1:1 ratio). The results from our work show that both of these NEs were successful in encapsulating curcumin and remained stable for an experimental timeframe of 8 weeks. However, the rate of degradation of curcumin was higher for MPE when compared to SCE. Structural changes in droplet behaviour during the course of digestion were monitored using CLSM and droplet size distribution. Results suggests that the

increase in droplet size during simulated digestion is a combined effect of digestive enzymes and the influence of rapid changes in pH and ionic strength of the gastric intestinal fluids. Results from *in vitro* digestion showed that both the NEs developed in this work could successfully deliver curcumin. Although not statistically significant SCE showed slightly higher bioaccessibility when compared to the MPE. Nevertheless, it should be noted that it is practically impossible to simulate the complex physiological processes that occur in the human gastrointestinal tract and there is always need for better *in vitro* digestion studies with advanced techniques. Results from this work could be useful in understanding the release of lipophilic bioactives encapsulated in NE systems for food and pharmaceutical applications.

6 GENERAL DISCUSSION

Nanoemulsions (NEs) have had remarkable progress over the last few years, in terms of research activities and application in the food industry. They were found to have numerous advantages over the conventional emulsions in terms of stability and shelf life. For beverage applications, formulating a NE and diluting it to a large extent to produce the product of desirable characteristics has been practiced. Food emulsions stabilized by proteins offer many advantages, e.g., use of natural ingredients, offer health benefits and raise lesser toxicological concerns when compared to the synthetic small molecule emulsifiers (Tweens, SDS etc.). However, usage of food proteins as emulsifiers in NEs is far more challenging than small molecules surfactants due to larger size of proteins, and their inability to readily adsorb on the droplet surface during homogenization giving rise to larger droplet sizes. Nevertheless, due to the advantages they come with, this has been taken as a challenge to develop NEs stabilized by proteins. The overall goal of this research was to develop oil-in-water (O/W) NEs stabilized by mixed sodium caseinate (SC) (a dairy protein) and pea protein isolates (PPI) (a pulse protein) and utilize them to encapsulate curcumin, a bioactive compound, and determine its stability, delivery and bioavailability through *in vitro* digestion studies. The O/W NEs in this study were prepared with canola oil and protein solution as oil (5 wt%) and aqueous phase (95 wt%), respectively.

Proteins have been widely used as emulsifiers to facilitate the formation of emulsions. They are amphiphilic in nature and thus the interfacial activity of proteins is because of the hydrophilic and lipophilic groups distributed in their structure. Food proteins, isolated from bovine milk (casein and whey proteins) are widely used as emulsifying agents in a variety of food products including beverages, ice creams, sports supplements, infant formula and coffee creamer (McClements, 2005). The sodium salt of casein, popularly referred to as sodium caseinate (SC), is essentially a soluble mixture of all four fractions of caseins (α_{s1} , α_{s2} , β and κ) (Radford & Dickinson, 2004). Due to its high solubility and well-defined hydrophobic and hydrophilic regions that help in rapid adsorption at the oil-water interface, SC has been exploited widely as an emulsifier for conventional emulsions and also NEs (Hunt & Dalgleish, 1994; Lee & Norton, 2013; Qian &

McClements, 2011; Zhao et al., 2015). Hence, as a part of the first objective, different concentration (2.5 – 10 wt%) of SC as a sole emulsifier was used in the preparation of 5 wt% oil-in-water NEs (SCEs) and their long-term stability (6 months) was investigated. Previous studies in literature, associated with SC as sole emulsifier have only looked into droplet size but did not include any long-term stability studies (Liang et al., 2014; Randford & Dickinson 2004; Zeeb et al., 2014). To our best knowledge, the present work is one of its kind to report the stability of these NEs for a period of 6 months. All the SCEs developed in this work displayed an average droplet diameter less than 200 nm and remained stable for a period of 6 months. However, they displayed rapid cream layer formation, which was weak and re-dispersible upon gentle mixing. It was proposed that the excess un-adsorbed protein present in the continuous phase of these emulsions caused depletion flocculation and eventually lead to creaming of oil droplets. Similar behaviour was reported previously in the case of SC-stabilized conventional emulsions (Dickinson & Golding, 1997; Dickinson et al., 1997).

It was found that flexible proteins like casein that have a disordered structure are most surface-active compared to the globular proteins like pea that required to be unfolded before adsorption to the interface (Dickinson & McClements, 1995). Therefore, it is considered challenging to utilize globular pulse based proteins like pea to develop NEs for long-term stable applications. As a part of the second objective, PPI was utilized to partially replace SC in the development of NEs. In the mixed protein NEs (MPEs), SC and PPI was mixed in 1:1 ratio with a total aqueous-protein concentration of 5, 7.5 and 10 wt%. Therefore the objective was to utilize pea protein and investigate its efficacy as an emulsifier. To understand the mixed protein NEs (MPEs), individual PPI stabilized NEs (PPIEs) were also prepared as control. PPI failed to produce stable flowable NEs where the average droplet diameter was greater than 200 nm and also displayed excessive droplet and protein aggregation. A unique finding of this work is that, at higher concentrations of PPI (7.5 and 10 wt%), the emulsions transformed into viscoelastic gels, which could have numerous applications in food industry. Interestingly, MPEs did not display any creaming or aggregation, although, after a month of storage these NEs displayed protein sedimentation (indication of un-adsorbed protein in the continuous phase). But, in spite of the protein sedimentation, they remained stable to flocculation throughout the experimental timeframe of 6 months with an average droplet < 200 nm. From surface load and SDS-PAGE analysis of interfacial and serum layer, the presence of PPI at the interface along with SC was confirmed

indicating that PPI aided in droplet formation of these NEs. Absence of creaming and flocculation in these MPE indicates that the mutual presence of PPI and SC not only stabilized these NEs, but also curbed creaming. Using intrinsic fluorescence and surface hydrophobicity analysis of the protein solutions, it was proposed that the presence of excess SC and PPI under high-pressure homogenization led to the disintegration of PPI (alteration in structure) subunits followed by hydrophobic interactions between SC and PPI. In order to confirm whether the interactions between SC and PPI were at secondary structure level, FTIR spectroscopy was performed on these samples. Previously, researchers have widely used FTIR to determine the changes in secondary structure of proteins when subjected to high pressure homogenization and adsorbed at the oil droplet interface (Corzo-Martínez et al., 2015; Lee et al., 2009; Subirade et al., 1998). In our work, it was seen through FTIR that the structural changes did not happen at secondary level. Therefore, the SC-PPI entity prevented depletion flocculation effect of SC and interfered with PPI aggregation thereby preventing both the destabilizing mechanisms seen in individual protein-stabilized NEs. Previous attempts have been made by researchers in order to curb depletion flocculation induced in SC stabilized conventional emulsions and NEs. In this regard, whey protein isolate (Hunt & Dalgleish, 1994), polysaccharides (maltodextrin or xanthan gum) (Liang et al., 2014), various alcohols (ethanol, 1-propanol, 1-butanol) (Zeeb et al., 2014) have been used. Present work is therefore a novel in two ways; not only did it address the issue of depletion that is very critical in protein stabilized emulsions, but also utilized pea, a pulse based, globular protein, that aided in long-term stabilization of these mixed protein stabilized-NEs.

Oil-in-water NEs have been widely perused for encapsulation of bioactive compounds not only to utilize bioactive (for their numerous advantages on human health) but also to enhance their bioavailability (McClements et al., 2007; Sari et al., 2015). A kinetically stable emulsion not only protects bioactives from light and chemicals but also successfully delivers it to the human gut. Additionally, nanoemulsion-based delivery system has been shown to further improve bioavailability when compared with conventional emulsions (Anand et al., 2007; McClements et al., 2007; Sari et al., 2015; Wang et al., 2008). As a part of the third and fourth objectives, curcumin, a polyphenolic bioactive compound, was encapsulated in the oil phase of the MPE and SC to study its stability and bioaccessibility through *in vitro* digestion studies. Curcumin is said to have a number of beneficial biological effects on the human body (Anand et al., 2007). It is an oil soluble phytochemical extracted from powdered rhizomes of turmeric spice. The challenge in utilizing

curcumin comes from its extremely low water solubility, making it difficult to incorporate into food and challenging with adsorption in the GI tract (Ahmed et al., 2012). Previous studies on curcumin indicate that NEs were successful in encapsulating and delivering this compound (Ahmed et al., 2012; McClement et al., 2007). In our work it was found that curcumin did not have any effect on the long term stability of the SCE and MPE (in terms of droplet size). The stability of curcumin in the prepared NEs was evaluated as a function of time. It was seen that over 50% of encapsulated curcumin was degraded within a storage period of 8 weeks. Structural changes in droplet behaviour during the course of digestion were monitored using confocal laser scanning microscopy and droplet size distribution. Results reveal that the increase in droplet size and rupture of interfacial protein layer during simulated digestion is a combined effect of digestive enzymes and the influence of rapid changes in pH and ionic strength of the simulated gastric fluids. *In vitro* digestion studies have also shown that the MPE is as efficient as the SCE in delivering the bioactive compound. Overall a total of about 50% curcumin was accessible for adsorption as it was found to present in the aqueous micelle phase out of the NE oil droplets. Previous studies reveal that there was no advantage in terms of bioaccessibility of curcumin encapsulated in NE (10 wt% oil), when compared to a conventional emulsion (Ahmed et al., 2012). Bigger droplet size and weaker interface leads to more digestion and an increase in the bioaccessibility for conventional emulsions even with much smaller total interfacial area. Therefore, the applicability of NEs has to be questioned if bioaccessibility is the primary goal. Nevertheless, NEs remain stable for a longer time and stay unaffected to major destabilization mechanisms as compared to conventional systems. As in our case, the emulsion remained stable for an experimental time frame of 8 weeks and showed potential to remain stable for a time period of 1.5 years were droplet size distribution remained unchanged. In conclusion, not only did the MPE show its efficacy in encapsulating curcumin, it also successfully delivered the component making it similar bioaccessible compared to SCEs.

7 OVERALL CONCLUSION

Overall, the present research developed NE-based delivery system encapsulating a bioactive component, curcumin. The NEs were developed using a mixture of dairy (sodium caseinate) and pulse proteins (pea protein isolate) as emulsifiers. The efficacy of the dual protein-stabilized NE as a delivery vehicle for curcumin was assessed via *in vitro* digestion studies where bioaccessibility of curcumin encapsulated in the NEs was determined. The mixed protein nanoemulsions (NEs) developed in this work, displayed better stability when compared to their individual counter parts i.e. sodium caseinate (SCEs) and pea protein isolate (PPIEs) NEs.

Initially, 5 wt% O/W NEs were developed with various concentrations of SC as a sole emulsifier. All the SCEs remained stable with no change in droplet size over an experimental time frame of 6 months. However, excess un-adsorbed protein in the continuous phase of these SCEs, induced reversible depletion flocculation and creaming in them. Similar behaviour was previously reported with work involving SC as emulsifier to develop conventional and nanoemulsions (Dickinson & Golding, 1997; Liang et al., 2014). Quantitative estimation of depletion interaction energy was done based on the work from Radford and Dickinson (2004). It was found that depletion attraction decreased with a decrease in droplet size reconfirming the inherent advantage of NEs against depletion induced destabilization. The thermal energy of the system was so low that, the flocs formed due to depletion broke apart upon gentle mixing thereby, un-affecting the droplet size of these NEs over the experimental time frame. The thickness of the cream layer formed due to depletion interactions increased with an increase in protein concentration. The microstructure of the flocculated nanodroplets was confirmed using confocal microscopy while the structure of the un-disturbed cream layer and its compaction was recorded using an optical microscope. Long-term stability studies were done employing a photocentrifuge. In contrast to results from visual observation, stability analysis under accelerated gravitational field of the photocentrifuge revealed that the NEs with higher SC concentration (10 wt%) had least separation. This could be due to oversaturation of the instrument detector at high protein concentration, which prevented clear detection of droplet movement.

Next, in order to utilize a pulse based protein, pea protein isolate (PPI) was incorporated by partial replacement of SC partially (in 1:1 ratio) forming, mixed protein stabilized NEs (MPEs) were developed. The efficacy of PPI in stabilizing the MPEs and their long term stability was studied in detail. Individual PPI stabilized NEs (PPIEs) were also prepared as control. PPI failed to produce stable flowable NEs where the average droplet diameter was greater than 200 nm and also displayed excessive droplet and protein aggregation. Interestingly, at higher concentrations of PPI, the emulsions transformed into viscoelastic gels, which could have numerous applications in food industry. The MPEs displayed better stability when compared to SCEs and PPIEs, they remained stable over the 6 months storage period with no change in droplet size. Results from surface load analysis and SDS-PAGE of interfacial protein from MPE confirmed that both PPI and SC took part in stabilizing the droplets in the MPEs. It was hypothesised that the mutual presence of PPI and SC in the case of MPEs, resulted in their stability. It was hypothesised that excess PPI, SC present in the continuous phase of these NEs, form a PPI-SC entity. This entity not only prevents aggregation of PPIs, as observed in the PPIEs but also fall into size range such that depletion is induced as in the case of SCEs. Results from FTIR and surface hydrophobicity confirmed that the buried hydrophobic moieties were unravelled during co-homogenization of both the protein, thereby facilitating in better emulsification. We postulated that flexible and disordered casein molecules formed a coating around the disrupted globular protein, PPI thereby increasing the dispersibility of PPI-SC moiety in the continuous phase. From the scope of this work it can be concluded that MPEs are a not only a novel way of utilizing plant based protein but also curb depletion, a major destabilization phenomenon in protein stabilized emulsions.

Finally, curcumin, a highly water insoluble bioactive compound, was encapsulated in NEs stabilized by SC and mixed protein (SCE and MPE). *In vitro* digestion was performed on these encapsulated NE to determine the bioaccessibility of curcumin and also understand the structural changes an emulsion undergoes during digestion process. Results suggest that both the NEs were successful in encapsulating curcumin and remained stable for an experimental timeframe of 8 weeks. Results from confocal laser scanning microscopy and droplet size distribution suggests that the increase in droplet size during simulated digestion is a combined effect of digestive enzymes and the influence of rapid changes in pH and ionic strength of the simulated gastric fluids. SCE showed slightly higher bioaccessibility (statistically not significant) when compared to the MPE. This could be attributed to the thicker interfacial layer of the MPEs when compared to SCEs, due

to the presence of PPI. However, it should be noted that *in vitro* studies employed in this work only aid in understanding the behavior of these emulsions under simulated conditions and that it is practically impossible to simulate the complex physiological processes that occur in the human gastrointestinal tract. Hence, results from this work help aid in understanding the tentative behavior of the NEs when subjected to gastric and intestinal conditions in presence of two different interfacial systems.

Therefore, these MPEs not only utilized a pulse protein, PPI, in the development of NEs, but also show good applicability in terms of encapsulating bioactive ingredients for prospective applications in food and pharmaceutical industries. The knowledge developed from this work could be useful in understanding the effect of protein concentration, homogenization and mutual interaction of PPI and SC on the long-term stability of NEs. In conclusion, more research is needed in order to fully understand the role of PPI in stabilizing mixed NEs and the mechanism behind their stability; and determine the actual measure of bioavailability of curcumin (through *in vivo* studies) when encapsulated and delivered through these NEs. The knowledge developed from this research could thus be applied in food, beverage, cosmetic and pharmaceutical industries.

8 FUTURE STUDIES

The nanoemulsions (NEs) developed in this work were stable for at least 6 months. Long-term stability is a very important factor for real-life applications. Hence, these NEs definitely have potential for applications in food, pharmaceutical and chemical industries. Especially because they have been formulated with just 5 wt% oil, their application in beverage industry could be very useful. Beverage emulsions are usually made up with low concentration of oil with necessary flavour components, and then finally diluted to a large extent to produce the final product (Piorkowski & McClements, 2014). All the NEs developed in this work were stabilized by proteins. Proteins being healthier and safer in comparison to their small molecule surfactant counterparts, the potential usage of these products is enhanced in the market, especially with the new ongoing trend of organic and natural foods. However, the performance of proteins could be enhanced in a number of ways, to develop product of desired characteristics.

The pea protein isolate-stabilized NEs (PPIEs) were subjected to extensive flocculation. There could be a number of ways to enhance the stability of these emulsions and hence prevent flocculation of pea. Researchers have seen that ultra-sonication is one such way to improve the stability of emulsions by opening up the proteins' secondary structure, unravelling its hydrophobic parts, thereby creating stable droplet surface (Jafari et al., 2007; Leong et al., 2009). Solvent evaporation is another technique that can be used to further decrease the droplet size of the NEs (Lee & McClements, 2010). In this method a mixture of oil and organic solvent is homogenized with aqueous solution of protein, followed by evaporation of solvent making the oil droplets to shrink and form stable nano droplets. This could be incorporated in case of globular proteins like pea, to achieve small, stable droplets.

Another interesting aspect of the PPIEs is that at higher concentrations (7.5 and 10 wt%) they transformed into viscoelastic gels. It is noteworthy how by mere addition of 5 wt% oil to a concentrated pea protein solution and homogenizing it would develop a gel that may find potential applications in low fat-food based products. However, more investigation is needed in order to fully understand this behaviour. Extensive study on their viscosity and viscoelastic behaviour is

required. The behaviour of these gelled emulsions when subjected to stress should be understood. This will make it easier to incorporate them in commercial food products that typically undergo a series of processing conditions before being available for consumer.

In case of NEs stabilized by sodium caseinate (SCEs), they were subjected to depletion flocculation due to the excess sodium caseinate that formed sub-micelle and thus induced depletion. Therefore, it is important to develop these emulsions at those concentrations of protein that would be just sufficient for the mono-layer coverage of the droplets formed, such that there is no excess caseinate in the aqueous phase that would form sub-micelles to promote depletions effects.

The mixed protein stabilized NEs (MPEs) (stabilized by 1:1 ratio of sodium caseinate and pea protein isolate) were also stable for the experimental time frame of 6 months. Additional long-term stability studies (beyond 6 months) have revealed that, they have a potential to stay stable for a really long period (droplet size distribution remained unchanged for 1.5 years). The enhancement of the stability due to mutual presence of pea and casein is a remarkable finding of this work. However, lot more investigation is needed in order to establish the exact mechanism behind the stability of these systems. Based on the studies carried out in the scope of this work we proposed that during homogenization there were interactions between pea and casein that consequently stabilized the MPEs. Techniques such as nuclear magnetic resonance and circular dichroism may reveal how these two proteins are bound to each other in the solvent under high pressure homogenization that may lead to a better idea and understanding of this novel phenomenon. The protein solutions utilized to develop PPIEs, MPEs and SCEs were pre homogenized in the high-pressure homogenization. In this regards, it would be noteworthy to investigate the effect of pre-homogenization on protein solutions at various pressures on the final stability of these NEs. This could give us an idea of what pressure promotes mutual interactions of pea and casein and the extent of interaction that leads to enhanced stability of the NEs.

Confocal scanning laser microscopy is quite a powerful tool to visualize the structure of biopolymers at micrometer scale. Covalent labelling of proteins and polysaccharides using various fluorescent dyes allows the visualisation of a specific biopolymer in a complex mixture. Additionally, multiple labelling of proteins and polysaccharides is a technique that facilitates the study of the microstructure of the mixtures of biopolymers and the simultaneous localisation of the different components (van de Velde et al., 2003). In the present case, we used separate dyes to

stain the oil and protein phases respectively. It would be interesting to stain the two proteins with separate dyes (employing the method of multiple labelling) so that any specific structural changes in pea and casein in the mixed NE could be visible. In our work, although, confocal laser scanning microscopy did reveal that homogenization significantly reduced the size of PPI, it would be worthwhile to examine the structure of homogenized and un-homogenized protein under high resolution Transmission Electron Microscopy (TEM) and/ or scanning Electron Microscopy (SEM). This might throw some light on the three dimensional structure of pea and compliment the results.

Curcumin is a promising bioactive ingredient with large potential in pharmaceutical, cosmetic and food applications. However, its poor bioavailability is an issue researchers have been trying to battle out. Of the number of ways to do this, some studies showed that an adjuvant, piperine, enhanced serum concentration, extent of absorption and bioavailability of curcumin in both rats and humans with no adverse effects (Prasad et al., 2014; Shoba, 1998). It would be certainly interesting to understand the influence of piperin on bioavailability of these curcumin from our NEs. It would be a novel way to enhance the bioavailability of curcumin from emulsions.

In vitro studies performed in this study were simple experiments to understand the solubilization of curcumin in mixed micelles from NEs stabilized by different proteins. It was certainly a way to understand weather the mixed protein would be successful in encapsulating the curcumin and delivering it as efficiently as the most commonly used casein protein. However, a wide range of *in vitro* studies could be incorporated to understand the true bioavailability of these NEs. Inclusion of simulated mouth condition in the system would enhance the sophistication of the protocol followed. TIM[®] is an *in vitro* digestion set up much more sophisticated than the traditionally followed ones (Reis et al., 2008). TIM[®] offer insight into the fate of food and food constituents during digestion in the stomach and small intestine and fermentation in the large intestine that are unique and very close to the real system. In a way, it was developed to contribute to a reduction of animal models (*in vivo* studies) to understand the behaviour of various products in human digestive system. This was also used to perform digestion studies on emulsions and NEs systems too (Pinheiro et al., 2013; Reis et al., 2008). In the present case this would also give a more accurate measure of structural changes during digestion and bioavailability of curcumin.

9 REFERENCES

- Acosta, E. (2009). Bioavailability of nanoparticles in nutrient and nutraceutical delivery. *Current Opinion in Colloid & Interface Science*, 14(1), 3-15.
- Adebisi, A. P., & Aluko, R. E. (2011). Functional properties of protein fractions obtained from commercial yellow field pea (*Pisum sativum* L.) seed protein isolate. *Food Chemistry*, 128(4), 902-908.
- Aggarwal, B. B., Kumar, A., & Bharti, A. C. (2003). Anticancer potential of curcumin: preclinical and clinical studies. *Anticancer Research*, 23(1A), 363-398.
- Ahmed, K., Li, Y., McClements, D. J., & Xiao, H. (2012). Nanoemulsion-and emulsion-based delivery systems for curcumin: encapsulation and release properties. *Food Chemistry*, 132(2), 799-807.
- Akhtar, M., & Dickinson, E. (2007). Whey protein–maltodextrin conjugates as emulsifying agents: an alternative to gum arabic. *Food Hydrocolloids*, 21(4), 607-616.
- Aleandri, R., Schneider, J. C., & Buttazzoni, L. (1968). Evaluation of Milk for Cheese Production Based on milk Characteristics and Formagraph Measures. *Journal of Dairy Science*, 72(8), 1967-1975.
- Anand, P., Kunnumakkara, A. B., Newman, R. A., & Aggarwal, B. B. (2007). Bioavailability of curcumin: problems and promises. *Molecular Pharmaceutics*, 4(6), 807-818.
- Anton, M., Le Denmat, M., Beaumal, V., & Pilet, P. (2001). Filler effects of oil droplets on the rheology of heat-set emulsion gels prepared with egg yolk and egg yolk fractions. *Colloids and Surfaces B: Biointerfaces*, 21(1), 137-147.
- Aronson, M. P. (1989). The role of free surfactant in destabilizing oil-in-water emulsions. *Langmuir*, 5(2), 494-501.

- Avramenko, N. A., Low, N. H., & Nickerson, M. T. (2013). The effects of limited enzymatic hydrolysis on the physicochemical and emulsifying properties of a lentil protein isolate. *Food Research International*, *51*(1), 162-169.
- Baldwin, E. A., Hagenmaier, R., & Bai, J. (2011). *Edible coatings and films to improve food quality*. Boca Raton, FL: CRC Press.
- Barac, M., Cabrilo, S., Pesic, M., Stanojevic, S., Zilic, S., Macej, O., & Ristic, N. (2010). Profile and Functional Properties of Seed Proteins from Six Pea (*Pisum sativum*) Genotypes. *International Journal of Molecular Sciences*, *11*(12), 4973-4990.
- Biesalski, H. K., Dragsted, L. O., Elmadfa, I., Grossklaus, R., Müller, M., Schrenk, D., Weber, P. (2009). Bioactive compounds: Definition and assessment of activity. *Nutrition*, *25*(11), 1202-1205.
- Bouaouina, H., Desrumaux, A., Loisel, C., & Legrand, J. (2006). Functional properties of whey proteins as affected by dynamic high-pressure treatment. *International Dairy Journal*, *16*(4), 275-284.
- Bouwmeester, H., Dekkers, S., Noordam, M. Y., Hagens, W. I., Bulder, A. S., De Heer, C., Sips, A. J. (2009). Review of health safety aspects of nanotechnologies in food production. *Regulatory Toxicology and Pharmacology*, *53*(1), 52-62.
- Can Karaca, A., Low, N., & Nickerson, M. (2011a). Emulsifying properties of chickpea, faba bean, lentil and pea proteins produced by isoelectric precipitation and salt extraction. *Food Research International*, *44*(9), 2742-2750.
- Can Karaca, A., Low, N. H., & Nickerson, M. T. (2011b). Emulsifying properties of canola and flaxseed protein isolates produced by isoelectric precipitation and salt extraction. *Food Research International*, *44*(9), 2991-2998.
- Chang, Y., McLandsborough, L., & McClements, D. J. (2012). Physical properties and antimicrobial efficacy of thyme oil nanoemulsions: influence of ripening inhibitors. *Journal of Agricultural and Food Chemistry*, *60*(48), 12056-12063.

- Chen, J., & Dickinson, E. (1995). Protein/surfactant interfacial interactions Part 3. Competitive adsorption of protein+ surfactant in emulsions. *Colloids and Surfaces A: Physicochemical and Engineering Aspects*, 101(1), 77-85.
- Chen, L., Remondetto, G. E., & Subirade, M. (2006). Food protein-based materials as nutraceutical delivery systems. *Trends in Food Science and Technology*, 17(5), 272-283.
- Cofrades, S., Carballo, J., Careche, M., & Colmenero, F. J. (1996). Research note: emulsifying properties of actomyosin from several species. *LWT-Food Science and Technology*, 29(4), 379-383.
- Corzo-Martínez, M., Mohan, M., Dunlap, J., & Harte, F. (2015). Effect of Ultra-High Pressure Homogenization on the Interaction Between Bovine Casein Micelles and Ritonavir. *Pharmaceutical Research*, 32(3), 1055-1071.
- Coupland, J. N., & McClements, D. J. (1996). Lipid oxidation in food emulsions. *Trends in Food Science and Technology*, 7(3), 83-91.
- da Silva Gomes, R. A., Batista, R. P., de Almeida, A. C., da Fonseca, D. N., Juliano, L., & Hial, V. (2003). A fluorimetric method for the determination of pepsin activity. *Analytical Biochemistry*, 316(1), 11-14.
- Dagorn Scaviner, C., Gueguen, J., & Lefebvre, J. (1987). Emulsifying properties of pea globulins as related to their adsorption behaviors. *Journal of Food Science*, 52(2), 335-341.
- Dahan, A., & Hoffman, A. (2007). The effect of different lipid based formulations on the oral absorption of lipophilic drugs: the ability of in vitro lipolysis and consecutive ex vivo intestinal permeability data to predict in vivo bioavailability in rats. *European Journal of Pharmaceutics and Biopharmaceutics*, 67(1), 96-105.
- Damodaran, S. (1996). *Amino Acids, Peptides, and Proteins*. New York, NY: Marcel Dekker.
- Detloff, T., Sobisch, T., & Lerche, D. (2013). Instability Index. *Dispersion Letters Technical*, T4, 1-4.

- Dhuique Mayer, C., Borel, P., Reboul, E., Caporiccio, B., Besancon, P., & Amiot, M. J. (2007). β -Cryptoxanthin from citrus juices: assessment of bioaccessibility using an in vitro digestion/Caco-2 cell culture model. *British journal of nutrition*, 97(05), 883-890.
- Dickinson, E. (1986). Mixed proteinaceous emulsifiers: review of competitive protein adsorption and the relationship to food colloid stabilization. *Food Hydrocolloids*, 1(1), 3-23.
- Dickinson, E. (1992a). Faraday research article. Structure and composition of adsorbed protein layers and the relationship to emulsion stability. *Journal of the Chemical Society, Faraday Transactions*, 88(20), 2973-2983.
- Dickinson, E. (1992b). *Introduction to food colloids*. New York, NY: Oxford University Press.
- Dickinson, E. (1994). Protein-stabilized emulsions. *Journal of Food Engineering*, 22(1), 59-74.
- Dickinson, E. (2009). Hydrocolloids as emulsifiers and emulsion stabilizers. *Food Hydrocolloids*, 23(6), 1473-1482.
- Dickinson, E., & Golding, M. (1997). Depletion flocculation of emulsions containing unadsorbed sodium caseinate. *Food Hydrocolloids*, 11(1), 13-18.
- Dickinson, E., Golding, M., & Povey, M. J. (1997). Creaming and flocculation of oil-in-water emulsions containing sodium caseinate. *Journal of Colloid and Interface Science*, 185(2), 515-529.
- Dickinson, E., Rolfe, S. E., & Dalgleish, D. G. (1988). Competitive adsorption of α s1-casein and β -casein in oil-in-water emulsions. *Food Hydrocolloids*, 2(5), 397-405.
- Dickinson, E., Rolfe, S. E., & Dalgleish, D. G. (1989). Competitive adsorption in oil-in-water emulsions containing α -lactalbumin and β -lactoglobulin. *Food Hydrocolloids*, 3(3), 193-203.
- Donsì, F., Senatore, B., Huang, Q., & Ferrari, G. (2010). Development of novel pea protein-based nanoemulsions for delivery of nutraceuticals. *Journal of Agricultural and Food Chemistry*, 58(19), 10653-10660.

- Duranti, M. (2006). Grain legume proteins and nutraceutical properties. *Fitoterapia*, 77(2), 67-82.
- Erramreddy, V. V., & Ghosh, S. (2014). Influence of Emulsifier Concentration on Nanoemulsion Gelation. *Langmuir*, 30(37), 11062-11074.
- Fang, Y., & Dalgleish, D. G. (1997). Conformation of β -lactoglobulin studied by FTIR: effect of pH, temperature, and adsorption to the oil–water interface. *Journal of Colloid and Interface Science*, 196(2), 292-298.
- Fernández-García, E., Carvajal-Lérida, I., & Pérez-Gálvez, A. (2009). In vitro bioaccessibility assessment as a prediction tool of nutritional efficiency. *Nutrition Research*, 29(11), 751-760.
- Fernandez, P., André, V., Rieger, J., & Kühnle, A. (2004). Nano-emulsion formation by emulsion phase inversion. *Colloids and Surfaces A: Physicochemical and Engineering Aspects*, 251(1-3), 53-58.
- Fillery-Travis, A. J., Gunning, P. A., J., H. D., & Robins, M. M. (1993). Coexistent phases in concentrated polydisperse emulsions flocculated by nonadsorbing polymer. *Journal of Colloid and Interface Science*, 159(1), 189-197.
- Friberg, S. E., Lochhead, R. V., Blute, I., & Wårnheim, T. (2004). Hydrotropes—performance chemicals. *Journal of Dispersion Science and Technology*, 25(3), 243-251.
- Garti, N., Yaghmur, A., Leser, M. E., Clement, V., & Watzke, H. J. (2001). Improved oil solubilization in oil/water food grade microemulsions in the presence of polyols and ethanol. *Journal of Agricultural and Food Chemistry*, 49(5), 2552-2562.
- Gharsallaoui, A., Cases, E., Chambin, O., & Saurel, R. (2009). Interfacial and emulsifying characteristics of acid-treated pea protein. *Food Biophysics*, 4(4), 273-280.
- Ghosh, S., & Rousseau, D. (2010). Emulsion breakdown in foods and beverages. *Chemical Deterioration and Physical Instability of Food and Beverages*, 260-295.
- Gibbs, F., Selim, K., Inteaz, A., Catherine, N., & Mulligan, B. (1999). Encapsulation in the food industry: a review. *International Journal of Food Sciences and Nutrition*, 50(3), 213-224.

- Gradzielski, M. (1998). Effect of the cosurfactant structure on the bending elasticity in nonionic oil-in-water microemulsions. *Langmuir*, 14(21), 6037-6044.
- Graves, S. M., & Mason, T. (2008). Transmission of visible and ultraviolet light through charge-stabilized nanoemulsions. *The Journal of Physical Chemistry C*, 112(33), 12669-12676.
- Gueguen, J., Chevalier, M., Barbot, J., & Schaeffer, F. (1988). Dissociation and aggregation of pea legumin induced by pH and ionic strength. *Journal of the Science of Food and Agriculture*, 44(2), 167-182.
- Guerra, A., Etienne-Mesmin, L., Livrelli, V., Denis, S., Blanquet-Diot, S., & Alric, M. (2012). Relevance and challenges in modeling human gastric and small intestinal digestion. *Trends in Biotechnology*, 30(11), 591-600.
- Gutiérrez, J. M., González, C., Maestro, A., Sole, I., Pey, C., & Nolla, J. (2008). Nano-emulsions: New applications and optimization of their preparation. *Current Opinion in Colloid & Interface Science*, 13(4), 245-251.
- Gutiérrez, J. M., González, C., Maestro, A., Solè, I., Pey, C. M., & Nolla, J. (2008). Nano-emulsions: New applications and optimization of their preparation. *Current Opinion in Colloid & Interface Science*, 13(4), 245-251.
- He, W., Tan, Y., Tian, Z., Chen, L., Hu, F., & Wu, W. (2011a). Food protein-stabilized nanoemulsions as potential delivery systems for poorly water-soluble drugs: preparation, in vitro characterization, and pharmacokinetics in rats. *International Journal of nanomedicine*, 6, 521-533.
- Holst, B., & Williamson, G. (2008). Nutrients and phytochemicals: from bioavailability to bioefficacy beyond antioxidants. *Current Opinion in Biotechnology*, 19(2), 73-82.
- Hu, F. B. (2003). Plant-based foods and prevention of cardiovascular disease: an overview. *The American Journal of Clinical Nutrition*, 78(3), 544S-551S.
- Hu, L., Mao, Z., & Gao, C. (2009). Colloidal particles for cellular uptake and delivery. *Journal of Materials Chemistry*, 19(20), 3108-3115.

- Huang, Q., Yu, H., & Ru, Q. (2010). Bioavailability and delivery of nutraceuticals using nanotechnology. *Journal of Food Science*, 75(1), R50-R57.
- Hunt, J. A., & Dalglish, D. G. (1994). Adsorption behaviour of whey protein isolate and caseinate in soya oil-in-water emulsions. *Food Hydrocolloids*, 8(2), 175-187.
- Hur, S. J., Decker, E. A., & McClements, D. J. (2009). Influence of initial emulsifier type on microstructural changes occurring in emulsified lipids during in vitro digestion. *Food Chemistry*, 114(1), 253-262.
- Jafari, S. M., He, Y., & Bhandari, B. (2007). Production of sub-micron emulsions by ultrasound and microfluidization techniques. *Journal of Food Engineering*, 82(4), 478-488.
- Joshi, M., Adhikari, B., Aldred, P., Panozzo, J. F., Kasapis, S., & Barrow, C. J. (2012). Interfacial and emulsifying properties of lentil protein isolate. *Food Chemistry*, 134(3), 1343-1353.
- Kato, A., & Nakai, S. (1980). Hydrophobicity determined by a fluorescence probe method and its correlation with surface properties of proteins. *Biochimica et Biophysica Acta (BBA)-Protein Structure*, 624(1), 13-20.
- Kuhn, K. R., de Silva, F. G., Drummond, Netto, F. M., & da Cunha, R. L. (2014). Assessing the potential of flaxseed protein as an emulsifier combined with whey protein isolate. *Food Research International*, 58, 89-97.
- Lakowicz, J. R. (2013). *Principles of fluorescence spectroscopy*. New York, NY: Springer Science & Business Media.
- Lawrence, M. J., & Rees, G. D. (2000). Microemulsion-based media as novel drug delivery systems. *Advanced Drug Delivery Reviews*, 45(1), 89-121.
- Lee, L., & Norton, I. T. (2013). Comparing droplet breakup for a high-pressure valve homogeniser and a Microfluidizer for the potential production of food-grade nanoemulsions. *Journal of Food Engineering*, 114(2), 158-163.

- Lee, S.-H., Lefèvre, T., Subirade, M., & Paquin, P. (2009). Effects of ultra-high pressure homogenization on the properties and structure of interfacial protein layer in whey protein-stabilized emulsion. *Food Chemistry*, *113*(1), 191-195.
- Lee, S. J., & McClements, D. J. (2010). Fabrication of protein-stabilized nanoemulsions using a combined homogenization and amphiphilic solvent dissolution/evaporation approach. *Food Hydrocolloids*, *24*(6), 560-569.
- Leong, T. S. H., Wooster, T. J., Kentish, S. E., & Ashokkumar, M. (2009). Minimising oil droplet size using ultrasonic emulsification. *Ultrasonics Sonochemistry*, *16*(6), 721-727.
- Lerche, D. (2002). Dispersion stability and particle characterization by sedimentation kinetics in a centrifugal field. *Journal of Dispersion Science and Technology*, *23*(5), 699-709.
- Li, Y., Kim, J., Park, Y., & McClements, D. J. (2012). Modulation of lipid digestibility using structured emulsion-based delivery systems: comparison of in vivo and in vitro measurements. *Food and Function*, *3*(5), 528-536.
- Liang, Y., Gillies, G., Patel, H., Matia-Merino, L., Ye, A., & Golding, M. (2014). Physical stability, microstructure and rheology of sodium-caseinate-stabilized emulsions as influenced by protein concentration and non-adsorbing polysaccharides. *Food Hydrocolloids*, *36*, 245-255.
- Lin, W., Hong, J. L., Shen, G., Wu, R. T., Wang, Y., Huang, M. T., Heimbach, T. (2011). Pharmacokinetics of dietary cancer chemopreventive compound dibenzoylmethane in rats and the impact of nanoemulsion and genetic knockout of Nrf2 on its disposition. *Biopharmaceutics and Drug Disposition*, *32*(2), 65-75.
- Linares, E., Larre, C., Lemeste, M., & Popineau, Y. (2000). Emulsifying and foaming properties of gluten hydrolysates with an increasing degree of hydrolysis: role of soluble and insoluble fractions. *Cereal Chemistry*, *77*(4), 414-420.
- Liu, J., Verespej, E., Alexander, M., & Corredig, M. (2007). Comparison on the effect of high-methoxyl pectin or soybean-soluble polysaccharide on the stability of sodium caseinate-

- stabilized oil/water emulsions. *Journal of Agricultural and Food Chemistry*, 55(15), 6270-6278.
- Madene, A., Jacquot, M., Scher, J., & Desobry, S. (2006). Flavour encapsulation and controlled release—a review. *International Journal of Food Science and Technology*, 41(1), 1-21.
- Maldonado-Valderrama, J., Woodward, N. C., Gunning, A. P., Ridout, M. J., Husband, F. A., Mackie, A. R., Wilde, P. J. (2008). Interfacial characterization of β -lactoglobulin networks: Displacement by bile salts. *Langmuir*, 24(13), 6759-6767.
- Mason, T. G., Wilking, J. N., Meleson, K., Chang, C. B., & Graves, S. M. (2006). Nanoemulsions: formation, structure, and physical properties. *Journal of Physics: Condensed Matter*, 18(41), R635.
- Maynard, A. D., Aitken, R. J., Butz, T., Colvin, V., Donaldson, K., Oberdörster, G., Stone, V. (2006). Safe handling of nanotechnology. *Nature*, 444(7117), 267-269.
- McClements, D. J. (1994). Ultrasonic determination of depletion flocculation in oil-in-water emulsions containing a non-ionic surfactant. *Colloids and Surfaces A: Physicochemical and Engineering Aspects*, 90(1), 25-35.
- McClements, D. J. (2005). *Food emulsions: principles, practices, and techniques*. Boca Raton, FL: CRC press.
- McClements, D. J. (2007). Critical review of techniques and methodologies for characterization of emulsion stability. *Critical Reviews in Food Science and Nutrition*, 47(7), 611-649.
- McClements, D. J. (2012). Nanoemulsions versus microemulsions: terminology, differences, and similarities. *Soft Matter*, 8(6), 1719-1729.
- McClements, D. J., Decker, E. A., & Weiss, J. (2007). Emulsion-based delivery systems for lipophilic bioactive components. *Journal of Food Science*, 72(8), R109-R124.
- McClements, D. J., & Li, Y. (2010a). Review of in vitro digestion models for rapid screening of emulsion-based systems. *Food and Function*, 1(1), 32-59.

- McClements, D. J., & Li, Y. (2010b). Structured emulsion-based delivery systems: Controlling the digestion and release of lipophilic food components. *Advances in Colloid and Interface Science*, 159(2), 213-228.
- Morris, V. J., & Gunning, A. P. (2008). Microscopy, microstructure and displacement of proteins from interfaces: implications for food quality and digestion. *Soft Matter*, 4(5), 943-951.
- Muschiolik, G. (2007). Multiple emulsions for food use. *Current Opinion in Colloid & Interface Science*, 12(4), 213-220.
- Nedovic, V., Kalusevic, A., Manojlovic, V., Levic, S., & Bugarski, B. (2011). An overview of encapsulation technologies for food applications. *Procedia Food Science*, 1806-1815.
- Newling, B., Glover, P. M., Keddie, J. L., Lane, D. M., & McDonald, P. J. (1997). Concentration profiles in creaming oil-in-water emulsion layers determined with stray field magnetic resonance imaging. *Langmuir*, 13(14), 3621-3626.
- Nik, A. M., Wright, A. J., & Corredig, M. (2010). Interfacial design of protein-stabilized emulsions for optimal delivery of nutrients. *Food and Function*, 1(2), 141-148.
- Pan, M. H., Huang, T. M., & Lin, J. K. (1999). Biotransformation of curcumin through reduction and glucuronidation in mice. *Drug Metabolism and Disposition*, 27(4), 486-494.
- Patel, D., & Sawant, K. K. (2007). Oral bioavailability enhancement of acyclovir by self-microemulsifying drug delivery systems (SMEDDS). *Drug Development and Industrial Pharmacy*, 33(12), 1318-1326.
- Pinheiro, A. C., Lad, M., Silva, H. D., Coimbra, M. A., Boland, M., & Vicente, A. A. (2013). Unravelling the behaviour of curcumin nanoemulsions during in vitro digestion: effect of the surface charge. *Soft Matter*, 9(11), 3147-3154.
- Piorowski, D. T., & McClements, D. J. (2014). Beverage emulsions: Recent developments in formulation, production, and applications. *Food Hydrocolloids*, 42, 5-41.
- Porter, C. J. H., & Charman, W. N. (2001). In vitro assessment of oral lipid based formulations. *Advanced Drug Delivery Reviews*, 50, S127-S147.

- Prasad, S., Tyagi, A. K., & Aggarwal, B. B. (2014). Recent developments in delivery, bioavailability, absorption and metabolism of curcumin: the golden pigment from golden spice. *Cancer Research and Treatment: Official Journal of Korean Cancer Association*, 46(1), 2.
- Qian, C., & McClements, D. J. (2011). Formation of nanoemulsions stabilized by model food-grade emulsifiers using high-pressure homogenization: Factors affecting particle size. *Food Hydrocolloids*, 25(5), 1000-1008.
- Radford, S. J., & Dickinson, E. (2004). Depletion flocculation of caseinate-stabilised emulsions: what is the optimum size of the non-adsorbed protein nano-particles? *Colloids and Surfaces A: Physicochemical and Engineering Aspects*, 238(1), 71-81.
- Rao, J., & McClements, D. J. (2012). Food-grade microemulsions and nanoemulsions: Role of oil phase composition on formation and stability. *Food Hydrocolloids*, 29(2), 326-334.
- Reis, P. M., Raab, T. W., Chuat, J. Y., Leser, M. E., Miller, R., Watzke, H. J., & Holmberg, K. (2008). Influence of surfactants on lipase fat digestion in a model gastro-intestinal system. *Food Biophysics*, 3(4), 370-381.
- Sahay, G., Kim, J. O., Kabanov, A. V., & Bronich, T. K. (2010). The exploitation of differential endocytic pathways in normal and tumor cells in the selective targeting of nanoparticulate chemotherapeutic agents. *Biomaterials*, 31(5), 923-933.
- Sari, T. P., Mann, B., Kumar, R., Singh, R., Sharma, R., Bhardwaj, M., & Athira, S. (2015). Preparation and characterization of nanoemulsion encapsulating curcumin. *Food Hydrocolloids*, 43, 540-546.
- Sarkar, A., Goh, K. K., Singh, R. P., & Singh, H. (2009). Behaviour of an oil-in-water emulsion stabilized by β -lactoglobulin in an in vitro gastric model. *Food Hydrocolloids*, 23(6), 1563-1569.
- Sarkar, A., Horne, D. S., & Singh, H. (2010). Interactions of milk protein-stabilized oil-in-water emulsions with bile salts in a simulated upper intestinal model. *Food Hydrocolloids*, 24(2), 142-151.

- Schmitt, C., Bovay, C., & Frossard, P. (2005). Kinetics of formation and functional properties of conjugates prepared by dry-state incubation of β -lactoglobulin/acacia gum electrostatic complexes. *Journal of Agricultural and Food Chemistry*, 53(23), 9089-9099.
- Shaikh, J., Ankola, D., Beniwal, V., Singh, D., & Kumar, M. R. (2009). Nanoparticle encapsulation improves oral bioavailability of curcumin by at least 9-fold when compared to curcumin administered with piperine as absorption enhancer. *European Journal of Pharmaceutical Sciences*, 37(3), 223-230.
- Sharma, O. (1976). Antioxidant activity of curcumin and related compounds. *Biochemical pharmacology*, 25(15), 1811-1812.
- Shen, L., & Tang, C.-H. (2012). Microfluidization as a potential technique to modify surface properties of soy protein isolate. *Food Research International*, 48(1), 108-118.
- Shoba G, J. D., Joseph T, Majeed M, Rajendran R, Srinivas PS. (1998). Influence of piperine on the pharmacokinetics of curcumin in animals and human volunteers. *Planta Medica*, 64(4), 353-356.
- Sikorski, Z. (2001). Functional properties of proteins in food systems. *Chemical and Functional Properties of Food Proteins*, 113-136.
- Silva, H. D., Cerqueira, M. A., & Vicente, A. A. (2012). Nanoemulsions for food applications: development and characterization. *Food and Bioprocess Technology*, 5(3), 854-867.
- Smith, D., Galazka, V. B., Wellner, N., & Sumner, I. G. (2000). High pressure unfolding of ovalbumin. *International Journal of Food Science and Technology*, 35(4), 361-370.
- Solans, C., & Solé, I. (2012). Nano-emulsions: formation by low-energy methods. *Current Opinion in Colloid & Interface Science*, 17(5), 246-254.
- Stipanuk, M. H., & Caudill, M. A. (2013). *Biochemical, physiological, and molecular aspects of human nutrition*: Elsevier Health Sciences.
- Subirade, M., Loupil, F., Allain, A.-F., & Paquin, P. (1998). Effect of dynamic high pressure on the secondary structure of β -lactoglobulin and on its conformational properties as

- determined by Fourier transform infrared spectroscopy. *International Dairy Journal*, 8(2), 135-140.
- Tadros, T., Izquierdo, P., Esquena, J., & Solans, C. (2004). Formation and stability of nano-emulsions. *Advances in Colloid and Interface Science*, 108, 303-318.
- Taylor, S. J., & McDowell, I. J. (1992). Determination of the curcuminoid pigments in turmeric (*Curcuma domestica* Val) by reversed-phase high-performance liquid chromatography. *Chromatographia*, 34(1-2), 73-77.
- Tikekar, R. V., Pan, Y., & Nitin, N. (2013). Fate of curcumin encapsulated in silica nanoparticle stabilized Pickering emulsion during storage and simulated digestion. *Food Research International*, 51(1), 370-377.
- Tiyaboonchai, W., Tungpradit, W., & Plianbangchang, P. (2007). Formulation and characterization of curcuminoids loaded solid lipid nanoparticles. *International Journal of Pharmaceutics*, 337(1), 299-306.
- Tønnesen, H. H., & Karlsen, J. (1985). Studies on curcumin and curcuminoids. *Zeitschrift für Lebensmittel-Untersuchung und Forschung*, 180(5), 402-404.
- Tønnesen, H. H., Másson, M., & Loftsson, T. (2002). Studies of curcumin and curcuminoids. XXVII. Cyclodextrin complexation: solubility, chemical and photochemical stability. *International Journal of Pharmaceutics*, 244(1), 127-135.
- Tsoukala, A., Papalamprou, E., Makri, E., Doxastakis, G., & Braudo, E. E. (2006). Adsorption at the air–water interface and emulsification properties of grain legume protein derivatives from pea and broad bean. *Colloids and Surfaces B: Biointerfaces*, 53(2), 203-208.
- van de Velde, F., Weinbreck, F., Edelman, M. W., van der Linden, E., & Tromp, R. H. (2003). Visualisation of biopolymer mixtures using confocal scanning laser microscopy (CSLM) and covalent labelling techniques. *Colloids and Surfaces B: Biointerfaces*, 31(1), 159-168.
- Velikov, K. P., & Pelan, E. (2008). Colloidal delivery systems for micronutrients and nutraceuticals. *Soft Matter*, 4(10), 1964-1980.

- Walstra, P. (1993). Principles of emulsion formation. *Chemical Engineering Science*, 48(2), 333-349.
- Walstra, P. (1996). *Dispersed systems: basic considerations*. New York, NY: Marcel Dekker.
- Walstra, P. (2002). *Physical chemistry of foods*. New York, NY: Marcel Dekker
- Wanasundara, J. P., Abeysekara, S. J., McIntosh, T. C., & Falk, K. C. (2012). Solubility differences of major storage proteins of Brassicaceae oilseeds. *Journal of the American Oil Chemists' Society*, 89(5), 869-881.
- Wang, X., Jiang, Y., Wang, Y.-W., Huang, M.-T., Ho, C.-T., & Huang, Q. (2008). Enhancing anti-inflammation activity of curcumin through O/W nanoemulsions. *Food Chemistry*, 108(2), 419-424.
- Weiss, J., & McClements, D. J. (2000). Influence of Ostwald ripening on rheology of oil-in-water emulsions containing electrostatically stabilized droplets. *Langmuir*, 16(5), 2145-2150.
- Wooster, T. J., Golding, M., & Sanguansri, P. (2008). Impact of oil type on nanoemulsion formation and Ostwald ripening stability. *Langmuir*, 24(22), 12758-12765.
- Wu, J. & Muir, A. D. (2008). Comparative structural, emulsifying, and biological properties of 2 major canola proteins, cruciferin and napin. *Journal of Food Science*, 73, C210-C216.
- Ye, A. (2008). Interfacial composition and stability of emulsions made with mixtures of commercial sodium caseinate and whey protein concentrate. *Food Chemistry*, 110(4), 946-952.
- Ye, A. (2011). Functional properties of milk protein concentrates: emulsifying properties, adsorption and stability of emulsions. *International Dairy Journal*, 21(1), 14-20.
- Yerramilli, M., & Ghosh, S. (2016a). Long-term stability of sodium caseinate-stabilized nanoemulsions. *submitted to Journal of Food Science and Technology*.
- Yerramilli, M., & Ghosh, S. (2016b). Improved stabilization of nanoemulsions by partial replacement of sodium caseinate with pea protein isolate. *submitted to Food Hydrocolloids*.

Zeeb, B., Herz, E., McClements, D. J., & Weiss, J. (2014). Impact of alcohols on the formation and stability of protein-stabilized nanoemulsions. *Journal of Colloid and Interface Science*, 433, 196-203.

Zhao, Q., Long, Z., Kong, J., Liu, T., Sun-Waterhouse, D., & Zhao, M. (2015). Sodium caseinate/flaxseed gum interactions at oil–water interface: Effect on protein adsorption and functions in oil-in-water emulsion. *Food Hydrocolloids*, 43, 137-145.